Ulp1 is required for subtelomeric chromatin localization and function

by

Ulyss Karl Roesner

A thesis submitted in partial fulfillment of the requirements for the degree of

Master of Science

Department of Cell Biology
University of Alberta

Abstract

In yeast, subtelomeric chromatin is silenced and positioned at the inner nuclear membrane (INM) through the interaction of proteins that comprise the heterotrimeric SIR complex with INM proteins. Telomeres reside primarily at the INM using partially redundant tethering mechanisms mediated by the chromatin associated protein, Sir4. Telomere tethering has also been shown to require the posttranslational modification, SUMO (small ubiquitin-related modifier). SUMOylation of target proteins is transient and temporally regulated, with the addition of SUMO to target proteins requiring SUMO ligases and the removal of SUMO being accomplished by isopeptidases. The role of SUMOylation in telomere tethering was first established in studies showing that mutants lacking the SUMO ligase Siz2 show reduced INM association of telomeres, suggesting SUMOylation promotes telomere tethering to the INM. Since SUMO modifications are dynamic, we examined the role of deSUMOylation and the consequences of the accumulation of SUMO conjugates on telomere tethering to the INM. These studies focused on the deSUMOylase, Ulp1. By using the temperature sensitive, *ulp1-333* (*ulp1ts*) allele and the *ulp1K352E* coiled-coiled (CC) domain point mutant, increases in the accumulation of SUMO conjugates were observed. The accumulation of SUMO conjugates correlates with reduced telomere tethering to the NE at specific points in the cell cycle, with the *ulp1ts* mutant showing additional defects in subtelomeric silencing and growth. Failing to remove SUMO conjugates attributed to compromised Ulp1 function also caused a loss in the nuclear peripheral association of SIR complex components, Sir4 and Sir3. Mutants expressing the *ulp1ts* or the *ulp1K352E-V5*$_3$ alleles favored the interaction between the core scaffold nucleoporin, Nup170, with the INM

protein Esc1, which has been implicated in necessitating telomere tethering. In addition to this phenotype, the *ulp1ts* and the *ulp1K352E-V5*$_3$ mutants reduced the interaction between Nup170 and Sir4. The strength of the interaction between Sir4 and Sir3 is also increased in the *ulp1ts* mutant, suggesting changes in the organization of the SIR complex. Together, these data show that mutations in Ulp1 disrupt subtelomeric silencing and cause a distinct loss of telomere tethering in a cell cycle specific manner.

Dedication

To my loving family and friends...

without your support, I would have never made it this far in my journey forward

Acknowledgments

Foremost, I wish to acknowledge my supervisor, Dr. Richard Wozniak, for the strict guidance and supervision that he offered throughout the course of my studies. Without his tutelage and impressive attention to detail, my capabilities as a scientist would have never improved as much as they have in so short of a time.

Additionally, I wish to acknowledge my wonderful coworkers whose constant advice and witty incite made every day in the lab a pleasure. Specifically, I wish to thank Brett Roughhead for the personal support and the unforgettable memories. I would also like to thank Natasha Saik. Her consent, outgoing personality and fierce intellect always provided me with the encouragement to better my expertise within the lab. I would also like to acknowledge the contributions of both Tadashi Makio and Christopher Ptak. Without their unimaginable expertise at experimental design and their unparalleled love for science, the work presented here would not have been possible.

Also, to all of the friends who supported me; Avinash Seshachalam, Annapoorna Shruthi, Joe Wozniak, Dhavani Gudi, and Nicole Del Alba, I thank you all. Finally, I would like to thank my supportive family. Without their weekly Skype calls, I would not have found the courage to press forward and extend my abilities further into the realm of science.

Table of Content

List of Tables

List of Figures

List of Symbols or Abbreviations

µ	micro
µm	micrometer
µg	microgram
µL	microliter
5FOA	5-fluoroacetic acid
ade	adenine
ACS	ARS consensus sequence
ARS	autonomous replication sequence
℃	degrees Celsius
bp	base pair
CCD	charge-coupled device
ChIP	chromatin immunoprecipitation
d	day
DNA	deoxyribonucleic acid
ECL	enhanced chemiluminescence
EM	electron microscopy
FG	phenylalanine glycine
FISH	fluorescence in situ hybridization
G	gram
G1	gap 1 phase
G2	gap 2 phase
GAP	GTPase activating protein
GCR	gross chromosomal arrangement
GDP	guanosine-5′-diphosphate
GEF	guanine nucleotide exchange factor
eGFP	enhanced green fluorescent protein
GST	glutathione-S-transferase
GTP	guanosine-5′-triphosphate
GTPase	guanosine-5′-triphosphate hydrolase
h	hour
PrA	protein A
HML	hidden MAT left
HR	homologous recombination
HMR	hidden MAT right
IgG	immunoglobulin G
INM	inner nuclear membrane
kDa	kilo Dalton
LacI	lactose repressor
LacO	lactose operator
m	milli
M	molarity/mega
MAT	mating-type locus
mCherry	monomeric cherry
MDa	mega Dalton

mg	milligram
min	minute
mL	milliliter
mRNA	messenger ribonucleic acid
mRuby	monomeric ruby
nm	nano meter
NAD	nicotinamide adenine dinucleotide
NHEJ	non-homologous end joining
NE	nuclear envelope
NPC	nuclear pore complex
Nup	nucleoporin
OD	optical density
ONM	outer nuclear membrane
ORF	open reading frame
ORC	origin of recognition complex
PCR	polymerase chain reaction
Pom	pore membrane protein
rDNA	ribosomal DNA
RFPT	red fluorescent protein t
RNA	ribonucleic acid
RNP	ribonucleoprotein
S	synthesis phase
SAC	spindle assembly checkpoint
SC	synthetic complete medium
SDS-PAGE	sodium dodecyl sulfate polyacrylamide gel electrophoresis
sec	second
SIM	sumo interacting motif
SIR	Silent information regulator
SPB	spindle pole body
SUMO	small ubiquitin-related-modifier
TCA	trichloroacetic acid
Tel	telomere
TPE	telomere position effect
Ulp1	ubiquitin-like specific protease 1
ura	uracil
WT	wild type
YPD	yeast extract peptone dextrose medium

Chapter I: Introduction

Epigraph

"*There are many ways of going forward, but only one way of standing still.*"
Franklin D. Roosevelt

1.1 Overview

The eukaryotic cell is defined by the compartmentalization of its cellular processes into distinct organelles. One such organelle is the nucleus and it is surrounded by the nuclear envelope (NE) which sequesters the cellular genome into an enclosed space. The genome organizes at the NE based on different factors, one of which being gene content (reviewed in Cremer & Cremer, 2010). Gene poor heterochromatin tends to localize towards the nuclear periphery while gene-dense euchromatin dominates the nuclear interior. The genome is comprised of linear chromosomes. Positioned at the end of chromosomes are telomeres, which function as caps that protect chromosomes from unregulated DNA end resection. Telomeres are composed of repetitive elements that promote a transcriptionally repressive environment and the regions adjacent to the telomere are gene-poor. In budding yeast, the subtelomeric, gene-poor region contains binding sites for proteins that function to recruit the SIR (silent information regulatory) complex, which organizes subtelomeric chromatin into a repressive state and positions it at the nuclear periphery.

In budding yeast, the tethering of telomeres at the nuclear periphery occurs in a cell cycle dependent manner and through partially redundant pathways. Telomeres are positioned at the NE and only briefly oscillate away from the nuclear periphery until late S-phase of the cell cycle, where telomeres localize towards the nuclear interior to replicate (Hediger et al., 2002; Ebrahimi & Donaldson, 2008). Both G1-phase and S-phase telomere tethering pathways function independently from one another and require distinct mechanisms to facilitate the relocalization of subtelomeric chromatin towards the nuclear periphery. The reversible post translational protein modification, SUMO (small

ubiquitin-related modifier), has been implicated in this process, which potentially acts as a dynamic mechanism of control for the organization of subtelomeric chromatin at the nuclear periphery. Further characterizing the mechanisms that control the conjugation and removal of SUMO onto proteins localized within the subtelomeric region of chromatin is critical in understanding how subtelomeric chromatin is positioned at the nuclear periphery in a cell cycle dependent fashion.

1.2 The nuclear envelope and the nuclear organization of chromatin

The nuclear envelope (NE) consists of two membranes that define the boundary between the cytoplasm and the genomic material. It serves to encapsulate and compartmentalize the genomic material of the cell in a defined space, termed the nucleoplasm. The two membranes that compose the NE are the outer nuclear membrane (ONM) and the inner nuclear membrane (INM) (Watson, 1955). The ONM is continuous with the endoplasmic reticulum (ER) and contains proteins that can function mediate interactions with the cytoskeleton (Dreger et al., 2001). The INM faces the nucleoplasm and between the two membranes resides the perinuclear space. Chromatin has been shown to organize within the nucleus in a non-random fashion (Croft et al., 1999).

The organization of chromatin can be visualized in metazoans with electron microscopy. Electron micrographs of metazoan cells show darkly staining heterochromatin organizing along the nuclear periphery with lightly staining euchromatin positioned at the nuclear pores (Krull et al., 2010). In support of these observations, chromosomes have been shown to organize based on gene density. Chromosomes exist in spatially defined regions termed chromosomal territories (CTs) (reviewed in Cavalli &

Misteli, 2013). FISH (fluorescent in situ hybridization) of small human chromosomes (HSA) 18 and 19 showed gene poor HSA18 localizing towards the nuclear periphery while gene dense HSA19 localize more internally (Croft et al., 1999). Following anaphase, interphase chromatin can organize in a configuration known as the Rabl organization. The Rabl organization was first discovered in epithelial salamander larvae cells by Carl Rabl (Rabl, 1885). This chromatin configuration clusters centromeres to one end of the nucleus while telomeres interact with the opposite regions of the NE. The persistence of the Rabl organization following anaphase varies from different organisms and different cell types (reviewed in Cowan et al. , 2001). In *Saccharomyces cerevisiae* (budding yeast), interphase chromatin is positioned in a Rabl organization without the need to pass through anaphase. This arrangement of interphase chromatin in yeast also differs from the classical Rabl organization in a configuration referred to as 'Rabl-like' (Figure 1-1). In this orientation, centromeres cluster with the spindle pole body (SPB) opposite from the nucleolus, but the chromatin that extends from the centromere cluster loops back on itself, positioning telomeres at the NE between both the clustered centromeres and the nucleolus at the nuclear periphery (Figure 1-1) (Jin et al., 2000; Therizols et al., 2010).

Lining the nucleoplasmic face of the INM in higher eukaryotes is a polymer network of intermediate filaments known as the nuclear lamina. The lamina is composed of lamins which provide structural organization to the nucleus. The proteins that span the INM are referred to as NE transmembrane proteins or NETs. NETs associate with lamins and can function to organize chromatin at the nuclear periphery (reviewed in Stancheva & Schirmer, 2014). Mechanistically, anchoring at the nuclear periphery has been shown

through the indirect interaction of NETS, such as LAP2β or LBR (Lamin B receptor), with chromatin. HP1 (heterochromatin protein 1), cross links LBR to core histones H3/H4, establishing a link between proteins at the INM and the positioning of chromatin along the nuclear periphery (Polioudaki et al., 2001). Transcriptionally repressed chromatin has been shown to be positioned at the nuclear periphery through the binding of a complex consisting of the transcriptional repressor, cKrox and HDAC3, at lamina associated chromatin sequences, with LAP2β (Zullo et al., 2012). Additionally, lamins have been shown to directly bind DNA as well as play a role in the establishment of and the transition between gene expression states during the differentiation of embryonic stem cells (Zhao et al., 1996; Peric-Hupkes et al., 2010). Together, these observations suggest that chromatin binding at the nuclear periphery occurs both through the lamina and through the NETs that span the INM as well as demonstrate that positioning of chromatin at the nuclear periphery can establish the expression of different genes.

Budding yeast lack any discernible structure that resembles the nuclear lamina but still have INM-associated proteins. Some of these NE proteins function in much the same way as the lamina and NETs of higher eukaryotes to provide an anchor for heterochromatic regions (Taddei et al., 2004). An example of an INM protein that is involved in positioning chromatin to the nuclear periphery is Esc1. Mutants lacking Esc1 showed a loss in DNA anchoring and supercoiling (Andrulis et al., 2002). Additional research suggests that the yeast nuclear pore complex (NPC) basket proteins could be functioning with the INM proteins to form a scaffolding network in a similar manner to the lamina and NETs in higher eukaryotes (Strambio-de-Castillia et al., 1999; Niepel et al., 2005; Niepel et al., 2013).

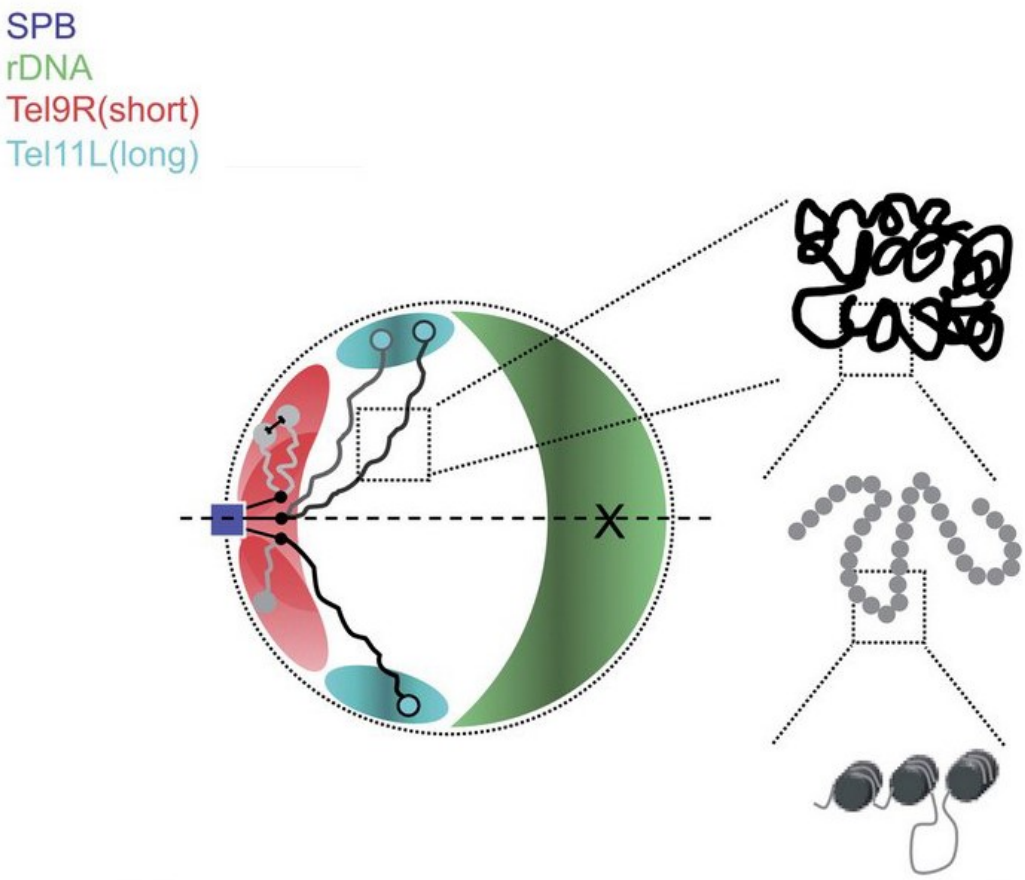

Figure 1-1. Rabl-like chromatin organization in interphase nuclei for *S. cerevisiae*

Above is the interphase chromatin organization for the yeast nucleus. The chromosomes extend from the centromeres (black circles) that cluster to one side of the nucleus at the spindle pole body (SPB) (dark blue). Facing the opposite side is the nucleolus where the rDNA organizes (green). Highlighted in red are the regions where shorter telomeres (such as the right arm of telomere 9 or Tel9) cluster at the nuclear periphery where light blue highlights the regions where longer telomeres (such as the left arm of telomere 11 or Tel11) cluster at the nuclear periphery. The chromatin in the yeast nucleus organizes in a 'Rabl-like' configuration during interphase because, unlike in higher eukaryotes, telomeres tend to loop back following extension from the centromere cluster, allowing for a 'relaxed' centromere-telomere polarization. Further highlighted by the grey box are a series of enlargements that depict the possible arrangement of the chromosome at smaller scales. At the smallest scale shown is a series of nucleosomes with a segment of nucleosome-free DNA looping out. Adapted from Zimmer et al., 2011.

Heterochromatin in higher eukaryotes is distinguished by H3K9 trimethylation but yeast lack this defining hallmark. Instead, heterochromatin-like regions in yeast include regions adjacent to telomeres (subtelomeric chromatin), tandem ribosomal RNA gene arrays (rDNA), and the silent mating type loci, HML and HMR. In the following sections, the structure of subtelomeric chromatin will be defined further and the mechanisms that promote silencing at these regions will also be characterized. In budding yeast, these heterochromatin-like regions are positioned at the NE and the mechanisms that promote this organization will be further explained below.

1.3 The repressive nature of telomeres and their structure

The sequence of telomeres and adjacent chromatin is repetitive. This includes the repetitive elements at the end of telomeres, which are known as the $TG_{(1-3)}$ repeats. The ends of telomeres are not blunt and extending from the 3′ strand is a G -rich overhang of ~300 bp (Shampay et al., 1984; Wang & Zakian, 1990). Regions encompassing ~25 kbp away from telomeres are generally referred to as subtelomeric chromatin. The subtelomeric region consists of two families of highly repetitive sequences that are classified as the Y′ and the X elements. Distally located from the X element, towards the end of roughly half of the telomeres, is the Y′ element. The Y′ element is highly conserved and localizes in 1-4 repeats that are flanked by $TG_{(1-3)}$ repeats on the side facing the end of the telomere (Chan & Tye, 1983; Louis et al., 1994; Louis & Haber, 1992). $TG_{(1-3)}$ repeats can be localized in between the Y′ and X elements or in between tandem Y′ elements and they are a source of genomic instability. This is because of their ability to recombine with other homologous telomeric sequences (Aksenova et al., 2013)

(Figure 1-2 A). Also located at the repetitive X and Y′ elements are the autonomously replicating sequences or ARSs (Chan et al., 1983). The more variable X elements are less characterized than the Y′ elements but they share a common ~475 bp element known as the X core. Within the X core region are binding sites for Abf1 (ARS-binding factor 1) and, in most instances, an ARS consensus sequences (ACS)(Pryde et al., 1995; Louis et al., 1994). Located towards the end of the telomere or in between the X and Y′ elements are the subtelomeric repeat (STR) elements. These elements are composed of tandem repeats of TTAGG sequences that provide a binding site for Reb1 and Tbf1 (reviewed in Louis et al., 1994). Tandemly positioned STRs can promote an anti-silencing effect for genes localized next to telomere repeats and thus display boundary activity (BA) that limits the spread of subtelomeric gene silencing (Fourel et al., 1999; Laroche et al., 1998).

Genes localized within the subtelomeric region normally experience position-dependent expression, being silenced when localized next to telomeric tracts of $TG_{(1-3)}$ repeats. This localization dependent silencing is known as the telomere position effect (TPE) and it was first characterized by Gottschling et al (1990). TPE was shown using an assay in which different genes were placed near the end of artificially reconstructed telomeres and their expression was monitored through colony coloration and the ability to grow on different media. Colonies with subtelomerically positioned *ADE2* displayed an *ade2-* phenotype. Similarly, strains with the *URA3* gene positioned subtelomerically failed to grown in the absence of uracil and were resistant to 5FOA (reviewed in Van Leeuwen & Gottschling, 2002). Both of these phenotypes indicated silencing. Colonies that display an *ade2-* phenotype display red coloration due to the accumulation of a red

pigment resulting from adenine auxotrophy and 5FOA resistance results from inhibiting the expression of *URA3*.

1.3.1 The organization of subtelomeric chromatin in regards to maintenance and silencing

Not only are the ends of telomeres protected from unregulated DNA strand resection by the 3′ overhang but proteins that bind at the subtelomeric region can also similarly protect and maintain the structure of subtelomeric chromatin. Within the subtelomeric region of chromatin are binding sites for various proteins that can serve to extend telomeres, cap telomeres to limit DNA strand resection, and organize subtelomeric chromatin into a repressive state. Rap1 (repressor/activator protein 1) binds double stranded DNA at $TG_{(1\text{-}3)}$ repeats and can function to regulate telomere length (Hardy et al., 1992a; Hardy et al., 1992b; Wotton et al., 1997), affect silencing (Hardy et al., 1992a; Hardy et al., 1992b; Kyrion et al., 1993), and protect telomere ends from resection (Negrini, et al., 2007; Vodenicharov et al., 2010). A negative feedback counting mechanism can be used to determine the number of Rap1 molecules that bind to subtelomeric chromatin and this counting mechanism can also be used to determine the number of interacting Rif proteins, whereby artificially increasing either protein onto subtelomeric chromatin negatively impacts telomere length (Levy & Blackburn, 2004; Marcand et al., 1997). Both Rif proteins, Rif1 and Rif2, bind the C-terminus of Rap1 and regulate telomere length. Deletions in either *RIF1* or *RIF2* increase the length of telomeres while simultaneously deleting both *RIF1* and *RIF2* generates even longer telomeres, suggesting that the two proteins regulate telomere length through alternative mechanisms (Hardy et al., 1992a; Hardy et al., 1992b; Wotton et al., 1997).

Figure 1-2. Organization of subtelomeric chromatin

The heterochromatic-like regions in yeast are silenced by the binding and nucleation of the Sir complex. A) A diagram outlining the sequences that comprise the subtelomeric region. At the region most distal from the centromere (dark blue circle) resides the telomere which consists of TG repeats that leave the end of the chromosome with a 3′ overhang. The region adjacent to the telomere cap is the conserved Y′ sequence that can organize in 1-4 tandem repeats depending on the chromosome. Most proximal to the centromere is the X core sequence and in between the X and Y′ sequences is another series of TG repeats. B) The 'fold back' structure of the yeast telomere with Rap1 bound Rif1, Rif2, and the SIR complex. The ssDNA binding CST complex and the dsDNA binding yKu heterodimer can be seen binding at the end of the telomere. C) The extendible telomere configuration. The CST complex outcompetes the ssDNA binding complex, RPA, and in conjugation with the yKu heterodimer, promotes the recruitment of telomerase to the end of telomeres. Adapted from Kupiec, 2014.

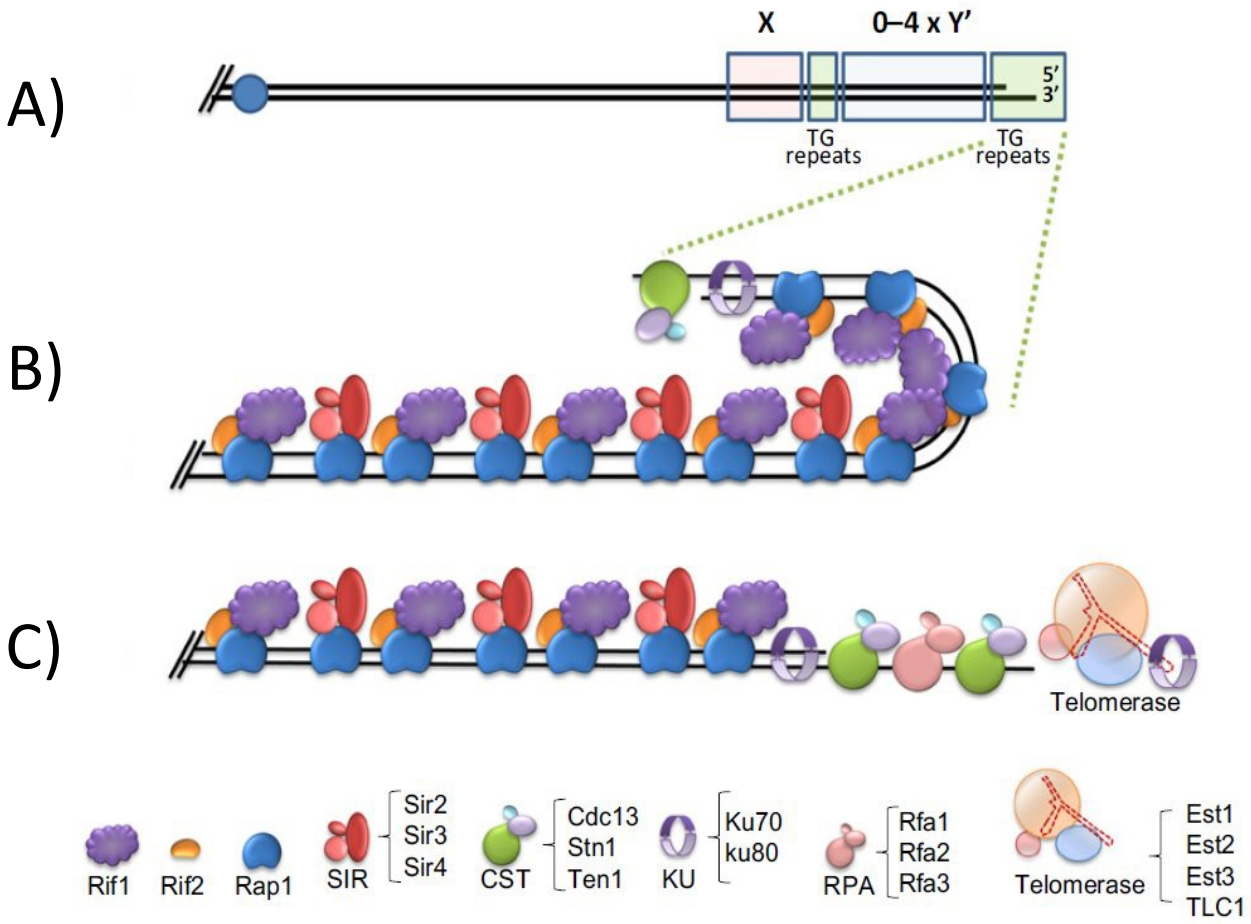

Figure 1-2. Organization of subtelomeric chromatin

Additionally, the yKu heterodimer is recruited to subtelomeric chromatin and plays a role in mediating telomere length and regulating gene silencing (Boulton & Jackson, 1996a; Boulton & Jackson, 1996b; Martin et al., 1999; Laroche et al., 1998; Mishra & Shore, 1999). Deleting either *YKU70* or *YKU80* promotes a loss of subtelomeric silencing that can be rescued through additional deletions of *RIF1/2* (Mishra & Shore, 1999). Coupled with the fact that telomeres are shorter in the absence of the yKu heterodimer, the yKu heterodimer is implicated in maintaining the structural organization of telomeres (Laroche et al., 1998). The ability of the yKu heterodimer to antagonize the functionality of the Rif proteins and maintain the structure of subtelomeric chromatin is thought to come from its ability to recruit telomerase though interactions with telomerase RNA (Stellwagen et al., 2003).

Telomerase is a holoenzyme that maintains the ends of telomeres from unregulated DNA end resection by adding $TG_{(1\text{-}3)}$ repetitive sequences to the end of critically short telomeres. Telomerase functions to synthesize telomere repeats through its reverse transcriptase function by templating DNA synthesis with the telomerase RNA subunit, Tlc1 (Singer & Gottschling, 1994). This process prevents the critical shortening of telomeres. Critically shortened telomeres activate double strand break (DSB) arrest within the cell leading to senescence (reviewed in Jain & Cooper, 2010).

Telomerase is composed of Est1, Est2, Est3, and Tlc1 (Hughes et al., 2000). Telomerase is recruited to DNA sequences with extended G-rich tracts either through an interaction between the yKu80 component of the yKu heterodimer, or through an interaction with Cdc13, the ssDNA binding component of the CST complex (Stellwagen et al., 2003; Evans & Lundblad, 1999). The Est1 component of telomerase binds the

telomere binding protein, Cdc13, and promotes telomerase recruitment to the 3′ G-rich overhang (Evans & Lundblad, 1999; Pennock, et al., 2001)(Figure 1-1 C). There are data to suggest that Cdc13 recruits telomerase based on the length of the initial G-rich sequence because yKu80 telomerase recruitment shows no sequence specificity (Stellwagen et al., 2003). By inducing gross chromosomal rearrangements (GCR) and isolating chromosomal recovery events that involved the addition of $TG_{(1-3)}$ sequences, telomerase-mediated extension events could be observed based on the length of the initial G-rich overhang. In mutant strains where the ability of yKu80 to interact with telomerase RNA is inhibited, telomerase recruitment at $TG_{(1-3)}$ rich junctions is not affected but recruitment to overhangs with three or less $TG_{(1-3)}$ junctions is completely abolished. This indicates yKu80 potentially function at alternative DNA binding sites then Cdc13 in order to recruit telomerase. Because yKu80 and Cdc13 are the only two proteins known to recruit telomerase, these data suggest that yKu80 most likely recruits telomerase to sites independently of their sequence while Cdc13 preferentially recruits telomerase to sites with extended G-rich tracts. Components of the SIR (silent information regulator) complex also associate to subtelomeric chromatin through an interaction with Rap1 (Rusché et al., 2002). Rap1-mediated recruitment of the Sir protein, Sir4, at subtelomeric chromatin initiates SIR complex assembly. The function of the SIR complex is to promote the silencing and subsequent recruit of subtelomeric chromatin to the NE.

1.3.2 The establishment of silent heterochromatin in yeast

Silencing of heterochromatic-like regions occurs through the binding and spreading of the SIR complex (Rine & Herskowitz, 1987). This heterotrimeric complex is

composed of Sir2, Sir3 and Sir4 at silenced subtelomeric chromatin (Rusché et al., 2002). Within the subtelomeric region, Rap1 binds at repetitive $TG_{(1-3)}$ repeats to promote the recruitment of Sir4 along with Sir3 to some extent (Luo et al., 2002). Initial complex assembly is dependent on the interaction between Sir proteins and Rap1, but complex spreading occurs because of the greater affinity Sir proteins have with hypoacetylated H4K16. Hypoacetylated histone tails are generated through the NAD^{+}-dependent deacetylation functionality of Sir2 (Braunstein et al., 1993). This allows for the Sir proteins to nucleate along chromatin, which is mediated through the interaction of the Sir3-BAH domain with the N-terminus of H4 (Onishi et al., 2007; Rusché et al., 2002). Interestingly, Rap1 has been shown to be unable to bind histones but was found at core heterochromatin the same distance from $TG_{(1-3)}$ tracts as Sir proteins that have spread from the initial point of complex assembly. This implies that subtelomeric chromatin can loop in order to account for distal Rap1 localization (Strahl-Bolsinger et al., 1997; Wright et al., 1992)(Figure 1-2 B).

SIR complex assembly at the HM loci is dependent mainly on the E silencer that flanks either the HML or the HMR locus and Sir1. Within the E (essential) silencer at HM loci are binding sites for Rap1 and ORC (Origin of replication) that binds the ACS while the I (important) silencer has binding sites for Abf1 and the ACS. Rap1 binding at the E silencer allows for the subsequent recruitment of Sir4 in order to promote silencing but unlike at subtelomeric chromatin, Sir1 was found to be indispensable for the establishment of silenced chromatin at this locus. When Sir1 is artificially bound at HMR through a GAL4 DNA binding domain, this interaction was sufficient to silence the HMR locus even in the absence of Rap1 binding (Chien et al., 1993). In order to mediate the

spread of silencing at HM loci, a boundary is established at either region flanking the loci. Boundary activity at the HMR locus is established on both the left and right side, with the right side establishing BA with greater efficiency (reviewed in Sun et al., 2011). On the right side of HMR is the $tRNA^{thr}$ gene that establishes a barrier against the spread of silencing through the binding of TFIIIC at box a and box b promoter elements of the *tRNA* gene (Donze & Kamakaka, 2001). Recruitment of PolIII is not necessary to establish BA but its recruitment to the *tRNA* gene requires upstream binding of TFIIIB (Valenzuela et al., 2009). Additionally, BA is maintained at the right side of HMR by the nearby depletion of histones through the activity of chromatin remodelers such as RSC, DNA Pol ε, or Rtt109. These chromatin remodelers work independently from the histone acetyltransferase (HAT) activity of complexes such as SAGA, SAS-1, and NuA4 in order to establish a boundary, preventing the spread of silenced chromatin (Dhillon et al., 2009; Oki & Kamakaka, 2005). There is no natural boundary flanking the HML locus but it has been speculated that the binding of several Rap1 molecules at upstream activator sequences of ribosome protein genes (UAS_{rpg}) could function to form a gap between nucleosomes, making them inaccessible to the spreading SIR complex (Bi & Broach, 1999).

At rDNA, silencing is maintained by Sir2. Deleting *SIR2* has been shown to upregulate the expression of genes inserted at rDNA while deleting either *SIR3* or *SIR4* was shown not to alter the expression of genes inserted at rDNA (Smith & Boeke, 1997; Fritze et al.,1997). One of the consequences of Sir2-dependent rDNA silencing was to prevent intrachromosomal recombination between rDNA arrays during meiosis (Gottlieb & Esposito, 1989).

1.4 Telomere positioning

In yeast, telomeres are positioned at the NE. Initial observations that telomeres were located at the nuclear periphery came from fluorescence in situ hybridization (FISH) studies of Y′ stained telomeres. Telomeres were found at the nuclear periphery but only appeared stained in 3-8 foci. Over half of yeast telomeres have a Y′element, but the number of labeled foci was considerably less, indicating that telomeres are clustering at the nuclear periphery (Gotta et al., 1996). The positioning of telomeres occurs through the physical interactions between proteins localized within the subtelomeric region with proteins positioned at the NE and this perinuclear positioning of telomeres occurs in a cell cycle dependent manner. Telomeres tend to oscillate on and off the periphery but are consistently peripherally localized during G1-phase and early S-phase of the cell cycle. As the cell progresses into late S-phase, telomeres tend to favor a nucleoplasmic localization and briefly come off the periphery to replicate. Peripheral localization is reestablished once the cell transitions into M-phase (Hediger et al., 2002; Ebrahimi & Donaldson, 2008).

Mechanistically, telomere tethering occurs via partially redundant pathways between the yKu heterodimer and Sir4. The ability of proteins to function as chromatin tethers was shown through the generation of lex-A-protein fusion constructs with proteins implicated in tethering chromatin at the NE. These fusion constructs bind specific lex-A binding sites downstream of chromatin labeled through the insertion of a tandem *lacO* array probed for by coexpressing LacI-GFP (Hediger et al., 2002). By using this system, labeled chromatin can be visualized as a bright focus and the localization of this focus can be determined in regards to the nuclear periphery (Taddei et al., 2004). The yKu70

fusion construct was shown to bind chromatin to the nuclear periphery and the mechanism of this chromatin binding was different from either the yKu80 or Sir4 fusion constructs, indicating distinct perinuclear tethering pathways for each of these proteins. By inhibiting the interaction between the yKu80 protein with Sir4 through generation of the *yku80-4* point mutant, the ability of either Sir4 or yKu80 to promote telomere tethering at the NE could be separated (Taddei et al., 2004). By using this system, the yKu heterodimer was shown to anchor chromatin at the nuclear periphery during G1-phase of the cell cycle independently of Sir4. Telomeres were shown to mislocalize from the periphery as well. By deleting either *ESC1* or *YKU70*, the perinuclear positioning of either the right arm of LacI-GFP labeled telomere 6 (Tel 6R) or the left arm of LacI-GFP labeled telomere 14 (Tel 14L) was reduced. Deleting both *ESC1* and *YKU70* caused telomeres to localize randomly within the nucleus indicating that G1 phase tethering is dependent on Esc1 and yKu70. Interestingly, yKu70 could still anchor chromatin to the periphery in the absence of Esc1 and deleting *ESC1* does not noticeably reduce the perinuclear positioning of Tel 14L, suggesting that there is an alternative G1-phase anchor that targets telomeres at the nuclear periphery (Figure 1-3; Taddei et al., 2004).

S-phase telomere tethering that was dependent on the yKu heterodimer required the interaction between yKu80 and telomerase with the integral SUN (Sad1-UNC-84) domain protein, Mps3. Specifically, binding of yKu80 to telomerase RNA necessitated the positioning of chromatin to the NE and this positioning was dependent on both the Est1 and Est2 telomerase subunits (Schober et al., 2009). The N-terminus of Mps3 was also required for the perinuclear positioning of chromatin at the NE (Figure 1-3)(Schober et al., 2009). A consequence attributed to the S-phase perinuclear positioning of

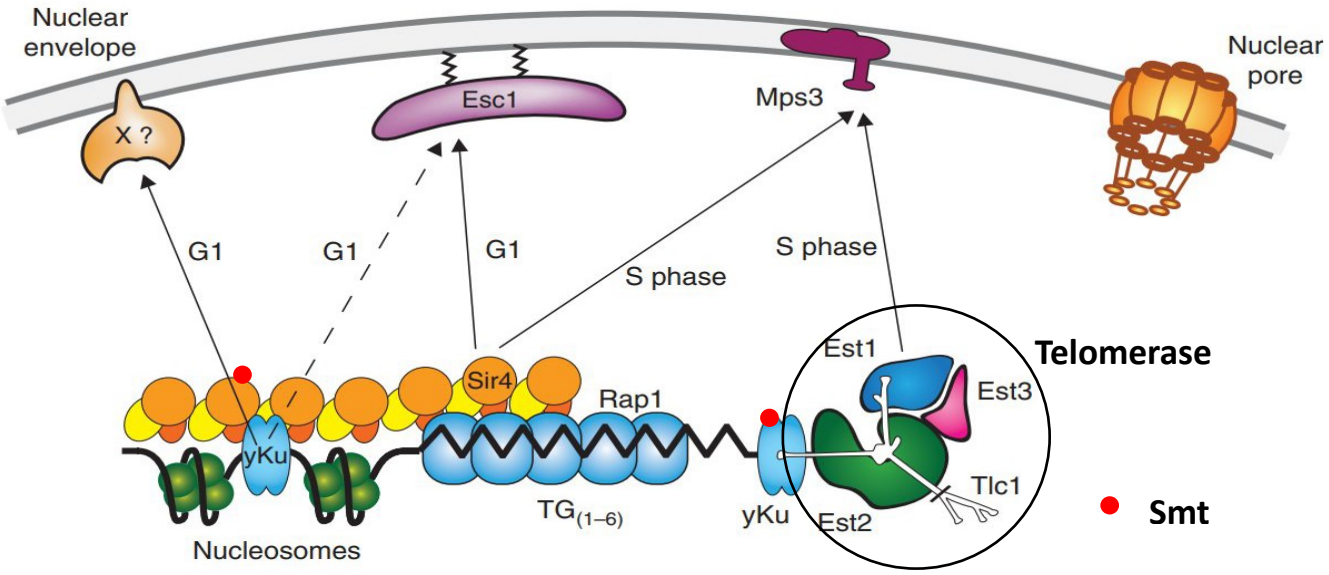

Figure 1-3. Telomere tethering at the nuclear envelope

Telomere tethering occurs through partially redundant pathways and is cell cycle dependent. During G1-phase of the cell cycle, Sir4 and the yKu heterodimer mediate telomere tethering through interactions with the perinuclear protein, Esc1, and this tethering is dependent on SUMOylation. Additionally, G1-phase telomere tethering occurs through the interaction between the yKu heterodimer with an unidentified partner(s) at the NE. S-phase telomere tethering occurs through the interaction between Sir4 and yKu80/Est1 with the transmembrane, SUN domain protein, Mps3. Adapted from Taddei et al., 2010.

telomeres was to restrict recombination between subtelomeric sequences which occurs when telomeres randomly localize within the nucleus (Schober et al., 2009).

Sir4-mediated telomere tethering occurs through the interaction of its partitioning and anchoring domain (PAD) with Esc1. $Sir4^{PAD}$ lex-A fusion constructs showed binding of chromatin to the nuclear periphery and this binding was only disrupted when both *ESC1* and *YKU70* are deleted. This indicated that there are two distinct G1-phase chromatin tethering pathways and that one of the chromatin tethering pathways is dependent on Sir4 (Taddei et al., 2004) (Figure 1-3). Deleting *SIR4* also caused a loss in the peripheral positioning of Tel 6R and Tel 14L at the NE during both G1-phase and S-phase of the cell cycle, indicating telomere tethering to the nuclear periphery is dependent on Sir4 (Figure 1-3)(Taddei et al., 2004). S-phase telomere tethering at the NE that is dependent on Sir4 occurs through the interaction of Sir4 with the N-terminus of Mps3. Deletion of *SIR4* or the N-terminal acidic residues in Mps3 led to telomere mislocalization (Bupp et al., 2007). The N-terminal residues of Mps3 were also found to be required for silencing, establishing that perinuclear tethering and silencing can be interconnected (Bupp et al., 2007).

The consequence of positioning telomeres to the nuclear periphery is thought to provide a transcriptionally repressive environment. By establishing this environment, homologous recombination between repetitive silenced regions within rDNA or subtelomeric chromatin is thought to be inhibited (Schober et al., 2009; Fritze et al.,1997). This has been further shown by the positioning of the rDNA locus at the nuclear periphery. This perinuclear positioning was shown to promote rDNA stability and prevent homologous recombination (HR) between repetitive rDNA elements (Mekhail et

al., 2008). Additionally, telomere positioning and silencing are thought to be linked because heterochromatic, gene-poor regions have been shown to localize at the nuclear periphery (Bourgeois et al., 1985; Koehler et al., 2009; Tanabe et al., 2002). However, there is contrary evidence that shows telomere tethering can occur irrespective of silencing. Silenced, full length telomere 6 and a truncated telomere 7 with compromised silencing were shown to equally localize to the periphery, indicating distinct requirements for either silencing or anchoring (Mondoux et al., 2007). Furthermore, additional research shows a lack in correlation between silenced cells and perinuclear positioned telomere 7 indicating that telomere positioning and silencing often occur irrespective of one another (Tham et al., 2001).

1.5 The role Nups play in organizing chromatin

The perinuclear positioning of telomeres can be affected by other proteins associated with subtelomeric chromatin. Indeed, Tbf1 and Reb1 were both found to antagonize telomere tethering to the NE (Hediger et al., 2006). There is growing evidence implicating the importance of proteins that constitute the nuclear pore complex (NPC) in organizing chromatin and mediating subtelomeric tethering at the NE. The NPC is a proteinaceous complex at the NE that is composed of approximately 30 proteins, termed nucleoporins or Nups. Nups reside in distinct subcomplexes within the NPC. These subcomplexes are organized at the NE in several rings; an outer ring that faces the cytoplasm and nucleoplasm, two centrally localized inner rings, and a transmembrane ring that is embedded in the envelope, which provides an anchor for NPC structure. Extending from the cytoplasmic facing outer ring, is the filamentous Nup subcomplex

and associated to the nucleoplasmic outer ring is the NPC basket. Nups have been implicated in many different cellular functions, one of which being the organization of chromatin at the nuclear periphery. The NPC basket has been shown to necessitate the organization of chromatin at the nuclear periphery by maintaining zones of heterochromatin exclusion (Krull et al., 2010). This suggests that active, euchromatic regions organize at the NPC. The preferentially association of active chromatin to the NPC supports a hypothesis known as the 'gene gating' hypothesis (Blobel, 1985). The gene gating hypothesis postulates that the three dimensional structure of the genome preferentially organizes actively transcribed genes to the NPC and a consequence of this genomic configuration would be to expedite the process of exporting nascent transcripts from the nucleus.

Research in *S. cerevisiae* has supported the 'gene gating' hypothesis by monitoring the change in localization for recently activated genes. Light et al., (2010) observed the localization of an inducible *INO1* promoter to the nuclear periphery and that this localization was dependent on the NPC basket. By labeling the sequence upstream of the *INO1* promoter with the *lacO*/LacI-GFP system, the localization of the locus could be monitored following either the induction of *INO1* by inositol starvation or repression through the subsequent addition of inositol following starvation. Removal of either Nups that comprised the NPC basket or proteins that were affiliated with the NPC basket failed to target either activated or recently repressed *INO1* to the nuclear periphery (Light et al., 2010). There is evidence that shows Nups are required for the functional organization of subtelomeric chromatin and the perinuclear positioning of telomeres. Specifically, mutations in Nups that comprise the outer ring complex were found to mislocalize the left

arm of telomere 11 (Tel 11L) from the nuclear periphery and to promote a loss of subtelomeric gene silencing (Therizols et al., 2006). Additionally, there is data that implicates the nuclear basket Nups in promoting subtelomeric silencing (Feuerbach et al., 2002; Galy et al., 2000), though there is evidence that contradict these claims (Hediger et al., 2002).

Nups have also been shown to localize at compartments outside of intact NPCs in order to regulate gene expression. In *Drosophila* cells, Nup98 and Sec13 were shown to colocalize with actively transcribed *RNAPII* regions on DAPI stained polytene chromosomes and to directly mediate expression of genes at regions enriched with either Nup. Additionally, both Nups showed immunofluorescence staining away from the NE, at interior chromatin labeled sites, supporting the notion that Nups can directly interact with chromatin at a compartment separate from NPCs and function to regulate gene expression (Capelson et al., 2010). In yeast, Chromatin immunoprecipitation (ChIP) of the core scaffold Nup, Nup170, coupled with DNA micro array analysis of Nup170-associated DNA revealed that Nup170 enriches at subtelomeric regions. Additionally, Nup170 was found to physically interact with both proteins of the RSC chromatin remodeling complex and Sir4. Mutants lacking Nup170 also showed a loss in the perinuclear localization of telomeres and a loss of subtelomeric gene silencing (Van de Vosse et al., 2013). Nup170 was also found to associate with Sir4 in a complex that is distinct from NPCs. By using a series of pulldowns with Sir4 tagged with Pr-A, Lapetina et al., (2017) showed that Sir4 only associates with a distinct set of nucleoporins, which they term the Snup complex. Support for the organization of this complex at subtelomeric chromatin comes from comparing a Sir4 chromatin immunoprecipitation sequencing

(ChIP-Seq) data set with the chromatin binding profile of Nup170 (Van de Vosse et al., 2013; Ellahi et al., 2015). There was significant overlap in the subtelomeric enrichment profile for both proteins indicating that the Snup complex organizes at subtelomeric chromatin, in a compartment separate from NPCs. Together, these data support the notion that Nups can function to maintain the organization of silenced chromatin and function to organize chromatin at the NE in compartments separate from the NPC.

Additional Snup complex components were the INM protein, Esc1, and the E3 SUMO ligase Siz2 (Lapetina et al., 2017). Siz2 has been implicated in facilitating the positioning of telomeres at the nuclear envelope presumably through its ability to SUMOylate proteins (Ferreira et al., 2011). In the following sections, the maturation, targeting, and the subsequent removal of SUMO (small ubiquitin-related modifier) will be further described and the components that necessitate this SUMO processing will be further elaborated on in order to rationalize studying SUMOylation as a means to facilitate the peripheral positioning of telomeres at the NE.

1.6 The post translational modification, SUMO

SUMOylation is the process of conjugating substrates with a SUMO protein modification to promote a biochemical or cellular response. SUMOylation was first discovered as a modification on nucleoporin associated RanGAP1 in the mid-1990s (Matunis et al., 1996; Mahajan et al., 1997). In higher eukaryotes, there are three different SUMO species. These species can be subdivided into two families, SUMO1 and SUMO2/3, the latter of which share 97% homology with one another. *S. cerevisiae* contain only 1 SUMO species encoded by *SMT3*.

SUMO substrate targeting occurs in a similar fashion to ubiquitylation. Both processes target internal lysine residues and the targeting of the modification to a substrate occurs via an E1 activating protein, an E2 conjugating protein, and an E3 ligase. In yeast, the E1-activating enzyme is a dimer that is composed of two subunits, Uba2 and Aos1 (also known as SAE1/2), and the E2 conjugating enzyme is Ubc9 (reviewed in Geiss-Friedlander & Melchior, 2007). The E3 ligases can be subdivided into the PAIS/SP-Ring family and the nucleoporin, RanBP2. The SP Ring family includes Siz1/2, Mms21, and Zip3 (Flotho & Melchior, 2013). Siz1/2 share 29% homology with one another and are closely related to the mammalian PIAS (Protein inhibitor of activated STAT) family of proteins (Suzuki et al., 2009; Takahashi et. al., 2003). Both ligases contain a SAP domain, which bind AT-rich DNA and a SP-Ring domain that contains its catalytic function. Each also contains a PINIT domain that can mediate their interaction with the target substrate along with SIMs (SUMO interacting motifs) that bind SUMO. These domains provide specificity and stability to the interaction of the E3 ligase with the target substrate to promote efficient modification (Johnson & Gupta, 2001; Song et al., 2004; Yunus & Lima, 2009).

1.6.1 SUMO processing and function

Initially, SUMO processing starts by maturating the immature SUMO modification by removing the C-terminal tripeptide (ATY) through the action of a SUMO isopeptidase, exposing a di-glycine motif within the protein. The E1-activating enzyme subsequently adenylates the exposed motif and forms a thioester bond at a catalytic cysteine residue within its Cys domain. The E2 enzyme is then recruited to the SUMO

intermediate via the C-terminal ubiquitin fold domain (UFD) of the E1 enzyme (Olsen et al., 2010). The modification is transferred to the E2 where, depending on the target substrate, it can be either directly applied to a target lysine residue within a SUMO consensus motif or, more commonly, targeted through the concerted action of an E3 ligase (Figure 1-4)(Bernier-Villamor et al., 2002). The SUMO consensus motif is a four residue site that is characterized by a large aliphatic residue (such as a leucine, isoleucine, or valine) next to a lysine residue, and ends in a glutamate residue. The E3 ligase functions to facilitate SUMOylation by locking the SUMO intermediate attached on the E2 into a favorable orientation with the target to allow for a nucleophilic attack onto the targeted lysine residue (Plechanovová et al., 2012). SUMOylation is reversible and is removed through a deSUMOylating enzyme, which also can function in SUMO maturation.

The consequences of SUMOylation within the cell have been shown to vary. Modifying substrates with SUMO has been shown to alter the interactions between proteins, affect protein stability, promote nuclear trafficking, allow for efficient DSB repair, and regulate many other cellular processes (Psakhye & Jentsch, 2012; Gostissa et al., 1999; Hannan et al., 2015; Churikov et al., 2016). Notably, SUMOylation plays a major role in recruiting components to DSB sites. Following the generation of single strand DNA (ssDNA) through DNA damage, Siz2 has been shown to be recruited to double strand breaks and SUMOylate RPA subunits that bind and shield ssDNA from exonuclease activity along with also SUMOylate components of the MRX complex, which promotes long-range resection (Chung et al., 2015; Psakhye & Jentsch, 2012). Interestingly, SUMOylation has also been implicated to mediate the perinuclear

positioning of telomeres. Siz2 has been shown to be essential for both G1-phase and S-phase telomere tethering at the NE. Not only did mutants lacking Siz2 show reduced telomere tethering at the NE, telomeres were longer when paired with either *RIF2* or *PIF1* (a DNA helicase) deletions. Additionally, in mutants lacking Siz2, S-phase mediated chromatin tethering at the NE by the yKu heterodimer has been shown to be rescued by the addition of SUMO, furthering suggesting that SUMO can mediate perinuclear chromatin tethering (Figure 1-3, Ferreira et al., 2011).

1.7 Ulp1- structure and function

Removal of the SUMO modification occurs through the deSUMOylating enzymes SENP1, 2, 3, 5, 6, and 7 in mammals and through Ulp1/2 in yeast (reviewed in Hickey et al., 2012). As a consequence of the cycling of SUMO, less than one percent of any given substrate is conjugated by SUMO at any time (reviewed in Geiss-Friedlander & Melchior, 2007). In yeast, Ulp1 (ubiquitin-like specific protease 1) is essential and is the sole protease required to maturate SUMO by cleaving the tripeptide located at the C-terminus of the SUMO protein modification. The Ulp1 protein consists of 3 domains; an N-terminal domain with karyopherin binding sites, a coiled-coiled domain, and a C-terminal catalytic cysteine domain. Knocking out *ULP1* is lethal due to a G2/M phase cell cycle arrest (Li & Hochstrasser, 1999). Because mutants that contain a deletion in *ULP1* are not viable, the initial step in characterizing the function of Ulp1 was done by generating a temperature sensitive allele (*ulp1-333*) by random PCR mutagenesis. The process of mutating Ulp1 resulted in generating a mutant ulp1 protein with nine different point mutations; three within the catalytic region, one within the CC domain, and 4

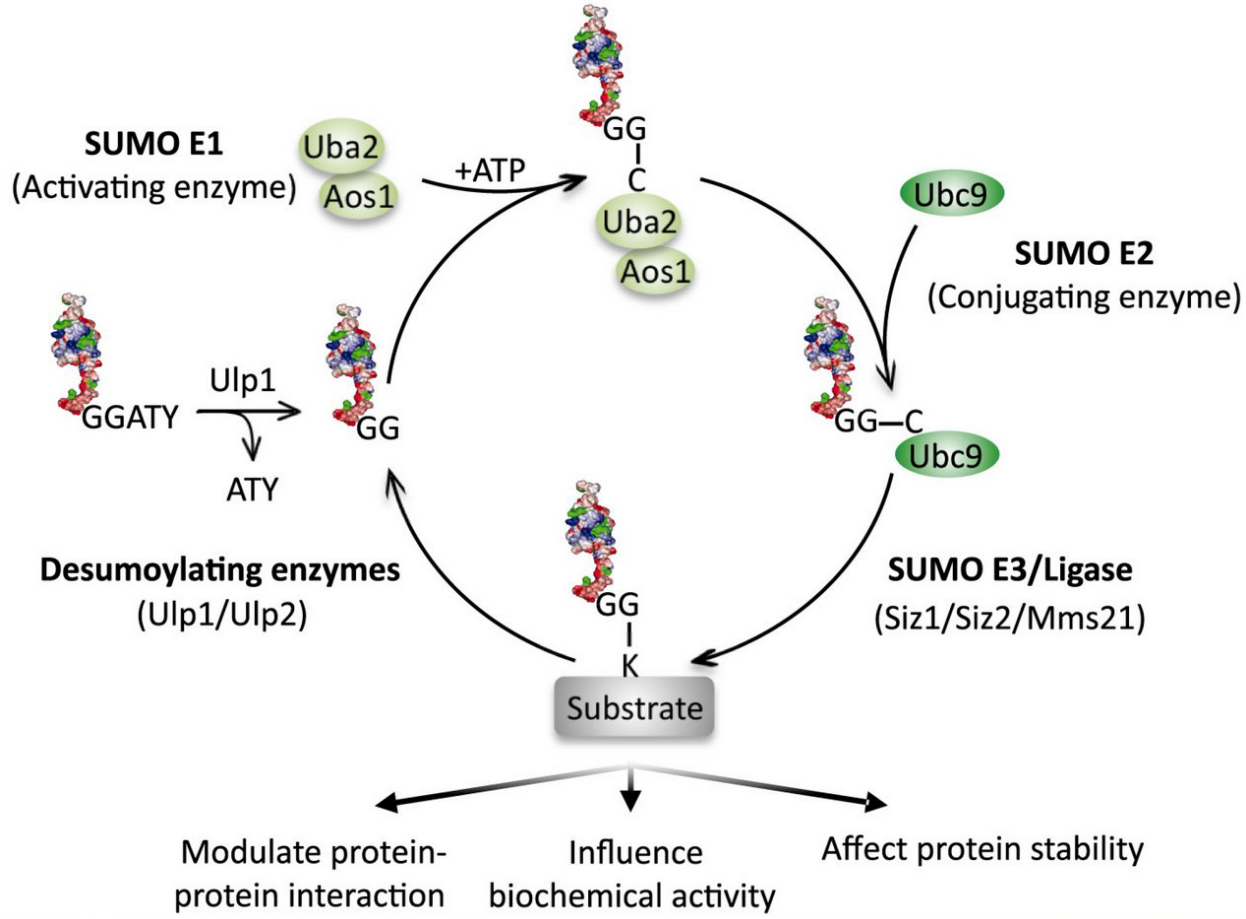

Figure 1-4. SUMO maturation and targeting in *S.cerevisiae*

SUMO is a small protein modification that promotes a biological change in function to target protein substrates. Initial maturation of SUMO occurs through the removal of the C-terminal tripeptide, exposing a di-glycine motif, through the isopeptidase, Ulp1. The mature SUMO is transferred to an E1 activating enzyme, Uba2/Aos1, forming an adenylated intermediate. Following this, the E1 enzyme transfers the modification to the E2 conjugating enzyme, Ubc9, and through the concerted action of an E3 ligase, a target modifiable lysine residue within a SUMO consensus motif is modified. The consequence of this modification varies and can promote a diverse range of different biological functions. Removal of the modification, in budding yeast, occurs through the deSUMOylating enzymes, Ulp1 and Ulp2. Adapted from Cremona et al., 2012.

within the NPC targeting domain (Li & Hochstrasser, 1999). At permissive temperatures, SUMO maturation is perturbed in mutants expressing the *ulp1-333* allele, with pre-SUMO shown to accumulate. In addition to this, SUMO conjugates were shown to accumulate in the *ulp1-333* mutant due to defects in the isopeptidase activity from mutating the catalytic domain of Ulp1. Upon shifting the *ulp1-333* mutant to restrictive temperatures, the SUMOylation pattern is markedly altered, with an overall reduction in the accumulation of SUMO conjugates (Li & Hochstrasser, 1999). Further experiments characterizing the function of Ulp1 did so by either mutating specific amino acid residues or by generating truncated mutant protein constructs that lacked specific regions of Ulp1. A point mutation within catalytic domain of Ulp1(C580S) was found to inhibit the ability of Ulp1 to cleave SUMO (Panse et al., 2003). Additionally, mutants that just expressed the catalytic domain of Ulp1 were not viable but viability could be restored by expressing a mutant protein construct containing the catalytic domain and the proximal residues that extend towards the N-terminus (Panse et al., 2003; Li & Hochstrasser, 2003).

Ulp1 is tethered to the nuclear basket of NPCs by the interaction between its N-terminus with the importins Kap95, Kap60, and Kap121 (Panse et al., 2003). Ulp1 can be mislocalized from the nuclear periphery by either truncating the N-terminal residues 1-337 *(ulp1NΔ338*) or through the removal of the NPC basket proteins (Nup60 or the Mlp proteins) (X. Zhao et al., 2004; Panse et al., 2003). Targeting Ulp1 to the NPC basket provides substrate specificity and this has been seen by observing effects resulting from a deletion in *ULP2* (Li & Hochstrasser, 2000; Panse et al., 2003). Deleting *ULP2* has been shown to accumulate different SUMO species than mutating Ulp1, suggesting that these two deSUMOylases target different substrates (Li & Hochstrasser, 2000). Also, Ulp2 has

been shown to localize within the nucleoplasm and not at the NE, where Ulp1 has been shown to localize (Panse et al., 2003). Together this suggests that by sequestering Ulp1 at the NPC basket, the substrates that it can recognize are different from the nucleoplasmic deSUMOylase, Ulp2. Mutants that lack Ulp2 also display a temperature sensitivity phenotype and this phenotype could be rescued by displacing Ulp1 from the NPC basket (Panse et al., 2003). This suggests that by displacing Ulp1 from the NPC basket, Ulp1 can substitute for functions normally performed by Ulp2.

The functional implications of targeting Ulp1 to the nuclear periphery have been examined in mutant constructs that alter the nuclear distribution of Ulp1. For example, the *ulp1NΔ338* mutant has been implicated in DNA damage repair. Rad52 foci were seen to accumulate within the *ulp1NΔ338* mutant, indicating an increase in double strand breaks (DSBs) (Therizols et al., 2006). By using a reporter system that utilizes a restriction enzyme to promote the formation of a DSB within the *ADE2* locus, the formation of colonies that can synthesis adenine (white) by HR versus accumulate red pigments from adenine auxotrophy (red) that is generated from non-homologous end joining(NHEJ) can be differentiated from one another. In the presence of this reporter construct, the *ulp1NΔ333* mutant showed a reduction of NHEJ mediated repair, indicating that the positioning of Ulp1 to the NPC is required to maintain a refractory environment for recombination at the nuclear periphery (Palancade et al., 2007; Therizols et al., 2006; Schober et al., 2009).

Ulp1 functions as a deSUMOylase and a loss in its localization can lead to alterations in SUMOylation that can have different consequences. Mislocalizing Ulp1 from the nuclear periphery has implicated a role for SUMOylation in mediating *GAL1*

transcription. Glucose acts by repressing galactose activated genes by the repressor Mig1 and corepressors, Ssn6 and Tup1 (Frolova et al., 1999; Treitel & Carlson, 1995). By shifting strains from glucose to galactose, the activation kinetics of *GAL1* can be monitored. The loss in Ulp1 localization to the NPC by replacing the N-terminal residues 172-340 with GFP showed an increase in inducible *GAL1* mRNA transcripts. This increase in *GAL1* mRNA transcripts could be observed when either Ssn6 or Tup1 were deSUMOylated, indicating that SUMOylation is required for normal *GAL1* derepression kinetics (Texari et al., 2013). Ulp1 is also involved in the deSUMOylation of Siz1 SUMOylated septin rings. Kap121 binding to Ulp1 and subsequent relocalization to NPCs was shown to be required for the SUMOylation of septin rings (Makhnevych et al., 2007).

1.7.1 The *ulp1K352E* mutant alters the SUMOylation of Scs2

While identifying the conjugates that accumulate from the different point mutations within the *ulp1-333* strain, a point mutant (K352E) in the coiled-coiled domain was found to specifically cause enhanced SUMOylation of 50 kDa and 70 kDa protein species. One of the proteins identified in this mutant was Scs2 (Felberbaum et al., 2012). Scs2 has been shown to contain a SUMOylation consensus site and is SUMOylated at lysine residue 180. Ulp1 was shown to specifically deSUMOylate Scs2 because mutants with SUMOylated Scs2 that expressed a deletion in *ULP2* did not affect the SUMOylation of Scs2 (Felberbaum et al., 2012).

Scs2 is a VAMP (Vesicle associated membrane protein) that localizes to both the endoplasmic reticulum (ER) and to the NE (Loewen & Levine, 2005). Scs2 is positioned

at both the ER and NE through its C-terminal transmembrane domain. By being localized at the ER, Scs2 has been shown to serve as a one of six associated membrane tethers that anchor cortical ER to the plasma membrane (Manford et al., 2012).

Scs2 also contains both a conserved VAP consensus domain and N-terminal MSP domain. Initially, Scs2 was found to counteract inositol auxotrophy (Nikawa et al., 1995) and has been seen to regulate phosphatidylinositol (PI) biosynthesis. When levels of intracellular inositol are low, Scs2 has been shown to upregulate PI biosynthesis through sequestration of the *INO1* suppressor, Opi1 (Loewen & Levine, 2005). Scs2 has been shown to bind Opi1 and other FFAT (two phenylalanines in an acidic tract) motifs through interactions with its MSP domain (Loewen & Levine, 2005). Interestingly, Scs2 has been implicated in mediating endocytic vesicular trafficking through interactions with Osh2 and 3 through MSP mediated FFAT binding(del Dedo et al., 2017).

1.8 Thesis Focus

The role of SUMOylation in mediating telomere tethering to the NE and the silencing of subtelomeric genes is ill-defined in the literature. Recent data have shown that cells lacking the E3 ligase Siz2 exhibit reduced telomere association with the NE. These observations have led us to further investigate the role of other regulators of cell SUMOylation. Specifically we have focused on Ulp1, as this isopeptidase plays a key role in both SUMO conjugation, through processing of the SUMO precursor, and deSUMOylation. Through the use of a temperature sensitive *ULP1* allele, alterations in SUMOylated conjugates can be observed. Additionally, specific SUMOylated conjugates (a prominent conjugate being Scs2) can be observed through the introduction of a point

mutation within the coiled-coiled domain of Ulp1. This thesis investigates the differing effects attributed to these two mutant *ulp1* alleles. Through the use of genetic and biochemical analysis, a role for Ulp1 in the NE localization of telomere and the silencing of subtelomeric genes was examined. Different mutations within Ulp1 showed mislocalization of telomeres away from the NE and a loss of subtelomeric silencing. Additionally, the interaction between proteins that promote telomere tethering was affected differently depending on the mutant *ulp1* allele examined. Furthermore, our results suggest that different mutations within Ulp1 alter the interaction between proteins of the SIR complex. Characterizing the different phenotypes that arise from mutating Ulp1 better define the complex mechanisms underpinning subtelomeric silencing and NE anchoring.

Chapter II: Experimental Procedures

2.1 Yeast strains and media

Yeast strains were grown at 30°C (unless otherwise indicated) in YPD (1% yeast extract, 2%bactopeptone, and 2% glucose) with constant agitation to mid-log phase (OD_{600} 0.5-1.0). Strains transformed with prototrophic yeast markers were selected for by growth in synthetic complete (SC) drop out media and 2% glucose lacking the necessary nutrient. Plates containing 5-FOA were made according to (Boeke et al., 1987). Yeast transformations by either autonomously replicating plasmid or PCR derived linear DNA were performed using the lithium acetate/polyethylene glycol method outlined by Giet & Woods, 2002. Briefly, overnight (5 ml) cultures were grown to early-logarithmic growth phase ($OD_{600} \leq 0.5$), harvested by centrifugation (Eppendorf 5810R, A-4-62 rotor at 6000 X g for 2 min), washed once with 1mL ddH_2O, and then washed with 300μL of transformation buffer (10mM Tris-HCl pH 7.5, 1mM EDTA, 100 mM LiOAc). Cells were resuspended with 50 μL of transformation buffer, 3μg/μL heat denatured salmon sperm, and 1-2 μg of the PCR-amplified transformation cassette of interest. Additionally, 300uL of PEG solution (0.8 g/mL polyethylene glycol 3350 dissolved in transformation buffer) was added, vortexed, and then incubated at 30°C for 45 min. Following incubation, cells were heat shocked at 42°C for 15 min in a hot water bath. Cells were then harvested by centrifugation (Beckman Coulter microfuge 18 centrifuge, 6000 X g) for 45 s and the resulting cell pellet was resuspended in YPD media and incubated 3 h prior to plating on the appropriate marker selection plates. The genomic manipulation of yeast strains, through the integration of tagging or deletion cassettes, was performed using the PCR-based, one-step method for gene modification (Longtine et al., 1998). DNA cassettes used for genomic integration were PCR-amplified using the Expand High

Fidelity PCR system (Roche Applied Science, Indianapolis, IN, USA). PCR templates were preferably isolated from genomic DNA, or less preferably, from DNA plasmids. For genomic integration from plasmid DNA for the carboxy terminal (C-terminal) protein A, $V5_3$, 13xMyc, eGFP, RFPT, mCherry, Ruby, and GFP tagging cassettes, ~60 bp oligonucleotide primers were designed with 40 bp 5′-overhangs that anneal to regions immediately upstream and downstream of the stop codon of the gene of interest. All positive colonies were primarily confirmed by PCR and, whenever possible, by Western Blotting or fluorescence microscopy. Due to potential genomic instability in regards to the *nup170Δ* strain, "fresh" haploids cultures were generated following tetrad dissection of diploid strains prior to use. Tetrads were genotyped by spreading on selective plates and analyzed by PCR. Positive transformants were grown overnight and frozen at -80°C for use in future experiments.

Table 2-1 Yeast Strains

All of the strains listed are not used in this dissertation.

Strain	Genotype	Reference
BY4741	*MATa his3Δ1 leu2Δ0 ura3Δ0 met15Δ0*	Brachmann et al., 1998
BY4742	*MATα his3Δ1 leu2Δ0 ura3Δ0 lys2Δ0*	Brachmann et al., 1998
CPY3606	*MATa his3Δ1 leu2Δ0 ura3Δ0 met15Δ0 ulp1-333-kanR*	This Study
CPY3608	*MATa his3Δ1 leu2Δ0 ura3Δ0 met15Δ0 ulp1-333::KAN smt3ΔATY-hphR*	This Study
CPY3854	*MATa his3Δ1 leu2Δ0 ura3Δ0 met15Δ0 ulp1-K352E-V5$_3$-kanR*	This Study
CPY3906	*MATa his3Δ1 leu2Δ0 ura3Δ0 met15Δ0 ulp1-K352E-hphR*	This Study
CPY4004	*MATa his3Δ1 leu2Δ0 ura3Δ0 met15Δ0 siz2Δ-natR*	This Study
CPY3888	*MATa his3Δ1 leu2Δ0 ura3Δ0 met15Δ0 scs2-K180R-kanR*	This Study

CPY3887	*MATa his3Δ1 leu2Δ0 ura3Δ0 met15Δ0 bar1Δ–natR scs2-K180R-kanR ulp1-K352E-V5$_3$-HIS*	This Study
DVY1534	*MATa leu2-3,112 ura3-1 trp1-1 ade2-1 can1-100 TELXIV-L::256xlacO-TRP1 his3::GFP-lacI-HIS3 SEC63-GFP-natR*	Van de Vosse et al., 2013
KRY1075	*MATa leu2-3,112 ura3-1 trp1-1 ade2-1 can1-100 TELXIV-L::256xlacO-TRP1 his3::GFP-lacI-HIS3 SEC63-GFP-natR ulp1K352E-kanR*	Derived from DVY1534
KRY1089	*MATa leu2-3,112 ura3-1 trp1-1 ade2-1 can1-100 TELXIV-L::256xlacO-TRP1 his3::GFP-lacI-HIS3 SEC63-GFP-natR ulp1K352EV5$_3$-kanR*	Derived from DVY1534
KRY1094	*MATa leu2-3,112 ura3-1 trp1-1 ade2-1 can1-100 TELXIV-L::256xlacO-TRP1 his3::GFP-lacI-HIS3 SEC63-GFP-natR ulp1K352EV5$_3$-kanR scs2K180R-hphR*	Derived from DVY1534
DVY1536	*MATa leu2-3,112 ura3-1 trp1-1 ade2-1 can1-100 TELXIV-L::256xlacO-TRP1 his3::GFP-lacI-HIS3 SEC63-GFP nup170Δ-kanR*	Derived from DVY1534
KRY1085	*MATa leu2-3,112 ura3-1 trp1-1 ade2-1 can1-100 TELXIV-L::256xlacO-TRP1 his3::GFP-lacI-HIS3 SEC63-GFP-natR ulp1-333-kanR*	Derived from DVY1534
KRY1092	*MATa leu2-3,112 ura3-1 trp1-1 ade2-1 can1-100 TELXIV-L::256xlacO-TRP1 his3::GFP-lacI-HIS3 SEC63-GFP-natR ulp1-333-kanR smt3ΔATY-hphR*	Derived from DVY1534
UCC3505	*MATa his3Δ200 leu2Δ1 ura3-52 lys2-801 trp1Δ63 ade2-101 ppr1::HIS3 adh4::URA3-TELVIIL ADE2-TEL-VR*	Gottschling et al., 1990
KRY1088	*MATa his3Δ200 leu2Δ1 ura3-52 lys2-801 trp1Δ63 ade2-101 ppr1::HIS3 adh4::URA3-TELVIIL ADE2-TEL-VR ulp1K352EV5$_3$-kanR*	Derived from UCC3505
KRY1077	*MATa his3Δ200 leu2Δ1 ura3-52 lys2-801 trp1Δ63 ade2-101 ppr1::HIS3 adh4::URA3-TELVIIL ADE2-TEL-VR ulp1-333-kanR*	Derived from UCC3505
KRY1093	*MATa his3Δ200 leu2Δ1 ura3-52 lys2-801 trp1Δ63 ade2-101 ppr1::HIS3 adh4::URA3-TELVIIL ADE2-TEL-VR ulp1-333-kanR smt3ΔATY-hphR*	Derived from UCC3505
KRY1073	*MATa his3Δ200 leu2Δ1 ura3-52 lys2-801 trp1Δ63 ade2-101 ppr1::HIS3 adh4::URA3-TELVIIL ADE2-TEL-VR siz2Δ-kanR*	Derived from UCC3505
KRY1083	*MATa his3Δ200 leu2Δ1 ura3-52 lys2-801 trp1Δ63 ade2-101 ppr1::HIS3 adh4::URA3-*	Derived from UCC3505

	TELVIIL ADE2-TEL-VR sir3Δ::kanR	
KRY1100	*MATa his3Δ1 leu2Δ0 ura3Δ0 met15Δ0 Sir4-GFP:HIS sur4-mCherry-natR*	This Study
KRY1091	*MATa his3Δ1 leu2Δ0 ura3Δ0 met15Δ0 Sir4-GFP:HIS sur4-mCherry-natR ulp1-333-kanR*	This Study
KRY1096	*MATa his3Δ1 leu2Δ0 ura3Δ0 met15Δ0 Sir4-GFP:HIS sur4-mCherry-natR ulp1-333-kanR smt3ΔATY-hphR*	This Study
KRY1090	*MATa his3Δ1 leu2Δ0 ura3Δ0 met15Δ0 Sir4-GFP:HIS sur4-mCherry-natR ulp1K352E-kanR*	This Study
KRY1101	*MATa his3Δ1 leu2Δ0 ura3Δ0 met15Δ0 Sir4-GFP:HIS sur4-mCherry-natR ulp1K352E-kanR-V5$_3$*	This Study
NS2144	*MATa his3Δ1 leu2Δ0 ura3Δ0 met15Δ0 Sir4-GFP:HIS sur4-mCherry-natR sizΔ-kanR*	This Study
NS2390	*MATa his3Δ1 leu2Δ0 ura3Δ0 met15Δ0 Sir4-GFP:HIS sur4-mCherry-natR nup170Δ-hphR*	This Study
KRY1098	*MATa his3Δ1 leu2Δ0 ura3Δ0 met15Δ0 Sir3-GFP-HIS sur4-mCherry-natR*	This Study
KRY1099	*MATa his3Δ1 leu2Δ0 ura3Δ0 met15Δ0 Sir3-GFP-HIS sur4-mCherry-natR ulp1K352E-V5$_3$-kanR*	This Study
NS2228	*MATa his3Δ1 leu2Δ0 ura3Δ0 met15Δ0 Sir3-GFP-HIS sur4-mCherry-natR ulp1K352E-V5$_3$-kanR sizΔ-kanR*	This Study
NS2318	*MATa his3Δ1 leu2Δ0 ura3Δ0 met15Δ0 Sir3-GFP-HIS sur4-mCherry-natR ulp1K352E-V5$_3$-kanR nup170Δ-kanR*	This Study
KRY1102	*MATa his3Δ1 leu2Δ0 ura3Δ0 met15Δ0 Esc1-eGFP-HIS Nop56-mCherry:natR*	This Study
KRY1103	*MATa his3Δ1 leu2Δ0 ura3Δ0 met15Δ0 Esc1-eGFP-HIS Nop56-mCherry:natR ulp1K352E-V53-kanR*	This Study
NS2400	*MATa his3Δ1 leu2Δ0 ura3Δ0 met15Δ0 Esc1eGFP-HIS Nop56-mCherry:natR nup170Δ-kanR*	This Study
KRY1139	*MATa his3Δ1 leu2Δ0 ura3Δ0 met15Δ0 Sir4-PrA-HIS Nup170x13MYC-natR*	This Study
KRY1129	*MATa his3Δ1 leu2Δ0 ura3Δ0 met15Δ0 Sir4-PrA-HIS Nup170x13MYC -hphR Sir3-V5$_3$siz2Δ-natR*	This Study
KRY1121	*MATa his3Δ1 leu2Δ0 ura3Δ0 met15Δ0 Sir4-PrA-HIS Nup170x13MYC-hphR Sir3-V5$_3$-*	This Study

	kanR ulp1K352E-V53-natR	
KRY1128	*MATa his3Δ1 leu2Δ0 ura3Δ0 met15Δ0 Sir4-PrA-HIS Sir3-V5$_3$-kanR nup170Δ-natR*	This Study
KRY1115	*MATa his3Δ1 leu2Δ0 ura3Δ0 met15Δ0 Sir4-PrA-HIS Nup170x13MYC -hphR Sir3-V5$_3$-kanR*	This Study
KRY1138	*MATa his3Δ1 leu2Δ0 ura3Δ0 met15Δ0 Sir4-PrA-HIS Nup170x13MYC-natR ulp1-333-kanR*	This Study
KRY1140	*MATa his3Δ1 leu2Δ0 ura3Δ0 met15Δ0 Sir4-PrA-HIS Nup170x13MYC-natR ulp1-333-kanR smt3_ΔATY-hphR*	This Study
CPY3748	*MATa his3Δ1 leu2Δ0 ura3Δ0 met15Δ0 Esc1-PrA-URA Nup170-x13MYC-natR*	This Study
NS2324	*MATa his3Δ1 leu2Δ0 ura3Δ0 met15Δ0 Esc1-PrA-URA Nup170-x13MYC-natR scs2D-kanR*	This Study
KRY1135	*MATa his3Δ1 leu2Δ0 ura3Δ0 met15Δ0 Esc1-PrA-URA Nup170-x13MYC-natR ulp1-333-kanR smt3 ΔATY-hphR*	Derived from CPY3749
KRY1136	*MATa his3Δ1 leu2Δ0 ura3Δ0 met15Δ0 Esc1-PrA-URA Nup170-x13MYC-natR ulp1-333-kanR*	Derived from CPY3750
KRY1130	*MATa his3Δ1 leu2Δ0 ura3Δ0 met15Δ0 Sir4-PrA-HIS Nup170x13MYC -hphR Sir3-V5$_3$scs2Δ-natR*	This Study
KRY1144	*MATa his3Δ1 leu2Δ0 ura3Δ0 met15Δ0 Sir4-PrA-HIS Sir3-V5$_3$-natR ulp1-333-kanR*	This Study
KRY1145	*MATa his3Δ1 leu2Δ0 ura3Δ0 met15Δ0 Sir4-PrA-HIS -hphR Sir3-natR ulp1-333-kanR smt3 ΔATY-hphR*	This Study
KRY1146	*MATa his3Δ1 leu2Δ0 ura3Δ0 met15Δ0 Sir4-GFP-HIS Sir3-Ruby-hphR*	This Study
KRY1147	*MATa his3Δ1 leu2Δ0 ura3Δ0 met15Δ0 Sir4-GFP-HIS Sir3-Ruby-hphR scs2Δ–kanR*	This Study
KRY1148	*MATa his3Δ1 leu2Δ0 ura3Δ0 met15Δ0 Sir4-GFP-HIS Sir3-Ruby-hphR siz2Δ-kanR*	This Study
DVY2338	*MATa his3Δ1 leu2Δ0 ura3Δ0 met15Δ0 Rap1-PrA-HIS Sir4x13MYC-hphR bar1Δ-natR*	Van de Voss et al., 2013
KRY1118	*MATa his3Δ1 leu2Δ0 ura3Δ0 met15Δ0 Rap1-PrA-HIS Sir4x13MYC-hphR siz2Δ kanR bar1D-natR*	This Study
KRY1125	*MATa his3Δ1 leu2Δ0 ura3Δ0 met15Δ0 Rap1-PrA-HIS Sir4x13MYC-hphR siz2S522A-V5$_3$-kanR bar1Δ-natR*	This Study

KRY1127	*MATa his3Δ1 leu2Δ0 ura3Δ0 met15Δ0 Rap1-PrA-HIS Sir4x13MYC-hphR siz2S527A-V5$_3$-kanR bar1Δ-natR*	This Study
KRY1124	*MATa his3Δ1 leu2Δ0 ura3Δ0 met15Δ0 Rap1-PrA-HIS Sir4x13MYC-hphR ulp1K352E-V5$_3$-kanR bar1Δ-natR*	This Study
KRY1119	*MATa his3Δ1 leu2Δ0 ura3Δ0 met15Δ0 Rap1-PrA-HIS Sir4x13MYC-hphR scs2D kanR bar1D-natR*	This Study
KRY1126	*MATa his3Δ1 leu2Δ0 ura3Δ0 met15Δ0 Rap1-PrA-HIS Sir4x13MYC-hphR nup170Δ kanR bar1Δ-natR*	This Study
KRY1022	*MATa his3Δ1 leu2Δ0 ura3Δ0 met15Δ0 Nup170-RFPT-natR Nic96-eGFP-HIS*	This Study
KRY1023	*MATa his3Δ1 leu2Δ0 ura3Δ0 met15Δ0 Nup170-RFPT-natR Nup49-eGFP-HIS*	This Study
KRY1081	*MATa his3Δ1 leu2Δ0 ura3Δ0 met15Δ0Nup170-RFPT-HIS Ulp1-eGFP-hphR*	This Study

2.2 Plasmids

The following plasmids were used in this dissertation: pRS313, CEN/HIS3 (Sikorski and Hieter, 1989) and pRS315, CEN/LEU2 (Sikorski and Hieter, 1989). The following plasmids were gifted by Dr. Susan Gasser, Friedrich Miescher Institute, Basel Switzerland: The plasmid pSR13 was used to tag telomeres with ~256xLacO::LEU2 and the plasimid pAFS78 that carried GFP-LacI::His3 was used to target tagged telomeres containing the 256xLacO array (Rohner et al., 2008). Genomic integration for C-terminal gene fusions were carried out by amplifying PCR cassettes from plasmids pGFP/HIS5 (EGFPF64L, S65T-HIS5), pmCherry/NAT (mCherry-NAT), pmRuby (mRuby/KanR) (Lee et al., 2013), and PRFP-T/HIS5 (RFP-T::HIS5) (Lee et al., 2013). Each of these plasmids was kindly gifted by Dr. Richard Rachubinski, University of Alberta, AB, Canada. Additionally, the pBXA plasmid (protein-A/HIS5) (Aitchison et al., 1995) and

pFA6a-13xMyc-kanMX6 plasmid (13xMYC-KanR) (Longtine et al., 1998) were used for C-terminal gene fusions. The following plasmid was generated for this work in which the inserts were PCR-amplified from genomic DNA using the Expand High Fidelity PCR system (Roche Applied Science, Indianapolis, IN, USA). The plasmid pTM1198 was made by modifying the plasmid pFA6-GFP(S65T)-kanMX6. The coding sequence for GFP(S65T), flanked by the Pac1 and Asc1 restriction enzyme sites, was replaced by the coding sequence for $V5_3$, by using the corresponding restriction enzyme sites.

Table 2- 2 Plasmids

Plasmid	Background	Source/Reference
pSR13	~256xLacO::LEU2	(Rohner et al., 2008)(Provided by Dr. Susan Gasser, Friedrich Miescher Institute, Switzerland)
pAFS78	GFP-LacI::HIS3	(Rohner et al., 2008) (Provided by Dr. Susan Gasser, Friedrich Miescher Institute, Switzerland)
pGFP	eGFP-S65T,F64L-HIS5	(Lee et al., 2013) (Provided by Dr.Richard Rachubinski, University of Alberta, Edmonton, AB)
pTagRFP-T	TagRFP-S158T-HIS5	(Lee et al., 2013) (Provided by Dr. Richard Rachubinski, University of Alberta, Edmonton, AB)
pBXA	Protein A-His5	(Aitchison et al., 1995)
p13xMYC	pFA6a-13xMyc-kanMX6	(Longtine et al., 1998)
pTM1198	pFA6a-3xV5-kanMX6	(Lapetina et al., 2017)
pmCherry	pFA6a-mCherry/NatR	(Lee et al., 2013) (Provided by Dr.Richard Rachubinski, University of Alberta, Edmonton, AB)
pmRuby	pFA6a-yomRuby/HphR	(Lee et al., 2013) (Provided by Dr.Richard Rachubinski, University of Alberta, Edmonton, AB)

2.3 Antibodies and Buffers

Table 2- 3 Antibodies

Antibody	Dilution	Type	Source/Reference
α-PrA	1:10000	Rabbit polyclonal	Sigma (Cat No: P3775)
α-Myc (9E10)	1:5000	Mouse monoclonal	Roche (Cat No: 11667149001)
α-V5 (ab27671)	1:5000	Mouse monoclonal	Abcam (Cat No: ab27671)
α-Scs2	1:5000	Rabbit polyclonal	(Kaiser et al., 2005)(Provided by Dr. Jason H. Brickner, Stanford University, California)
α-Smt3	1:5000	Rabbit polyclonal	Our Lab
α-Gsp1p	1:10000	Rabbit polyclonal	Our Lab
α-mouse IgG, HRP-conjugated (NXA931) goat	1:10000	Secondary HRP conjugated	GE Healthcare
Anti-rabbit IgG, HRP-conjugated (NA934) goat	1:10000	Secondary HRP conjugated	GE Healthcare

Table 2-4 Buffers

Buffer	Composition
Pre-lysis IP wash buffer	20 mM HEPES-KOH, pH 7.4, 110 mM KOAc, 2 mM MgCl2
IP wash buffer	20 mM HEPES-KOH, pH 7.4, 110 mM KOAc, 2 mM MgCl2, 0.1% Tween-20, 1:5000 dilution antifoam B
IP buffer	20 mM HEPES-KOH, pH 7.4, 110 mM KOAc, 2mM MgCl2, Tween-20, antifoam-B emulsion (1:5000), protease inhibitor pellets (complete EDTA-free)
PBS	137 mM NaCl, 2.7 mM KCl, 4.3 mM Na2HPO4, 1.4 mM KH2PO4, pH 7.4
PBS-T	137 mM NaCl, 2.7 mM KCl, 4.3 mM Na2HPO4, 1.4 mM KH2PO4, pH 7.4, 1% Tween-20
SDS-PAGE sample buffer	0.5 M Tris-base, 100 mM DTT, 15% glycerol, 6.5% SDS, 0.25% bromophenol blue
TE	10 mM Tris-HCl, 10 mM EDTA, pH7.5
Transformation	10 mM Tris-HCl, pH 7.5, 1 mM EDTA, 100 mM LiOAc

buffer	
Milk blocking buffer	5% skim milk powder, 0.1% Tween-20, 20mM Tris-HCl pH 7.5, 150 mM NaCl
Amido black	40% methanol, 10% acetic acid, 0.1% amido black
TES	10 mM Tris-HCl, 10 mM EDTA, pH7.5, 2% SDS

2.4 Growth and plating assays

In order to measure the doubling times of yeast cultures, strains were initially grown overnight at room temperature with consistent agitation and diluted the next morning to an OD_{600} of 0.05. OD_{600} readings were taken every 90 minutes over the course of 7.5 hours. Two independent cultures of each strain were examined. Tested cultures were grown in YPD media and doubling times were calculated following the protocol outlined by Richards (1928). Plating assays testing for growth were done with yeast cultures grown overnight and diluted down to mid log phase growth (~0.5-1.0 OD_{600}). Cultures were serially spotted onto YPD plates and grown at room temperature, 30°C, and 37°C for two days prior to imaging.

2.5 Subtelomeric gene silencing assay

Yeast strains used to assess subtelomeric gene silencing were derivatives of the UCC3505 strain in which the reporter genes *URA3* and *ADE2* are integrated adjacent to Tel 7L and Tel 5L, respectfully (Singer et al., 1994). *URA3* and an adjacent 81 bp sequence of telomeric repeats (TG_{1-3}) was inserted into chromosome VII at *ADH4*, which resulted in a ~15 kb truncation of the left arm of chromosome VII, removing native subtelomeric elements. As a consequence of this truncation, the 81 bp spacer sequence was extended to ~300 bp by telomerase, generating a new telomere (*adh4:URA3-TEL*)

where the *URA3* promoter is located ~1.3 kb from Tel 7L with transcription directed towards the telomere (Gottschling et al., 1990; Singer et al., 1994). Also, the *ADE2* gene and an adjacent 81 bp sequence of telomeric repeats (TG_{1-3}) is integrated directly into the Y′ element of Tel 5R creating a new telomere, *ADE-TEL*, with minimal truncation of the right arm of chromosome V (Singer et al., 1994). Cell cultures of this strain were grown overnight in YPD media and diluted down to mid log phase growth (~0.5-1.0 OD_{600}). Cultures were then serially spotted onto either YPD, synthetic complete (SC) –ura, or SC + 1mg/ml 5FOA plates and incubated at either room temperature or 30°C for 2 days prior to imaging.

2.6 Quantitative PCR

2.6.1 Yeast RNA isolation

RNA was isolated for qPCR analysis through the use of RNase free solutions from yeast cultures grown to mid log phase growth (~0.5-1.0 OD_{600}) and flash frozen with liquid nitrogen. Initially, RNA was isolated from frozen yeast samples by a series of exposures to 1mL water saturated phenol with vigorous shaking and then the cleared (Beckman Coulter; JLA 10.5, 5000 x g for 5 min at 23°C) supernatant was transferred to a l mL solution of 24:1 chloroform to isoamyl alcohol to remove excess phenol. After vigorous shaking and clearance by centrifugation (Beckman Coulter; JLA 10.5, 5000 x g for 5 min at 23°C), the resulting supernatant was subjected to 95% RNase-free ethanol (with 18mM NaOAc) solution for 2 h at -20°C in order to precipitate the RNA. Following RNA precipitation, RNA was pelleted from centrifugation (Beckman Coulter; JLA 10.5, 5000 x g for 5 min at 23°C), washed in 1 mL of 70% ethanol, re-pelleted by

centrifugation (Beckman Coulter; JLA 10.5, 5000 x g for 5 min at 23°), and left to dry for 1 h. The dried pellet was resuspended in 50μL of DEPC H_2O and 2μg of RNA (determined by spectrophotometry) was used for cDNA production.

2.6.2 cDNA production and qPCR

Sample RNA was first incubated with a DNase buffered solution (Invitorgen, Carlsbad, CA, USA) for 15min with a subsequent 1μL addition of EDTA and a 5 minute incubation at 65°C to quench the DNase. cDNA was amplified from sample RNA after the following steps: 2μL addition of primer mix (1:1 ratio of dNTPs to random primers, Invitorgen, Carlsbad, CA, USA), a 5 min incubation at 65°C followed by the addition of a 7 μL master mixture (4μL 5xFS Buffer, 2μL DTT, 1μL RNase out), and a final addition of 1μL Reverse Transcriptase II (Invitorgen, Carlsbad, CA, USA). A master mix of cDNA and the SYBR Green SuperMix (Low ROX, Quantabio, Beverly, MA, USA) was pipetted onto a 96 well PCR Microplate (Axygen Scientific, Union City, CA, USA) and cDNA was amplified by the Stratagene Mx30005P qPCR system with primers designed to generate PCR products 110-120 bp in length. 20ng of cDNA was amplified with the oligonucleotides listed in Table 2-5. Oligonucleotides for PCR-amplification to target cDNAs were designed to anneal within the 5′-end of the coding regions. The resulting C_t values of target genes for mutants of interest were normalized to internal loading controls (*ACT1* and *TUB2*) (ΔC_t) and finally normalized to WT ΔC_t values to determine change in fold expression ($\Delta\Delta C_t$).

Table 2- 5 Oligonucleotides used in qPCR

Target cDNA	Oligonucleotide Sequence
ACT1	Forward: ATCTGCCGGTATTGACCAAA
	Reverse: GGTACCACCGGACATAACGA
TUB2	Forward: GGTGTGACAACTTCATTGCG
	Reverse: CGTACCGACCATGAAGAAA
ARR3	Forward: CTGCAAAGTTTCCTGGGAGT
	Reverse: CAAAGGACCGATGACCCAAT
COS12	Forward: GGATCGACAAATTCAGGTTCAAATC
	Reverse: ACCAATTAGTTGCATCAGACTTCTC
GEX2	Forward: CGACCCGTCTCACCATGTAT
	Reverse: CATTTCAAGGAGGAGAAATCTGAG
YEL073C	Forward: GCATGGTCTAATACAGTTCCGTTAG
	Reverse: AAGGGTTTCATTCATCCAGATTACG
YER188	Forward: CACGCTATGGAAGAACCCTC
	Reverse: TCGTAAAAACCCTCACCTGC

2.7 Affinity purification with conjugated IgG Dynabeads

2.7.1 Affinity purification of protein A fusion proteins

Sir4, Esc1, and Rap1 were C-terminally tagged with the *Staphylococcus aureus protein* A (PrA) and affinity purified from yeast whole cell lysates as previously described (Alber et al., 2007a) with slight modification. Yeast cells expressing the respective protein tagged constructs of Sir4-PrA or Esc1-PrA were grown in 1L cultures

of YPD media to an OD_{600} of 0.8-1.0 and then harvested by centrifugation (Beckman Coulter; JLA 10.5, 5000 x g for 3 min at 23°C). Cells were pelleted and the resulting cell pellet was transferred to a syringe. Cells were then flash frozen by passage into liquid nitrogen in order to generate frozen yeast "noodles". Frozen cells were subsequently lysed using a planetary ball mill (PM100; Retsch, Haan, Germany) for 8 cycles with intermittent cooling by liquid N_2. For the first 4 cycles, the noodles were lysed at 450 rpm while for the latter 4 cycles; the speed was increase to 500 rpm. This resulted in 1-1.2 grams of lysed powder. One gram of lysed cell powder was then briefly warmed on ice prior to resuspension in 2mL of cold IP buffer containing protease inhibitor pellets (Roche Applied Science, Indianapolis, IN, USA). IgG conjugated Dynabeads were then washed while cell powder resuspended in IP buffer was simultaneously vortexed for 1 min in five 5 min intervals. The resulting lysed mixture was cleared by centrifugation (Eppendorf 5810R, A-4-62 rotor) at 1500 x g for 10 mins at 4°C. The supernatant of this mixture was exposed to washed, conjugated Dynabeads and both were incubated for 1hr at 4°C with constant agitation. After binding, the beads were separated from the input solution by a magnet and washed ten times with 1mL of IP buffer. Bound proteins were then eluted with an increasing concentration gradient of $MgCl_2$, followed by a wash of acetic acid. During the elution step, proteins bound to the beads were sequentially exposed to 500µL of different eluting solutions being 50mM $MgCl_2$, 0.5M $MgCl_2$, and 2M $MgCl_2$, followed by an elution of acetic acid for 3min with constant agitation. A final wash with SDS sample buffer was done to elute any remaining bound protein. Eluates were then subjected to overnight TCA precipitation at 4°C. The next day, samples were lyophilized in a CentriVap Centrifugal Vacuum (Labconco).

2.7.2 IgG-conjugated magnetic beads

Conjugation of IgG to magnetic beads was performed as previously described (Alber et al., 2007a). In brief, 8 mg IgG (Sigma-Aldrich, St. Louis, MO, USA) was dissolved in 800μL sodium-phosphate buffer (0.1 M $NaPO_4$ pH7.4) and then cleared by centrifugation (Eppendorf 5810R, F45-30-11 rotor at 20800 x g for 10 min at 4°C). To the cleared IgG, 2mL sodium-phosphate buffer was added followed by 1.33mL of 3 M ammonium sulfate pH 7.5. This IgG solution was used to resuspend 60mg of pre-washed Epoxy M-270 Dynabeads (Invitorgen, Carlsbad, CA, USA). Prior to the addition of IgG, the magnetic beads were equilibrated with 3.6mL sodium-phosphate buffer with rotation for 10min at room temperature and then washed once with 1mL sodium-phosphate buffer. Conjugation of IgG to the magnetic beads was facilitated by incubating the slurry at 30°C for 18-24 h with constant rotation. Following incubation, IgG-conjugated beads were washed extensively with rotation with the following solutions: once with 1mL 100mM glycine pH 2.5, once with 1mL 10mM Tris pH8.8, once with 1 mL 100 mM trimethylamine, pH 6.0, four times with 1mL PBS for 5min, once with 1mL PBS + 0.5% trition X-100 for 5min, once with 1mL PBS +0.5% triton X-100 for 15 min, followed by three consecutive washes with 1mL PBS for 5 min. Washed beads were then resuspended in 2mL PBS + 0.02% sodium azide and stored at 4°C.

2.8 Western blotting

2.8.1 Sample preparation

Cultures of interest were grown overnight and diluted down to mid log phase growth (~0.5-0.7 OD_{600}) prior to protein extraction. $1.9x10^7$ ml^{-1} cells from each culture

were centrifuged (Beckman Coulter microfuge 18 centrifuge, 6000 X g) for 1 min. Pelleted cells were washed and resuspended with 100μL of SDS PAGE sample buffer. Samples were then sonicated and boiled at 95°C for 3min and stored afterwards at -20°C for later use.

2.8.2 SDS-PAGE and Western blot analysis

Protein samples were resolved by SDS-PAGE containing 6-12% acrylamide in BioRad Mini Protean III units (BioRad, Hercules, CA, USA) and then transferred to nitrocellulose membranes using a GE Healthcare TE 22 Mini Tank Transfer Unit (GE Healthcare, Chalfront St. Giles, united Kingdom; 110 V for 1.2 h at 4°C). The protein transfer efficiency was assessed by amido-black staining and any excess stain was removed with a series of ddH_2O washes with constant shaking. Following transfer, nitrocellulose membranes were blocked with 5% skim milk powder resuspended in PBS-T (PBS containing 0.1% Tween-20) for 1h at 23°C. Primary antibodies listed in Table 2-3 were used to detect proteins of interest by probing the membrane overnight at 4°C in 5% skim milk powder resuspended in PBS-T. Membranes were then washed three times with varying volumes of PBS-T for 5min each. Bound primary antibodies were detected by either using goat anti-mouse or goat anti-rabbit HRP-conjugated secondary antibodies (see Table 2-2) and ECL (GE Healthcare, Chalfront St. Giles, United Kingdom). Exposure times were at set intervals of 1/60s, 30s, 1min, 3min, and 10min.

2.8.3 Protein quantification

Mutant samples with copurifying proteins from PrA-tagged pulldowns were compared to unmodified samples through the ImageQuant software (GE). A threshold for total pixel intensities (TPI) was determined by a rolling ball function that subtracted low background pixel intensities. TPI from PrA tagged stains following affinity purification was determined for a fraction of the total input protein and for the 50mM $MgCl_2$ elution, 0.5M $MgCl_2$ elution, 2M $MgCl_2$ elution, acetic acid elution, and the SDS PAGE sample buffer elution of the copurifying proteins of interest. Total TPI for each elution were summed and set as a fraction to input (TPIIP/TPIInput). This ratio was normalized to a similar ratio of total TPI over the TPI of input for the bait protein (TPIIPPrA/TPIPrAInput). The resulting fraction (TPIIP/TPIInput) / (TPIIPPrA/TPIPrAInput) from mutants of interest is then scaled to WT, where WT is set to 1 and fold change in protein concentration is determined based on the degree of variation in protein concentration each mutant has from 1.

2.9 Fluorescence Microscopy

All images were acquired using the Deltavision Olympus IX-71 base epi fluorescence microscope equipped with a PLAPON WD 150 micron DIC 60X oil emersion objective and an Coolsnap HQ2 high resolution CCD camera. All cells used for live cell imaging were grown in YPD liquid culture and suspended in a small volume of SC media to ~10^6 cells/μL. Prior to imaging, 1.8 μL of cell suspension was spotted onto a microscope slide. Images were deconvolved with the accompanying Deltavision

software, softWoRx, and rendered using the Image J software (National Institute of Health) for display.

2.10 Image Analysis

2.10.1 Subnuclear localization of telomere 14L

Yeast cells containing the ~256xLacO array of repeats inserted into ~19kb from Tel 14L and the interacting protein, LacI, fused to GFP were grown in YPD media supplemented with adenine (40μg/mL) and visualized with the Deltavision Olympus IX-71 base epi fluorescence microscope. Before imaging, cells were washed once with ddH_2O and resuspended in SC media. Telomere (Tel 14L) localization within the nucleus was determined based on proximity to Sec63 C-terminally fused with GFP. Images were acquired as 15 consecutive 200 nm stacks in the Z-axis. Only the middle stack containing the brightest foci was counted. The subnuclear positioning of the telomere was determined by dividing the telomere distance from the NE (TD) by the nuclear radius (r). The TD/r ratio (R) was used to group telomeres into three concentric zones of equal volume. Zone 1 represents foci with ratios $\leq$ 0.184 x R, zone 2 foci with rations > 0.184 x R and < 0.422 x R, and zone 3 represents foci with ratios $\geq$ 0.422 x R.

2.10.2 The subnuclear localization of Sir proteins: Sir4-eGFP and Sir3-eGFP localization in regards to the NE

Mutants expressing the *SIR4* gene with the C-terminal eGFP fusion construct were imaged in the presence of additional mutations being *nup170Δ, siz2Δ, scs2Δ, ulp1ts, ulp1ts smt3-ΔATY, ulp1K352E-V53,* and *scs2K180R*. Also, strains expressing the *SIR3*

gene with the C-terminal eGFP fusion construct were imaged in the presence of additional mutations being *siz2Δ, ulp1K352E-V53₃,* and *nup170Δ.* The nuclear envelope (NE) was visualized by expressing the mutant Sur4-mCherry construct. Sir4-GFP or Sir3-GFP localization in regards to the NE was defined as the degree of overlap (as colocalizing) with the NE marker Sur4-mCherry. Cells expressing either Sir4-GFP or Sir3-GFP with coexpressed Sur4-mCherry were imaged as 15 consecutive 200 nm stacks in the Z-axis. Images were deconvolved using the iterative 15 cycle conservative ratio in the softWoRx program and rendered using Image J (National Institute of Health). Distinct Sir4-GFP or Sir3-GFP foci were counted, and grouped as either complete or partial signal overlap was observed between either Sir4-GFP or Sir3-GFP with Sur4-mCherry. Percent colocalization was then expressed as the number of colocalizing Sir4-GFP or Sir3-GFP foci divided by the total number of Sir4-GFP or Sir3-GFP foci. These values were then plotted on a bar graph and error bars show 1 Standard Deviation.

2.10.3 Esc1-eGFP exclusion from the nucleolar region

Esc1 localization around the NE was assessed by C-terminally fusing the *ESC1* gene with eGFP and Nop56-mCherry was coexpressed to denote the nucleolus. The reference strain containing the Esc1-eGFP and Nop56-mCherry protein fusion constructs were transformed with PCR cassettes containing either the *nup170Δ* or *ulp1K352E-V53₃* mutant constructs. Images of a reference strain and the mutant constructs were taken as 15 consecutive 200 nm stacks in the Z-axis. Images were deconvolved using the iterative 15 cycle conservative ratio in the softWoRx program and rendered using Image J (National Institute of Health). Only those cells in which the Esc1-eGFP and Nop56-

mCherry signals were clearly visible in the middle focal stacks were counted. Those cells in which the Esc1-eGFP signal were excluded from regions of the NE abutting the nucleolus and those cells that showed a clear localization at the NE adjacent to the nucleolus were counted. The percentage of the total cells showing exclusion was plotted.

2.10.4 Double-tagged colocalization quantification using MatLab

Images of cells expressing either the C-terminally tagged eGFP/RFPT gene fusion constructs or GFP/mRuby gene fusion constructs were acquired as 15 consecutive 200 nm stacks in the Z-axis. Mutant strains expressing both Sir4-GFP and Sir3-mRuby and either the *siz2Δ or scs2Δ* mutant alleles were imaged and compared to a reference strain expressing Sir4-GFP and Sir3-mRuby. Additionally, mutant strains expressing Nup170-RFPT and either Ulp1eGFP, Nup49-eGFP, or Nic96-eGFP were imaged and the degree of overlap between fluorescently labeled loci was determined. Images were deconvolved using the iterative 15 cycle conservative ratio in the softWoRx program and rendered using a custom macro (Capitanio, 2016) in Image J(National Institute of Health) to separate specific fluorescent channels prior to importing processed images into MATLAB 2015a (MathWorks). In order to determine colocalizing foci, the following procedure is based on the pipeline outlined by Wu and Rifkin (2015). Masks to exclude background signal for each separate fluorescence channel were generated through Image J (National Institute of Health) and applied to each image through the ARO software. The ARO software then applies a 3D Gaussian distribution fit to local intensity maximum (spots) that are defined by a random forest classifier and projects a GUI (graphical user interphase) for spot training by the user. The parameters set by the GUI are True and

False, allowing the user to supervise the spot detection for additional rounds of spot detection. After multiple rounds of training the random forest classifier by the user, (total trained spots ~1000), colocalized spots are identified as overlapping if they are within ~300 nm or 5 pixels apart from one another. The percent of colocalization for spots in either fluorescence channel was determined to be total overlapped foci over the total identified foci. All colocalization experiments were done using three biological replicates and the averages of those replicates were graphed.

Chapter III: A role for the deSUMOylase Ulp1 in subtelomeric chromatin localization and gene silencing

3.1 Overview

By removing the SUMO E3 ligase Siz2, SUMOylation has been implicated to play a role in the peripheral positioning of telomeres (Ferreira et al., 2011). Impaired SUMOylation has also been shown to alter the targeting of transcription factors, suggesting that SUMOylation could impact gene expression (Bertolotto et al., 2011; Lee et al., 2011). The silencing of subtelomeric genes and telomere tethering to the NE are thought to be closely related to one another due to the positioning of silenced chromatin at the nuclear periphery, so changes in SUMOylation could affect both processes (Bourgeois et al., 1985; Koehler et al., 2009; Tanabe et al., 2002). Due to the dynamic nature of SUMOylation, prolonged SUMOylation could show distinct effects on telomere positioning and gene expression. By inhibiting the removal of SUMO through mutating the isopeptidase, Ulp1, an increase in SUMO conjugates can be observed. This was first characterized by the generation of a temperature sensitive *ulp1* allele, *ulp1-333* (Li & Hochstrasser, 1999). Not only did the *ulp1-333* (*ulp1ts*) mutant accumulate SUMO conjugates, but the *ulp1ts* mutant also had additional defects in SUMO maturation and growth (Li & Hochstrasser, 1999). During the process of characterizing the different point mutations within the encoded protein of the *ulp1ts* mutant*,* a specific point mutation within the coiled-coiled (CC) domain of Ulp1 (*ulp1K352E*) showed an increase in the level of Scs2 SUMOylation (Felberbaum et al., 2012). The consequence of this SUMOylation has yet to be characterized

The data in Chapter III show phenotypic consequences resulting from mutating Ulp1. Distinct phenotypes were seen in the ulp1 mutants in regards to growth, silencing, and telomere positioning. Alterations in NE morphology could also be seen in mutants

expressing the *ulp1K352E* allele. Additionally, proteins that promote telomere tethering were seen to mislocalize away from the NE in the different ulp1 mutants. Together, these results highlight how Ulp1 can function to promote the positioning of telomeres at the NE and alter the silencing state of subtelomeric genes.

3.2 Results

3.2.1 The specific effects that different *ulp1*mutant alleles have on growth

Various studies of Ulp1 function have utilized a temperature sensitive *ulp1* allele (the *ulp1-333,* subsequently referred to as *ulp1ts*) (Li & Hochstrasser, 1999). The *ulp1ts* mutant contains multiple single nucleotide changes that alter 9 amino acid residues in the encoded protein, including changes in the Ulp1 catalytic domain that are predicted to alter its isopeptidase function. Consistent with this, cells that produce this mutant ulp1 protein contain altered levels of SUMO conjugates (Li & Hochstrasser, 1999). Moreover, the *ulp1ts* mutant cells contain decreased levels of mature SUMO due to its reduced ability to remove the C-terminal ATY residues of pre-SUMO and produce the mature form of SUMO used in conjugation. We have examined the contribution of the SUMO maturation defect on the growth phenotype of the *ulp1ts* mutant by introducing a gene encoding mature SUMO into this mutant. Consistent with previous studies (Li & Hochstrasser, 1999), we observed that in both liquid cultures and on culture plates, *ulp1ts* cells grew at 23°C but their growth was arrested at 37°C (Figure 3-1). In *ulp1ts* cells supplemented with mature SUMO (*ulp1ts smt3-ATYΔ*) growth at all temperatures was improved, suggesting that the growth inhibition of *ulp1ts* cells was in part due to a defect in SUMO maturation. We also examined the growth characteristics of a Ulp1 point

Figure 3-1. Determining the effects that different mutant *ulp1* alleles have on growth.

A-C) Overnight cultures of the indicated strains were diluted to 0.05 $O.D._{600}$/ml of YPD media and cultures were then incubated at the indicated temperatures. At 90 minute intervals, the culture OD was determined and plotted versus time. Growth curves for each strain at the indicated temperatures were done in duplicate and plotted is the average of the two replicates. D) Overnight cultures of the indicated strains were serially diluted 10-fold and each was spotted onto YPD plates. Plates were then grown at the temperatures shown for 2 days and images of the plates were captured.

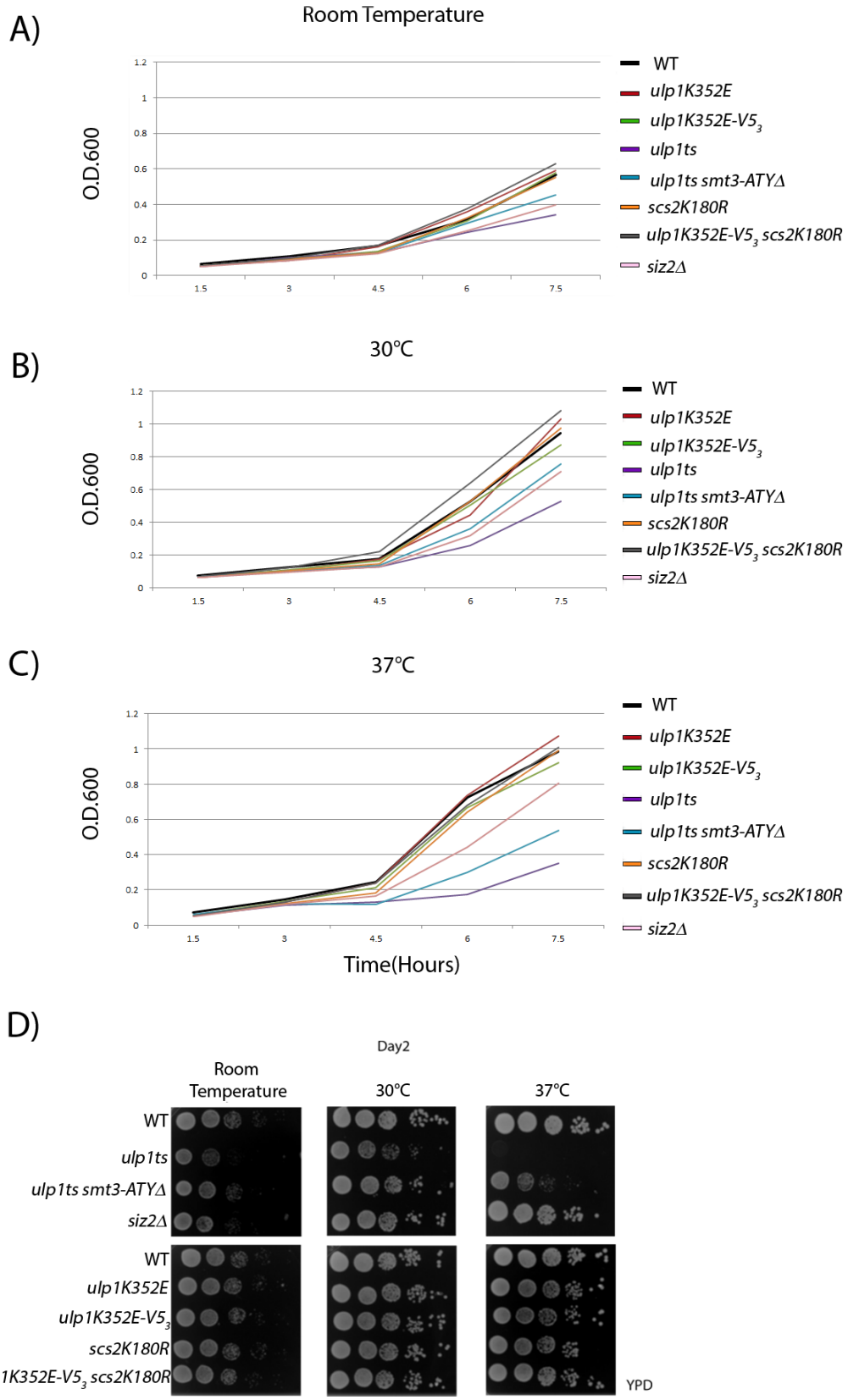

Figure 3-1. Determining the effects that different mutant *ulp1* alleles have on growth.

mutant (*ulp1K352E*) that was previously identified by characterizing the effects various point mutations residing within the mutant *ulp1ts* protein had on its function to process and maturate SUMO. A distinct phenotype of this mutant was the increased SUMOylation of a single protein identified as Scs2 (Felberbaumet al., 2012, also see Figure 3-2). The *ulp1K352E* mutant showed no obvious growth defect at any of the tested temperatures. Additionally, tagging the *ulp1K352E* with $V5_3$ (*ulp1K352E-V5*$_3$), which further increases levels of the SUMOylated ~55 kDa species (see Figure 3-2 B), also showed no obvious growth defects (see Figure 3-1). The growth of three other strains used in this study were also examined: a Scs2 point mutant that blocks its SUMOylation (*scs2K180R*; Felberbaum et al., 2012), a Scs2, Ulp1 double mutant (*scs2K180R*, *ulp1K352E*), and a *SIZ2* null mutation (siz2Δ). Of these three mutant strains, only the *siz2*Δ mutant show a visible growth defect. This mutant appeared to grow slower than WT, most noticeability at room temperature (Figure 3-1 A-D, Table 3-1).

3.2.2 Alterations in Ulp1 function increase levels of SUMO conjugates.

To further assess the functional consequence of the various *ulp1* mutants, we examined the effects of the various *ulp1* mutants on cellular levels of SUMO conjugates. As discussed above, the isopeptidase function of the ulp1 mutant protein is compromised in the *ulp1ts* mutant and previous observations suggested that this mutant contains increased cellular levels of SUMO conjugates (Li & Hochstrasser, 1999). However, the loss of Ulp1 is also predicted to restrict free mature SUMO available for conjugation, thus potentially inhibiting SUMOylation. Cellular levels of SUMO conjugates were examined using western blot analysis and anti-SUMO antibodies (Figure 3-2 A&B). The

Table 3-1. Doubling time in hours.

		Temperatures	
Strains	Room Temperature	30°C	37°C
WT	1.92 ±0.04	1.63 ±0.02	1.56 ±0.04
ulp1K352E	1.73 ±0.04	1.45 ±0.05	1.38 ±0.02
ulp1K352E-V5$_3$	1.83 ±0.05	1.61 ± 0.01	1.49 ±0.05
ulp1ts	2.23 ±0.1	2.01 ±0.01	2.15 ±0.06
ulp1ts smt3-ΔATY	1.95 ±0.06	1.71 ±0.01	1.93 ±0.02
scs2K180R	1.84 ±0.03	1.53 ±0.01	1.42 ±0.13
ulp1K352E-V5$_3$ scs2K180R	1.71 ±0.05	1.52 ± 0.01	1.39 ±0.02
siz2Δ	2.06 ±0.09	1.71 ±0.01	1.49 ±0.11

ulp1ts mutant showed a slight increase in SUMO conjugates at room temperature relative to WT cells consistent with previous observations (Li & Hochstrasser, 1999). Both mature SUMO and the SUMO precursor were detected at room temperature in mutant cells expressing the *ulp1ts* allele suggesting that at this temperature, the *ulp1ts* protein was still capable of processing the SUMO precursor. By contrast, at 30°C, the *ulp1ts* mutant cells contained low levels of mature SUMO and increased levels of the SUMO precursor. Consistent with these low levels of mature SUMO, the *ulp1ts* mutant cells showed decreased levels of SUMO conjugates relative to WT cells. These observations suggested that low levels of mature SUMO in the *ulp1ts* mutant cells may limit the levels of SUMO conjugates in these cells. To test this, the *SMT3* allele that encodes cellular SUMO was replaced in the *ulp1ts* mutant with an allele that encodes a mature SUMO peptide that lacks the C-terminal tripeptide (*ulp1ts smt3-ATYΔ*). At both room temperature and 30°C, the increased levels of mature SUMO in the *ulp1ts smt3-ATYΔ* strain (Figure 3-2 A) produced an increase in the accumulation of SUMO conjugates. These results suggest that phenotypes observed in the *ulp1ts smt3-ATYΔ* are unlikely to arise from low levels of mature SUMO.

The SUMOylation profile of the *ulp1K352E* point mutant was also examined. In this mutant, it was previously observed that SUMOylation of Scs2 is increased (Felberbaum et al., 2012). Similarly, we observed an increase in levels of a SUMOylated protein of a mass (~55 kDa) predicted for SUMO-modified Scs2 in the *ulp1K352E* point mutant, albeit weakly (Figure 3-2 B). The levels of ~55 kDa species was further increased in the *ulp1K352E-V5*$_3$ mutant strain. In addition, we observed increased levels of a ~43 kDa SUMOylated protein, the identity of which remains undefined

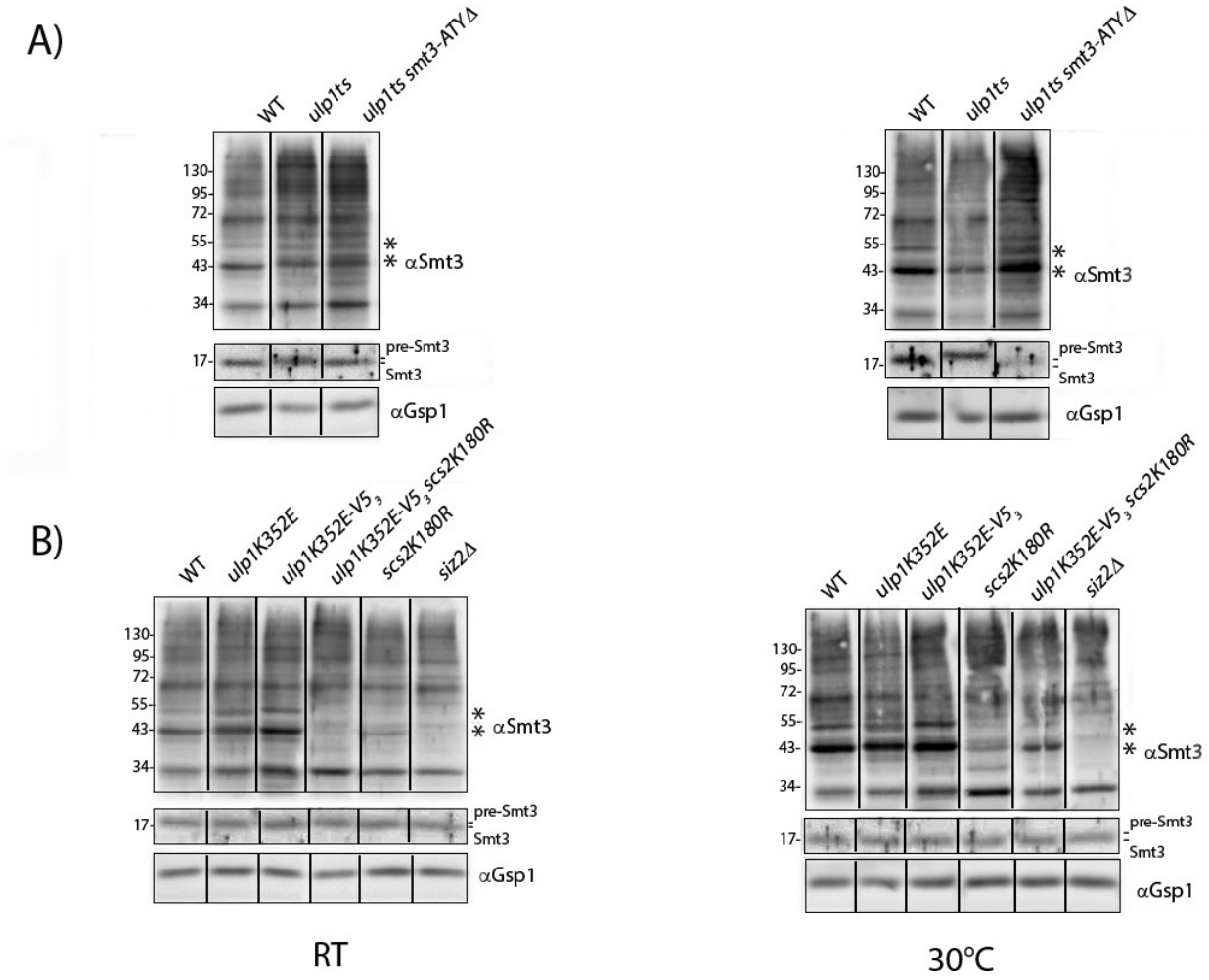

Figure 3-2. Alterations in Ulp1 function increase levels of SUMO conjugates.

A&B) The indicated mutants were grown asynchronously to an O.D.$_{600}$ of ~ 1 at either room temperature (RT) or 30°C. Whole cell lysates were isolated and polypeptides were separated by SDS-PAGE. Protein species were analyzed by western blotting and SUMOylated conjugates were probed with antibodies directed against SUMO (anti-Smt3). Species at ~17 kDa represent the processed and unprocessed forms of SUMO. Asterisks indicate species with increased levels of SUMOylation. The solid line between each lane represents cuts made to align the SUMOylation profile of each mutant for the ease of comparison. Western blot images shown for mutants grown at RT or 30°C were imaged at the same exposure and were blotted from the same gel for each respective temperature. The position of mass markers is shown in kDa. Gsp1 was used as a loading control.

(Figure 3-2 B). Previous reports suggested that mutating a SUMOylation site at lysine residue 180 (*K180R)* blocks Scs2 SUMOylation. Consistent with these data, we observed an *scs2K180R* mutant strain that lacks the 55 kDa SUMOylated species (Figure 3-2 B, Felberbaum et al., 2012). In addition, levels of the 43 kDa species were clearly reduced. Of note, the 55 kDa and 43 kDa species, were also absent from strains lacking Siz2 (Figure 3-2 B) (*siz2*Δ).

3.2.3 Telomere tethering is disrupted in *ulp1* mutants

Previous studies (Ferreira et al., 2011) have shown that deletion of the gene encoding the E3 ligase Siz2 disrupts telomere tethering to the NE, suggesting SUMOylation contributes to the localization of chromatin at the nuclear periphery. Considering these results and the altered levels of SUMO conjugates observed in the *ulp1* mutant strains, we examined the perinuclear positioning of telomeres in various *ulp1* mutant strains, including the *ulp1ts* and *ulp1ts smt3-ATYΔ* at 25°C and the *ulp1K352E* and *ulp1K352E-V5*$_3$ at 30°C. To assess telomere positioning at the NE, the localization of telomere 14L (Tel 14L) was examined by inserting an array of *lacO* repeats within the subtelomeric region on the left arm of this chromosome. The *lacO* tagged Tel 14L was then visualized by producing LacI-GFP in these cells, which binds the *lacO* repeats and appears as a single focus. In order to distinguish between peripherally or nucleoplasmically localized foci, the nucleus is subdivided into three concentric zones of equal volume and foci were counted as localizing at or adjacent to the nuclear periphery (zone 1) or within more interior regions of the nucleoplasm (zones 2-3) (Figure 3-3 A).

Figure 3-3. Telomere tethering at the nuclear periphery is disrupted in the different *ulp1* mutants.

A) Telomere positioning was analyzed by fluorescently labeling an array of subtelomerically integrated *lacO* on the left arm of telomere 14 (Tel 14L) with coexpressed LacI-GFP. The subnuclear positioning of the labeled focus within a single focal plane was determined in regards to the NE demarked by Sec63-GFP. Schematic to the left of the representative images indicate the method used to score the localization of the foci at or away from the nuclear periphery in a single focal plane by dividing the volume of the nuclear section into 3 concentric zones. B) Quantification of Tel 14L at the nuclear periphery in both G1-phase (no budded) and early S-phase cells (small budded). Bars show the average percentage of foci with zone1 localization from 150 cells. Indicated strains were grown overnight and diluted to an $O.D._{600}$ of ~ 1 at 30°C. C) Quantification of Tel 14L localization at the periphery for the *ulp1ts* strains during both G1-phase and early S phase. Strains were grown overnight at RT and diluted to an $O.D._{600}$ of ~1 the following day at 25°C prior to imaging. Bars show the average percentage of foci with zone1 localization from 150 cells. Error bars represent 1 standard deviation for 3 biological replicates (n=3). Asterisks denote a p-value of $\leq$0.01. Significance was determined by a 2 way homoscedastic t- Test.

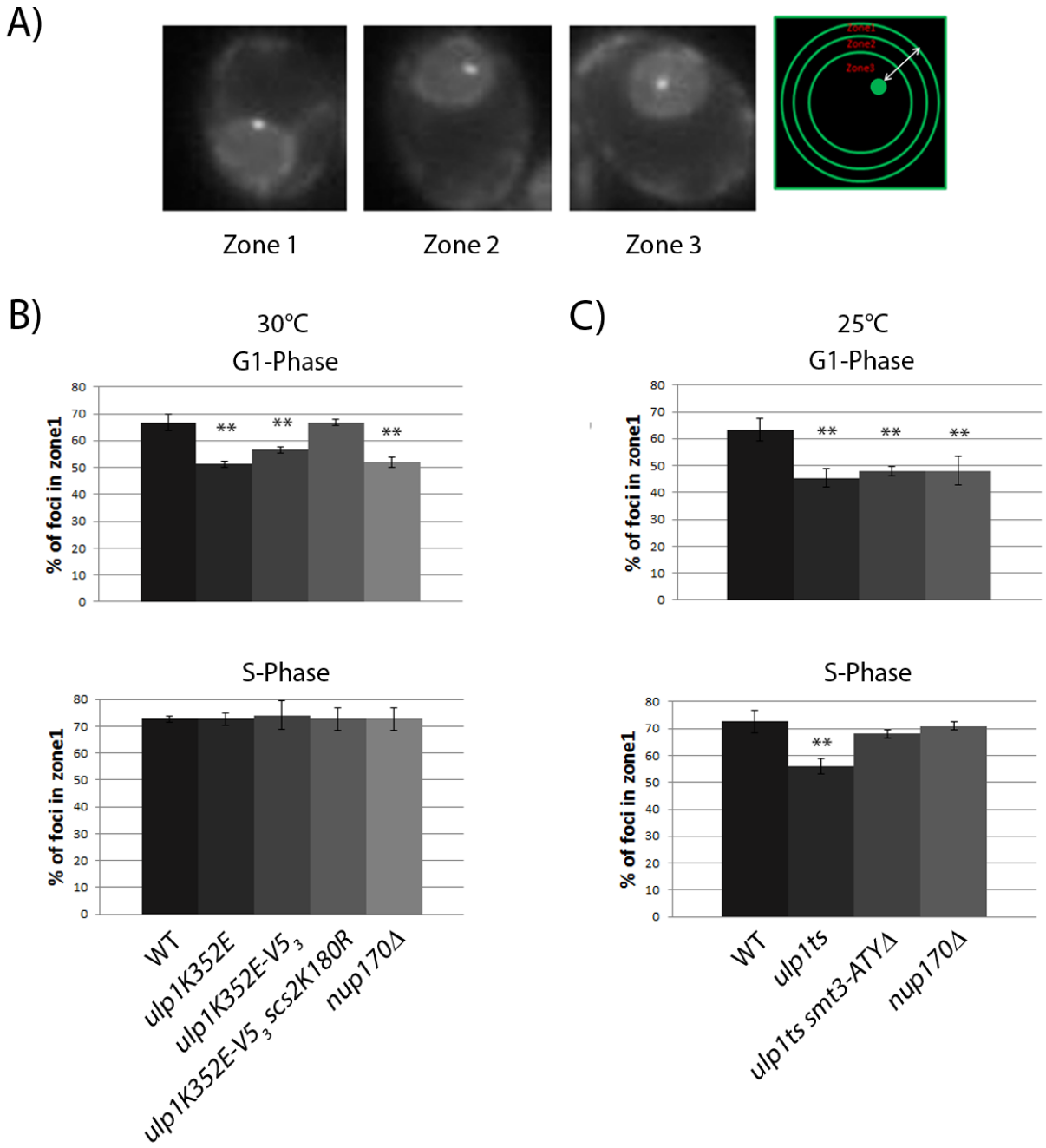

Figure 3-3. Telomere tethering at the nuclear periphery is disrupted in the different *ulp1* mutants.

It is well known that telomeres detach from the periphery during late S-phase, so the telomeres of cells identified as either in G1-phase (no bud) or early S-phase (small budded) were counted (Hediger et al., 2002; Ebrahimi & Donaldson, 2008). When compared to WT cells, the *ulp1ts* mutant cells showed reduced perinuclear positioning of Tel 14L in both G1-phase and early S-phase cells. Notably, the early S-phase defect in the positioning of telomeres at the NE in the *ulp1ts* mutant cells could be rescued by expression of mature SUMO (*ulp1ts smt3-ATY*Δ). These results would suggest that Tel 14L association with the NE requires free mature SUMO, and thus likely involves SUMOylation events that support telomere anchoring at the NE during early S-phase (Figure 3-3 C). A similar analysis was performed on the *ulp1K352E* and *ulp1K352E-V5*$_3$ mutant cells. In these mutants we observed that Tel 14L association with the NE was only altered in G1-phase, while early S-phase cells appeared similar to their WT counterparts. This phenotype mimics what was observed in a *nup170Δ* mutant, where the loss of Nup170 was shown to disrupt the positioning of subtelomeric chromatin at the nuclear periphery specifically during G1-phase of the cell cycle (Van de Vosse et al., 2013). These results suggest that both the *ulp1K352E* and *ulp1K352E-V5*$_3$ mutants affect the same G1-phase perinuclear telomere tethering mechanism that is altered in the *nup170Δ* mutant (Figure 3-3 B). Surprisingly, introduction of the *scs2K180R* allele in to the *ulp1K352E-V5*$_3$ mutant strain (*ulp1K352E-V53 scs2K180R*) rescued the G1-phase perinuclear telomere tethering defect (Figure 3 B). This suggests that inhibiting Scs2 SUMOylation in cells expressing the *ulp1K352E-V5*$_3$ mutant allele is sufficient to rescue the observed telomere tethering defect attributed to SUMOylated Scs2.

3.2.4 The *ulp1ts* mutant disrupts subtelomeric silencing regardless of SUMO processing

The expression of genes positioned within subtelomeric chromatin is often repressed. Various factors contribute to establishing this repressed state including the chromatin-binding proteins, such as the Sir proteins (Brachmann et al., 1995; Andrulis et al., 2002), and the association of subtelomeric chromatin with the NE (Zullo et al., 2012; Hediger et al., 2002; Ebrahimi & Donaldson, 2008). Considering that the *ulp1* mutants alter the NE association of telomeres, we examined the effects of these mutants on subtelomeric gene silencing using a reporter gene silencing assay. For these experiments, a *URA3* gene was inserted within the subtelomeric region on the left arm of telomere 7 (Tel 7L) (Gottschling et al., 1990). This subtelomeric *URA3* gene is silenced in the majority of a WT cell population and as a consequence, these cells fail to grow in medium lacking uracil. Alternatively, they grow in medium containing 5FOA, a compound that is metabolized to a toxic product in the presence of the *URA3* gene product (Gottschling et al., 1990). When silencing is reduced and *URA3* is expressed, cells grow in the absence of uracil and die in the presence of 5FOA (Gottschling et al., 1990). Previous research has shown that the loss of proteins of the SIR complex, including Sir3 and Sir4, disrupts the silencing state of subtelomeric chromatin and as shown in Figure 3-4, a *sir3*Δ mutant exhibits phenotypes consistent with a loss of silencing including growth in the absence of uracil and sensitivity to 5FOA (also see Brachmann et al., 1995; Van de Vosse et al., 2013). Interestingly, cells containing the *ulp1ts* or *ulp1ts smt3-ATY*Δ allele showed a loss of silencing (Figure 3-4). By contrast, neither the *ulp1K352E* nor the s*iz2Δ* mutants showed a loss of silencing even though both

showed mislocalization of Tel 14L from the nuclear periphery. These results suggests that Ulp1 plays a role in subtelomeric gene silencing and that its function as a deSUMOylase is required for the silencing state of genes localized within subtelomeric regions.

3.2.5 Ulp1 is required for silencing of endogenous subtelomeric genes

To further assess the role of Ulp1 in subtelomeric gene silencing, qRT-PCR was performed on WT and mutant cells to examine mRNA levels encoded by several subtelomeric genes located on different chromosomal arms. As a *nup170*Δ mutant was previously shown to exhibit a loss of subtelomeric gene silencing, this strain was used as a control to detect a loss of silencing (Van de Vosse et al., 2013). The levels of mRNAs encoded by five subtelomeric genes previously shown to be derepressed in the *nup170*Δ mutant, *ARR3*, *COS12*, *GEX2*, *YEL073c*, and *YER188w* were examined. As shown in Figure 3-5, in the *nup170*Δ mutant, mRNA levels of these genes were increased two-fold or greater as compared to WT cells. When this analysis was extended to the *ulp1* mutants, we observed that the *ulp1ts* mutant grown at 25^{o}C contained increased mRNA levels derived from *GEX2* and *COS12*, which are located on the right arm of chromosome 11 and the left arm of chromosome 7, respectively (Figure 3-5). However, no significant change was observed in the *ARR3*, *YEL073c*, and *YER188w* gene products. Similarly, no changes in the levels of any of the examined gene products were detected in the *ulp1K352E*, *ulp1K352E-V5*$_3$, *siz2Δ*, or *scs2K180R* mutants. Together, these results suggest that Ulp1 promotes the silencing of subtelomeric genes.

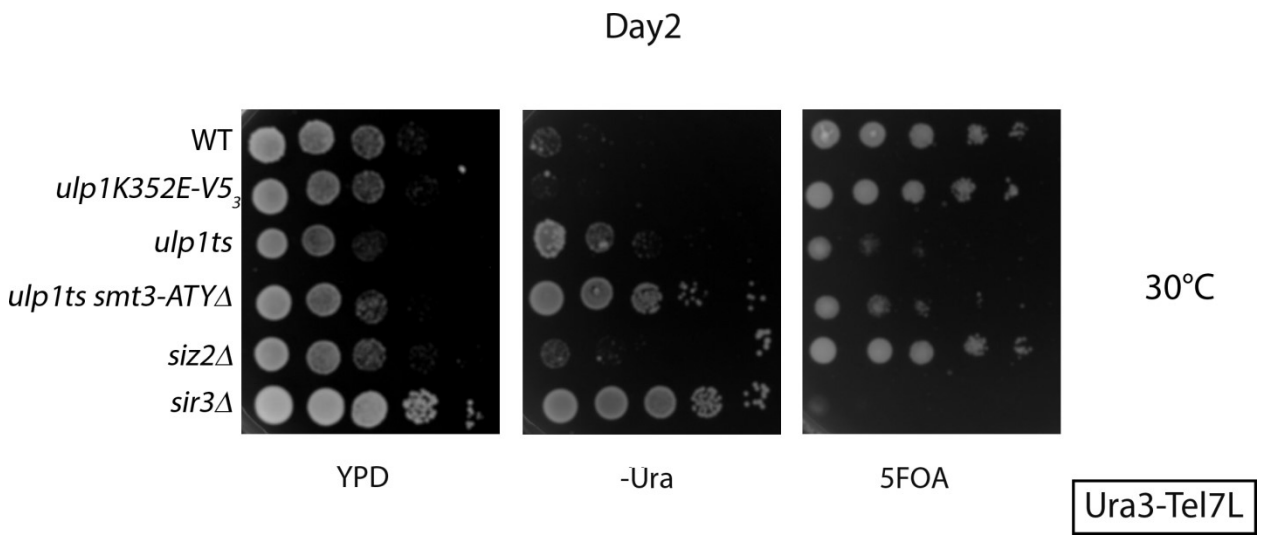

Figure 3-4. The *ulp1ts* mutant disrupts subtelomeric silencing regardless of SUMO processing.

Shown is a subtelomeric silencing assay using strains with *URA3* inserted within the left arm of telomere 7. Indicated strains were serially diluted 10-fold and plated on non-selective YPD medium or on selective medium (lacking either uracil or containing 5FOA) in order to determine *URA3* gene expression. The indicated mutants were imaged following 2 days of growth at 30°C.

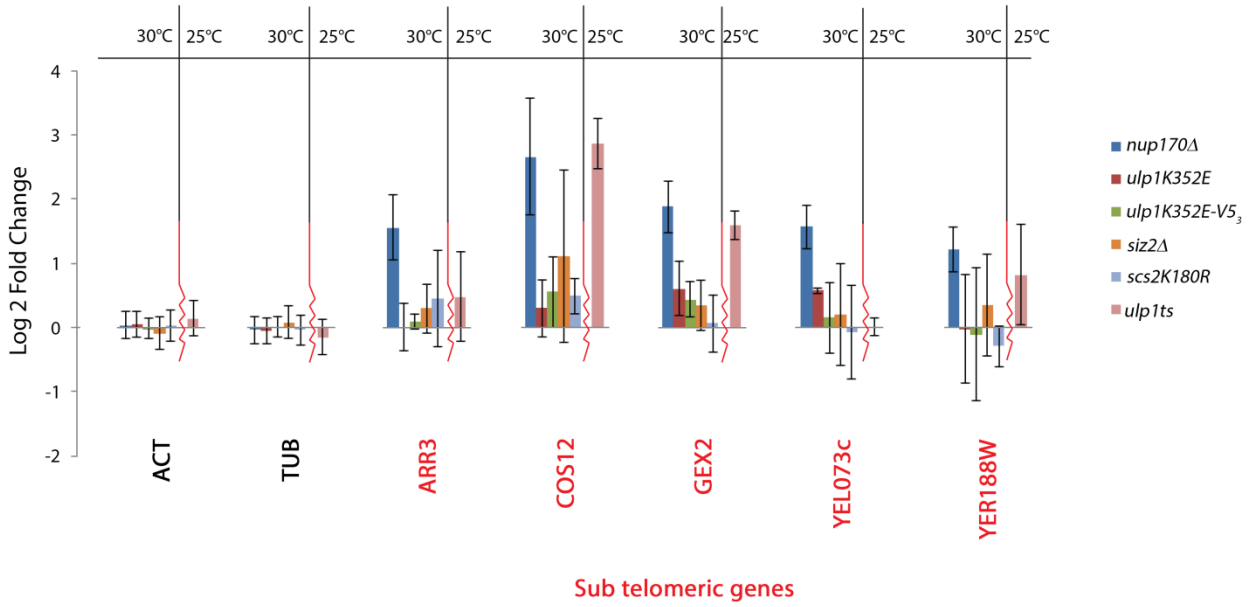

Figure 3-5. The *ulp1ts* mutant affects subtelomeric silencing at multiple loci.

RT-qPCR analysis showing fold change in gene expression for various subtelomeric genes. Overnight cultures of the indicated strains were diluted to an $O.D._{600}$ of ~ 1 at either 30°C or 25°C. Log2-fold change was determined for each subtelomeric gene by normalizing the ΔC_t values of each indicated strain to the ΔC_t value of WT, generating a $\Delta\Delta C_t$ value. Bars represent the average $\Delta\Delta C_t$ value of three biological replicates. Error bars represent 1 standard deviation. The threshold indicating significant fold-change was set to 1 Log2 fold change to show two fold changes in gene expression.

3.2.6 Mutations in Ulp1 mislocalize Sir proteins and alter nuclear morphology

Several NE associated proteins have been implicated in binding subtelomeric proteins and contributing to telomere localization. Among these are the NPC protein Nup170 and two membrane proteins, Esc1 and Mps3 (Van de Vosse et al., 2013; Taddei et al., 2004; Bupp et al., 2007). These proteins have been shown to interact with the subtelomeric chromatin protein, Sir4 (Taddei et al., 2004; Bupp et al., 2007; Van de Vosse et al., 2013). Previous work from our lab has shown that Nup170 also is present in a complex with the SUMO E3 ligase Siz2, consistent with a role for SUMOylation pathways in telomere association with the NE (Lapetina et al., 2017). Considering the physical interactions of Nup170 with Sir4 and the potential role of SUMOylation in regulating this interaction, we investigated the role of Ulp1 in the NE association of Sir4 and its binding partner, Sir3. The positioning of Sir4 at the nuclear periphery through the interaction between Sir4 and the INM proteins Esc1 and Mps3 occurs in a cell cycle dependent manner, so G1-phase and early S-phase cells were counted to determine cell cycle specific changes in Sir4 perinuclear positioning (Taddei et al., 2004; Bupp et al., 2007). The localization of Sir4-GFP was then examined in the WT and the *ulp1ts* and *ulp1K352E* mutants, and the position of the NE in these cells was determined using an NE/ER protein, Sur4, that is endogenously tagged with mCherry. Sir4-GFP localization to the nuclear periphery was reduced in the *ulp1ts* and *ulp1K352E* mutants both in G1- and early S-phase cells (Figure 3-6 A-B). This phenotype was similar to that observed in the *nup170Δ* mutant, where Sir4 also showed to reduced levels of NE association in both G1-phase and early S phase cells (Figure 3-6, also see Van de Vosse et al., 2013; Lapetina et al., 2017). The *siz2Δ* showed no loss in the nuclear peripheral positioning of

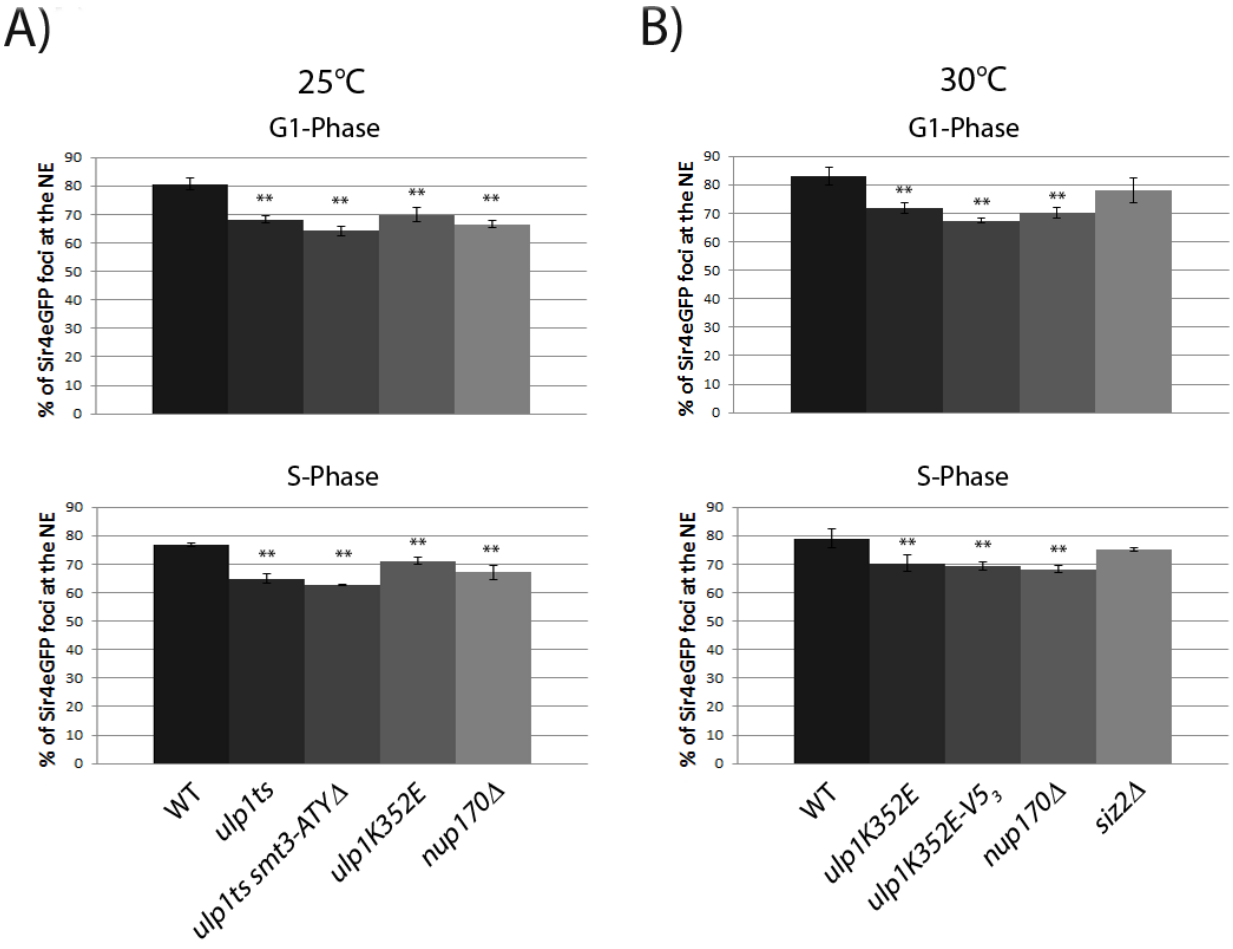

Figure 3-6. Mutations in Ulp1 mislocalize Sir4 away from the NE.

A) Quantification of Sir4-GFP localization at the NE. The percent Sir4 localization at the NE is expressed as the ratio of peripheral Sir4-GFP foci over the total identified GFP foci within the nucleus. Bar represents the average of three biological replicates totaling 150 cells. Sir4 localization for the *ulp1ts* mutants and *ulp1K352E* mutant was determined at 25°C in both G1 (no bud) and early S-phase (small budded) cells. B) Quantification of Sir4-GFP localization in the *ulp1K352E* and the *ulp1K352E-V5$_3$* strains at 30°C. No budded and small budded cells were counted and Sir4 peripheral localization was determined the same way as 3-6 A. Bar represents the average of 3 biological replicates for 150 cells Error bars represent 1 standard deviation. Asterisks denote a p-value of $\leq$0.01. Significance was determined by a 2 way homoscedastic t- Test.

Sir4 in either G1-phase or early S-phase cells (Figure 3-6 A-B). Sir3 localization was also examined in both the *ulp1K352E-V5$_3$* and *nup170Δ* mutants and showed a similar degree of mislocalization from the nuclear periphery as Sir4 (Figure 3-8). This loss in the perinuclear positioning of Sir4 and Sir3 could indicate a possible mechanism behind the reduced NE association of telomeres seen in the *ulp1ts, ulp1K352E-V5$_3$*, and *ulp1ts smt3-ATYΔ* mutants (see Figure 3-7).

Labeling the NE also enabled observations to be made of nuclear shape in the *ulp1* mutants. Interestingly, in the *ulp1K352E* mutant, nuclei often appeared 'dumbbell' or 'bean' shaped (Figure 3-8). This phenotype was exacerbated in the *ulp1K352E* point mutant containing a $V5_3$ tag (*ulp1K352E-V5$_3$*). As mentioned above, the addition of the $V5_3$ tag to the *ulp1K352E* further increased SUMOylation of conjugates potentially including Scs2 (see Figure 3-2, compare *ulp1K352E* and *ulp1K352E-V5$_3$*) suggesting that the increase in SUMOylation of these conjugates could be contributing to these NE perturbations (Figure 3-8 A). Surprisingly, nuclear abnormalities were less apparent in the *ulp1ts* mutant but there appeared to be a loss in the association of cortical ER with the plasma membrane and the occurrence of NE extensions, which have been commonly referred to as escapades or flares (Campbell et al., 2006; Hattier et al., 2007). The cortical ER disassociation along with the NE escapades appeared to be rescued with the addition of mature SUMO (Figure 3-8 B). A similar observation regarding altered NE morphology and cortical ER disassociation for the *ulp1K352E-V5$_3$* and *ulp1ts* mutants were also seen when the NE was labeled with Sec63-GFP (Figure 3-3, data not shown). Together, these data indicate that Sir4 and Sir3 localization at the nuclear periphery is reduced in the

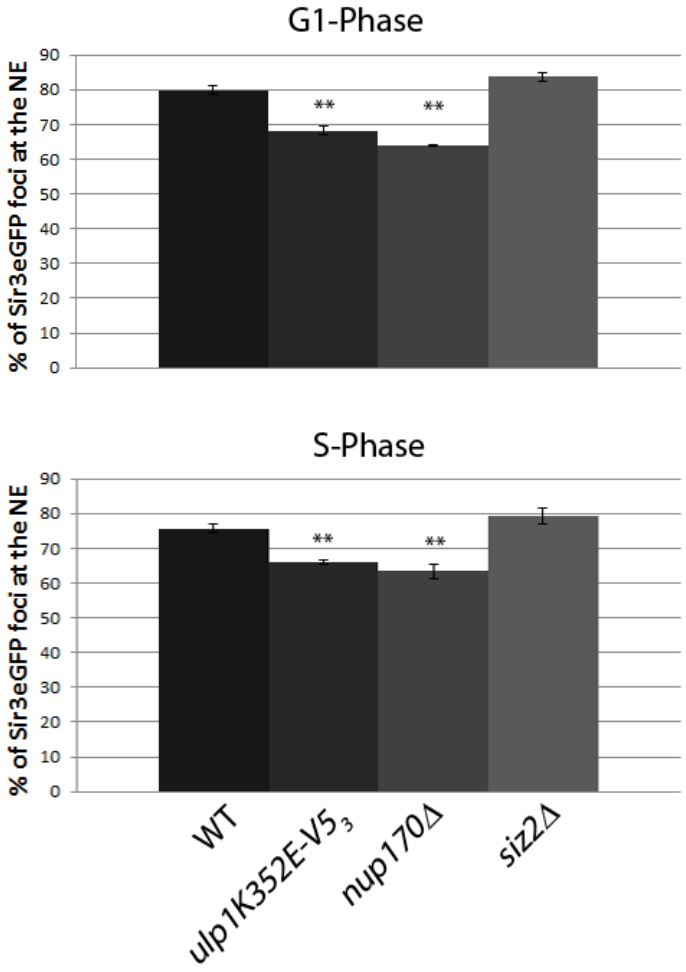

Figure 3-7. A mutation in Ulp1 mislocalizes Sir3 from the nuclear periphery.

Quantification of Sir3-GFP localization at the NE. The percent Sir3 localization at the NE is expressed as the ratio of peripheral Sir3-GFP foci over the total identified GFP foci within the nucleus. Bars represent the average of three biological replicates totaling 150 cells. Sir3 localization for the indicated strains at 30°C in both G1 (no bud) and early S-phase (small budded) cells. Error bars represent 1 standard deviation. Asterisks denote a p-value of $\leq$0.01. Significance was determined by a 2 way homoscedastic t- Test.

different ulp1 mutants and that a mutant with the point mutation in the coiled-coiled domain of Ulp1 showed an increase in the frequency of observable NE abnormalities.

3.2.7 The *ulp1K352E-V5$_3$* mutant shows mislocalization of Esc1 into regions of the NE adjacent to the nucleolus

Esc1 is positioned at the nuclear periphery, where it interacts with Sir4 and Nup170 to establish telomere tethering. Additionally, Siz2 has been shown to interact with all of these proteins and together, these proteins function at the nuclear periphery to tether telomeres (Lapetina et al., 2017). Mutating any of these proteins reduces telomere tethering at the periphery. Because Esc1 is localized at the nuclear periphery to promote the association of telomeres, its positioning at the NE could be dependent on the proteins that function to recruit telomeres to the nuclear periphery. This has been shown to be the case when deleting either Nup170 or Siz2 mislocalizes Esc1 to regions of the NE that are adjacent to the nucleolus, where normally it is excluded (Lapetina et al., 2017; Niepel et al., 2013; Andrulis et al., 2002). Mutants that lack Siz2 also reduce the exclusion of Esc1 from regions of the NE adjacent to the nucleolus, suggesting that SUMOylation could also be playing a role in Esc1 positioning. Following these observations, the exclusion of Esc1 from regions where the nucleolus abuts the NE was observed in cells expressing the *ulp1K352E-V5$_3$* mutation. This mutant has been shown to accumulate SUMO conjugates and mislocalize telomeres away from the nuclear periphery (Figure 3-2 and Figure 3-3). Confirming data shown by Lapetina et al. (2017), deleting *NUP170* leads to a significant loss of Esc1 exclusion from regions of the NE that are adjacent to the nucleolus, to where the percentage of excluded Esc1 is reduced to ~30% in both G1-phase and early S-phase cells. This loss in Esc1exclusion is seen to a lesser extent in cells expressing the

Figure 3-8. The *ulp1K352E-V5$_3$* mutant altered nuclear morphology.

A) Epifluorescence live cell imaging of asynchronous cultures expressing Sir4-GFP and its localization in regards to the nuclear envelope (NE), demarked by Sur4-mCherry. A) Cells from the indicated strains were grown up overnight and diluted the following day to an O.D.$_{600}$ of ~ 1 at 30°C prior to imaging. Arrows indicate NE abnormalities. B) Live cell imaging of asynchronous cultures expressing either the *ulp1ts* allele or both the *ulp1ts* allele and mature SUMO. Cells were grown overnight and diluted to an O.D.$_{600}$ of ~ 1 at 25°C prior to imaging. Arrows indicate displaced cortical ER and NE escapades. The white scale bars represents 2μm.

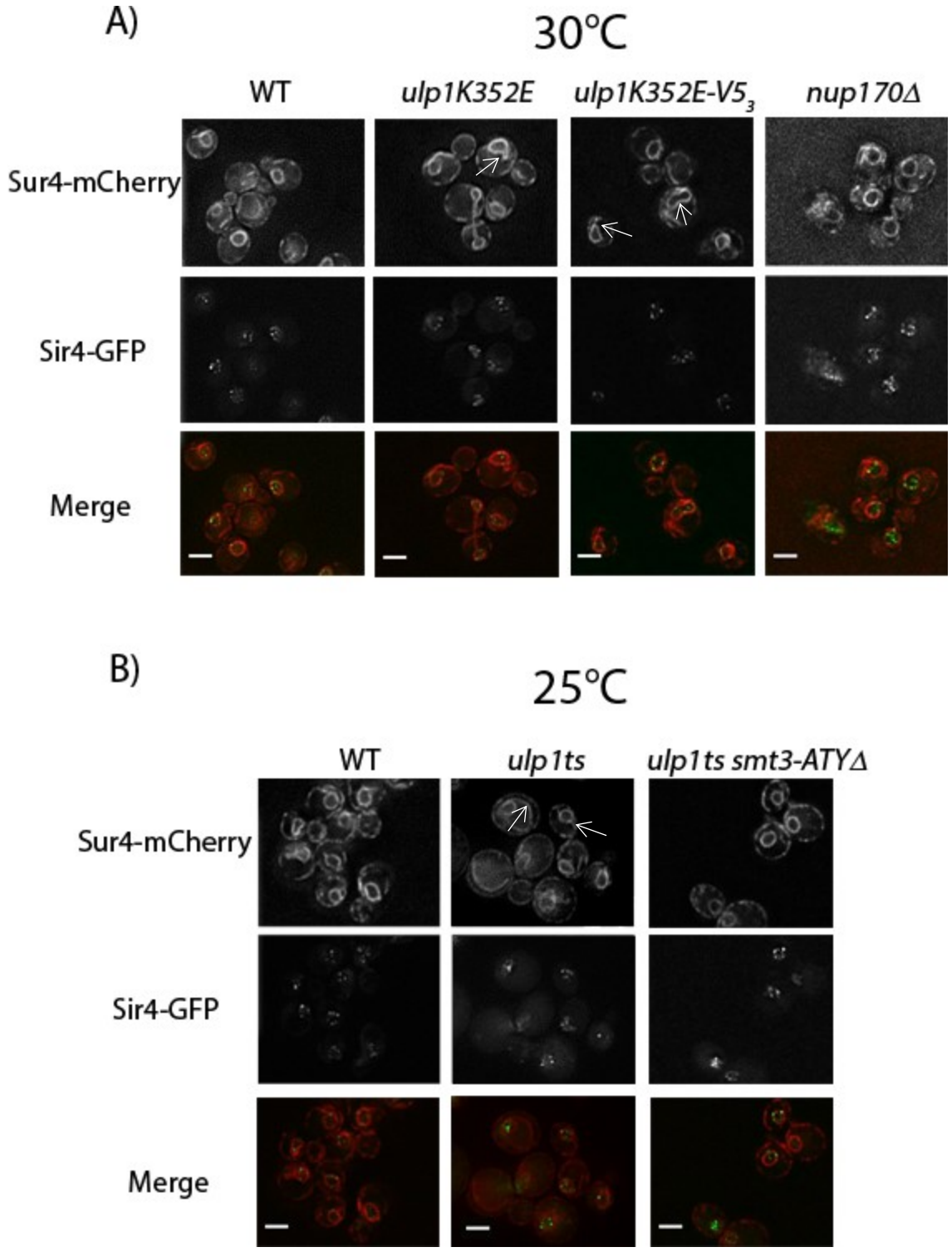

Figure 3-8. The *ulp1K352E-V5$_3$* mutant altered nuclear morphology.

ulp1K352E-V5₃ point mutant (Figure 3-9). These data suggest that the normal distribution of Esc1 along the NE is affected by mutants expressing the *ulp1K352E-V5₃* and that a loss in telomere tethering might contribute to a loss in Esc1 exclusion from the NE region adjacent to the nucleolus.

3.3 Discussion

The *ulp1ts* strain has severely diminished growth at higher temperatures and grows slowly at more permissive temperatures. There is a general accumulation of SUMO conjugates at lower temperatures but once shifted to higher temperatures, there is a precipitous drop in the accumulation of SUMO conjugates due to loss in cell viability and the inability of Ulp1 to maturate SUMO (Li & Hochstrasser, 1999). There was no detectible deficiency in growth for either the *ulp1K352E* or the *ulp1K352E-V5₃* mutants (Figure 3-1). There was an observable growth defect for the *ulp1ts* mutant, which could be partially rescued by expression of mature SUMO, at all tested temperatures (Figure 3-1). Due to the pleiotropic effects attributed to the *ulp1ts* allele, rescuing SUMO maturation by supplementing cells with endogenously expressed mature SUMO does not completely alleviate the temperature sensitivity phenotype. This persistent temperature sensitivity phenotype could be due to the increase in total SUMO conjugates (Figure 3-2 A).

Mutants expressing either the *ulp1K352E* or the *ulp1K352E-V5₃* alleles increased the accumulation of a ~43 kDa and ~55 kDa species. Introducing the *scs2K180R* mutation that eliminates SUMOylation of Scs2 eliminated the accumulation of the 55 kDa species, supporting data shown by Felberbaum et al., (2012) that this band correlates

to SUMOylated Scs2 (Figure 3-2). Additionally, C-terminally tagging of *ulp1K352E* with $V5_3$ increased the accumulation of the 43 kDa and 55 kDa species, indicating that tagging this ulp1 mutant further affects the ability of this protein to deSUMOylate target substrates. Interestingly, deleting *SIZ2* prevented the accumulation of either the 43 kDa or 55 kDa species, suggesting that Siz2 is the E3 SUMO ligase that conjugates SUMO to these target substrates (Figure 3-2 B).

Silencing and the perinuclear association of telomeres are thought to be connected. Observations in the organization of condensed chromatin in higher eukaryotes show darkly staining heterochromatic regions that organize at the periphery and genes localized at the nuclear periphery show silencing (Bourgeois et al., 1985; Peric-Hupkes et al., 2010; Koehler et al., 2009; Tanabe et al., 2002; Krull et al., 2010). Additionally, silenced regions are tethered to the periphery through the SIR complex with proteins that line the INM (Taddei et al., 2004). A loss in both subtelomeric silencing and the perinuclear positioning of telomeres was seen to occur in both the *ulp1ts* and *ulp1ts smt3-ATYΔ* mutants, which supports data that shows that the NE serves as a region that is refractory for gene expression (Figure 3-3, Figure 3-4, Figure 3-5). However, evidence from Mondoux et al. (2007) suggests that the two processes are not necessarily dependent on one another. Telomeres exhibiting different states of subtelomeric gene expression transiently localized on or away from the periphery, regardless of the silencing state. A similar phenotype was seen in both the *ulpK352E* and *ulp1K352E-$V5_3$* mutants. Both mutants displayed specific G1 phase telomere tethering defects in the absence of any noticeable loss in silencing (Figure 3-3 and 3-4). This suggests that silencing does not necessarily require telomere tethering at the NE. Instead, Sir complex

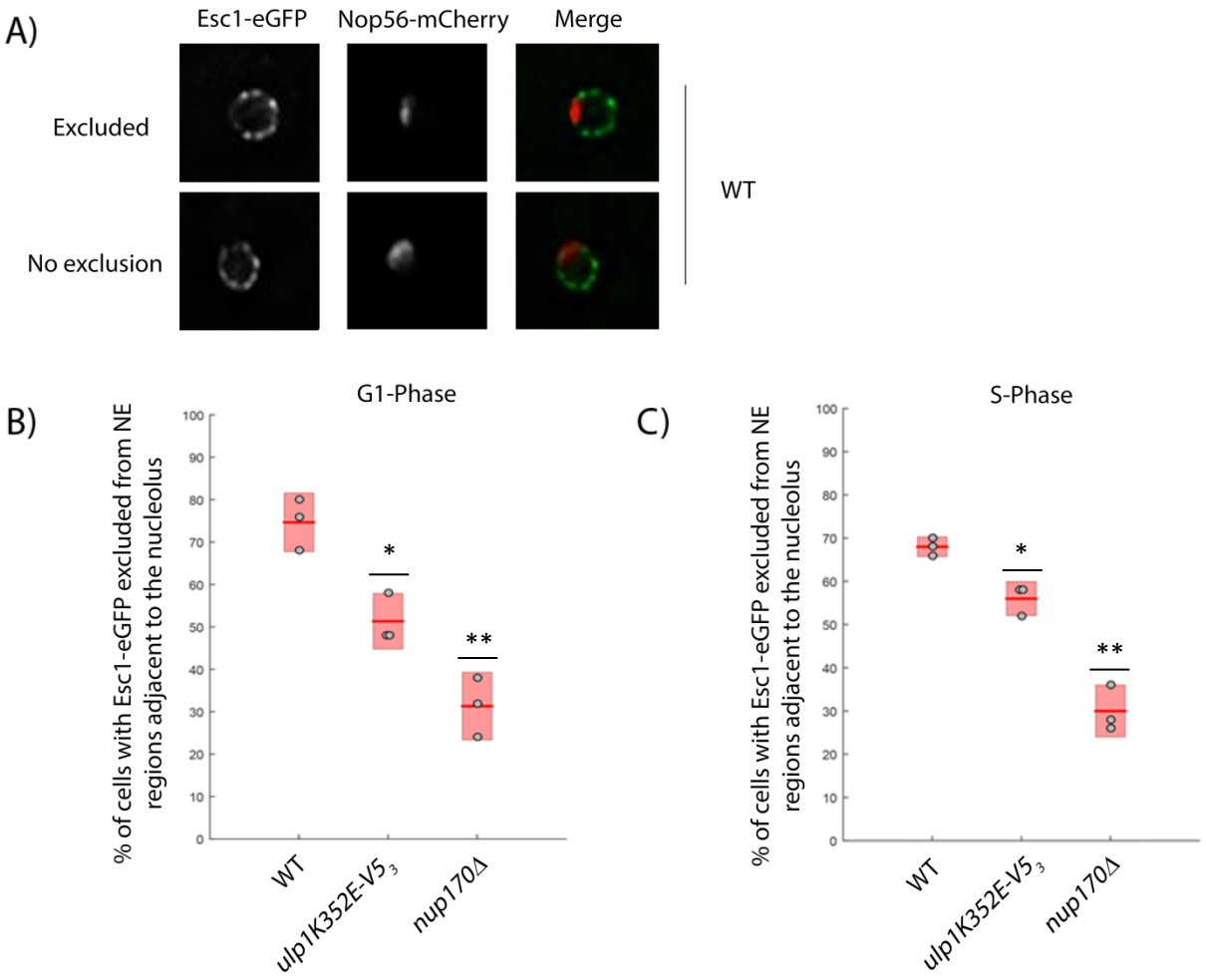

Figure 3-9. The *ulp1K352E-V5₃* mutant shows mislocalization of Esc1 into regions of the NE adjacent to the nucleolus

A) Epifluorescence microscopy of WT cells expressing Esc1-eGFP and the nucleolar marker Nop56-mCherry. The top panel indicates exclusion of Esc1 from the NE adjacent to the nucleolus while the bottom panel shows a loss of exclusion, indicating mislocalization of Esc1 into these regions. B) Quantification of Esc1 exclusion for the *ulp1K352E-V5₃* mutant during G1-phase of the cell cycle (no bud). The percentage of cells with Esc1-eGFP excluded from the NE regions adjacent to the nucleolus was determined by the total number of cells with a loss of Esc1 exclusion set as a ratio for the total number of cell counted for Esc1 exclusion. C) Quantification of Esc1 exclusion for the *ulp1K352E-V5₃* mutant during early S-phase of the cell cycle (small budded). The percentage of Esc1 exclusion from regions of the NE adjacent to the nucleolus was determined in the same manner as for Figure 3-9 B. Each circle represents one replicate that is an average of 50 cells showing Esc1 exclusion from the indicated region. The red line is the average for the three replicates. The pink box is 1 standard deviation. Asterisks indicate p-values $\leq$ 0.01 (*) or $\leq$0.001 (**). Significance was determined by a 2 way homoscedastic t- Test.

assembly on chromatin might be the deciding factor for subtelomeric gene silencing while the perinuclear positioning of chromatin facilitates other processes, such as DSB repair (Therizols et al., 2006; Chien et al., 1993; Horigome et al., 2016).

Telomeres are tethered to the NE using different mechanisms during G1- and S-phase of the cell cycle. G1-phase telomere tethering occurs through partially redundant pathways, involving the yKu heterodimer and Sir4. Additionally, SUMOylation was found to necessitate telomere tethering (Hediger et al., 2002; Ferreira et al., 2011). Interestingly, expressing either the *ulpK352E* or *ulp1ts* alleles was found to contribute to the mislocalization of Tel 14 away from the NE during the G1-phase of the cell cycle (Figure 3-3B). This loss in telomere tethering at the NE during the G1-phase of the cell cycle seen in the ulp1 mutants could be a result from the reduction in the isopeptidase activity of Ulp1. This suggests that the removal of SUMO from target substrates is required to position telomeres at the NE in a cell cycle dependent manner. Mutants that express a deletion in *SIZ2* also show a loss in telomere tethering at the NE, suggesting that a loss in SUMOylation also mislocalizes telomeres away from the NE. Together, these data suggest that the cycling of SUMO is required for the positioning of telomeres at the NE.

Additionally, the cycling of SUMO on specific substrates could affect the ability of telomeres to localize at the NE. Mutants expressing the *ulpK352E* allele increase the SUMOylation of Scs2 (Felberbaum et al., 2012, Figure 3-2 B). The *siz2Δ* mutant not only reduces telomere tethering but also reduces the accumulation of the 55 kDa SUMOylated species, which is likely Scs2 (Felberbaum et al., 2012, Figure 3-2 B). Together, these data suggest that the cycling of SUMO on Scs2 necessitates the localization of telomeres to

the NE. Furthermore, Scs2 is likely positioned at the INM where it could be targeted by either Siz2 or Ulp1, which are both positioned at the INM. Interestingly, Taddei et al., (2004) postulates that there are alternative NE anchored proteins that promote G1-phase telomere tethering due to the ability of yKu70 to mediate the G1-phase positioning of chromatin at the nuclear periphery, in the absence of Esc1. Cumulatively, these data suggest that Scs2 could locate at the INM, where it would function as an alternative G1-phase NE telomere tether. Potentially, the lack of SUMO cycling on Scs2 could impact its ability to function as a G1-phase telomere tether.

Notably, there were distinct differences in the perinuclear positioning of telomeres observed between the *ulpK352E-V5*$_3$ and the *ulp1ts* mutants, with the *ulp1ts* mutant showing additional defects in the perinuclear positing of telomeres during early S-phase of the cell cycle. This loss in telomere tethering at the NE could be rescued with the addition of mature SUMO, suggesting that the availability of mature SUMO plays a role in mediating telomere tethering to the NE during early S-phase of the cell cycle. Deleting *SIZ2* also reduces the ability of telomeres to localize at the nuclear periphery during early S-phase of the cell cycle (Ferreira et al., 2011). Together, these data strengthen the observation that the availability of SUMO plays a role in establishing early S-phase telomere anchoring at the NE (Figure 3-3 C).

The Sir complex mediates subtelomeric silencing and Sir4 is involved in anchoring telomeres to the NE. Sir4 is essential in organizing the SIR complex, which implicates it as a platform for SIR complex assembly (Luo et al., 2002; Rudner et al., 2005; Rusché et al., 2002). Because Sir4 provides a platform to promote SIR complex assembly and maintains telomere anchoring at the NE, removal of Sir4 causes changes in

silencing, protein localization, and telomere tethering (Ellahi et al., 2015; Lapetina et al., 2017; Taddei et al., 2004). Telomeres are no longer tethered to the NE when the isopeptidase activity of Ulp1 is impaired by introducing mutations in encoded protein (Figure 3-3 B-C). The different ulp1 mutants also show mislocalization of both Sir3 and Sir4 away from the NE. Together, this supports evidence that telomeres favor a more nuclear interior distribution as opposed to localizing at the periphery because Sir3 and Sir4 are also localizing away from the NE (Figure 3-6 and Figure 3-7). Thus, the loss in telomere tethering at the nuclear periphery from impaired Ulp1 function could be attributed to the mislocalization of Sir4 and Sir3 away from the nuclear periphery (Figure 3-6).

Additional defects in NE morphology could be seen in the *ulp1K352E-V5*$_3$ mutant. 'Dumbbell' or 'bean' shaped NE abnormalities occurred more frequently in the *ulp1K352E-V5*$_3$ mutant (Figure 3-6). Preventing the SUMOylation of Scs2 by mutating lysine 180 to arginine (*scs2K180R* allele) in cells expressing the *ulp1K352E-V5*$_3$ allele, these NE abnormalities are lost (Chris Ptak and Natasha Saik, unpublished observations). These data suggest that an increase in the SUMOylation of Scs2 increases the frequency of NE abnormalities. These NE bulges or protrusions could be due to alterations in phospholipid biogenesis. Scs2 functions to sequester Opi1, a suppressor for the *INO1* activator genes *INO2* and *INO4*, during moments of low inositol, which upregulates phosphatidyl inositol (PI) biosynthesis (Loewen & Levine, 2005; Nikawa et al., 1995). SUMOylated Scs2 drives sequestration of Opi1 to the NE and promotes unregulated *INO1* expression (Natasha Saik, unpublished observations). Upregulating *INO1* expression would increase the total amount of nuclear membrane by increasing PI

biosynthesis, potentially altering membrane fluidity and structure (Fajardo et al., 2011; Berterame et al., 2016). Similar effects have been seen in temperature sensitive secretory (sec) pathway mutants. Growing a *sec6-4* mutant at non-permissive temperatures displayed a bilobed yeast nuclei and this abnormality was dependent on phospholipid biosynthesis (Walters et al., 2018). The consequences regarding mutating Sec proteins vary from the mislocalization of nuclear proteins to promoting defects in NPC assembly, indicating that abnormal phospholipid biosynthesis has pleotropic consequences (Ryan & Wente, 2002). This leaves open the possibility that the *ulp1K352E-V5*$_3$ mutant is contributing to an increase in phospholipid biosynthesis and that this increase in phospholipid biosynthesis is also contributing to the mislocalization of both telomeres and Sir proteins away from the NE.

Chapter IV: The effect that different Ulp1 mutants have on the interactions between INM-associated proteins

4.1 Overview

Subtelomeric chromatin interacts with the NE anchored proteins, Esc1 and Mps3, through the interaction of Sir4 (Bupp et al., 2007; Taddei et al., 2004). There is additional evidence that links the SUMO E3 ligase Siz2 as being necessary for the perinuclear positioning of telomeres (Ferreira et al., 2011). There is also evidence that the interaction between Nup170 and Esc1, which are both proteins that promote telomere anchoring at the NE periphery, is reduced when *SIZ2* is deleted (Lapetine et. al., 2017). These data indicate that a loss in Siz2, which SUMOylates substrates at the INM, can affect the ability of proteins at the NE to interact with telomere tethers. Additionally, these data correlate with a loss of perinuclear positioned telomeres, suggesting that Siz2 mediated SUMOylation could play a role in the organization of proteins at the NE.

In order to address the consequences that cells producing ulp1 mutant constructs have on the interaction between proteins localized at the INM, the interaction between proteins that promote the recruitment of subtelomeric chromatin was assessed. The data in chapter IV show how different ulp1 mutants change the ability of proteins localized at the INM to interact, suggesting consequences that result from impairing the isopeptidase activity of Ulp1. These results expand on data in chapter III, which show that both telomeres and proteins that promote telomere tethering mislocalize away from the NE as a consequence from producing mutant ulp1. By using both the *ulp1ts* and *ulp1K352E-V5*$_3$ mutants, the organization of the SIR complex was also examined in order to determine how impairing the isopeptidase function of Ulp1 affects the organization of subtelomeric chromatin.

Ulp1 is anchored at the nuclear periphery through interactions with the NPC basket. In order to address whether Ulp1 could localize to other compartments outside of the NPC to regulate the positioning of subtelomeric chromatin, the localization of Ulp1 in regards to components of the Snup complex, which localize in compartments separate from the NPC to mediate subtelomeric anchoring at the NE, was assessed. We show that in the different ulp1 mutants, the interaction between proteins at the NE and the localization of proteins that promote the positioning and organization of subtelomeric chromatin are altered. Together these data further show consequences that result from the loss in the localization of subtelomeric chromatin at the NE.

4.2 Results

4.2.1 The interaction between Nup170 and Sir4 is disrupted in cells expressing different mutant *ulp1* alleles

In order to further characterize consequences that result from the reduced anchoring of telomeres at the nuclear periphery, endogenously expressed, C-terminally tagged PrA constructs of either Sir4 or Esc1 were inserted into strains that expressed mutant *ulp1* alleles. Mutants expressing the *ulp1ts* or *ulp1ts smt3-ATYΔ* allele were grown at 25°C and compared to WT grown at the same temperature. This was done to distinguish between consequences that were a result of the reduced isopeptidase activity of Ulp1 in mutants expressing *ulp1ts* allele on the ability of subtelomeric proteins to associate with proteins at the NE from the defect in SUMO maturation that is also present in the *ulp1ts* mutant (Figure 3-2A). Mutants not expressing these alleles were grown at 30°C. Affinity purified cell extracts from the *siz2Δ*, the *nup170Δ*, the *ulp1ts*, and the

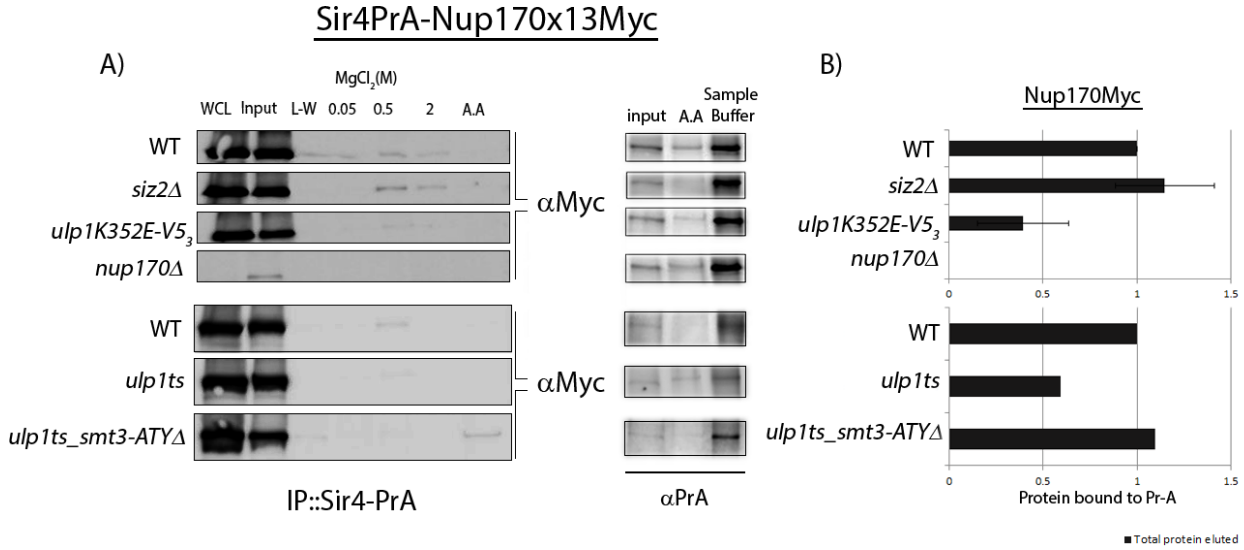

Figure 4-1. The interaction between Nup170 and Sir4 is disrupted in the ulp1 mutants.

A) Affinity purification of Nup170x13Myc with Sir4-PrA. Whole cell lysates produced from cryo-milled cultures of the indicated strains. Lysates from equal amounts (total number of cells) of each strain were incubated with IgG conjugated Dynabeads to bind PrA tagged Sir4. Nup170x13Myc was subsequently eluted from Sir4-PrA in a stepwise fashion with an increasing $MgCl_2$ concentration gradient, ending with a final wash of acetic acid (left panels). Sir4-PrA was eluted from IgG conjugated beads using washes of acetic acid followed by sample buffer (right panels). Nup170x13Myc and Sir4-PrA were visualized by western blot analysis B) Quantification of Nup170x13Myc eluted from Sir4-PrA. The total pixel intensity (TPI) for the eluted Nup170x13Myc (TPI-IP) was summed and set as a ratio to Input (TPI-Input) (TPI-IP/TPI-Input). TPI-IP/TPI-Input was then set as a ratio of the TPI-IP/TPI-Input for the eluted Sir4-PrA ([(TPI-IP/TPI-Input) Nup170x13Myc/(TPI-IP/TPI-Input) Sir4-PrA)]). The Nup170x13Myc and Sir4-PrA TPI ratio for the indicated mutants was normalized to WT. Fold-change in TPI is shown as variation from 1. Plotted TPI for proteins eluted from 3 biological replicates (Top graph). Plotted TPI for proteins eluted from 2 biological replicates. Error bars represent 1 standard deviation.

ulp1K352E-V5$_3$ mutants were probed for copurifying proteins. Initially, the interaction between Sir4 and Nup170 was characterized. Nup170 has been shown to be important for the localization of Sir4 at the NE (Van de Vosse et al., 2013). Deleting *NUP170* also mislocalizes telomeres away from the NE. Because both Sir4 and Nup170 are required to promote the positioning of subtelomeric chromatin at the NE, investigating the interaction between these proteins would elucidate downstream consequences that result from the mislocalization of telomere away from the NE. Deleting *SIZ2* did not appear to alter the copurification of Nup170x13Myc from Sir4-PrA (see also Lapetina et. al., 2017). However, both the *ulp1ts* and *ulp1K352E-V5$_3$* mutant show a reduction in total copurifying Nup170x13Myc with Sir4-PrA (Figure 4-1 A-B). These data indicate that the ulp1 mutants show reduction in the amount of Nup170 bound to Sir4. Even though there is a detectable SUMO maturation defect within mutants expressing the *ulp1ts* allele, SUMOylated conjugates still accumulate (Figure 3-2 A; Li & Hochstrasser, 1999), suggesting that the accumulation of SUMO conjugates could be affecting the interaction between Nup170x13Myc with Sir4-PrA (Figure 4-1). Interestingly, by restoring mature SUMO to the *ulp1ts* strain by producing mature SUMO (*ulp1ts smt3-ATYΔ*), the interaction between Nup170 and Sir4-PrA appeared more similar to WT counterparts. Curiously, this suggests that further increasing the availability of mature SUMO in mutants expressing the *ulp1ts* allele can alleviate the loss in copurification of Nup170x13Myc from Sir4-PrA.

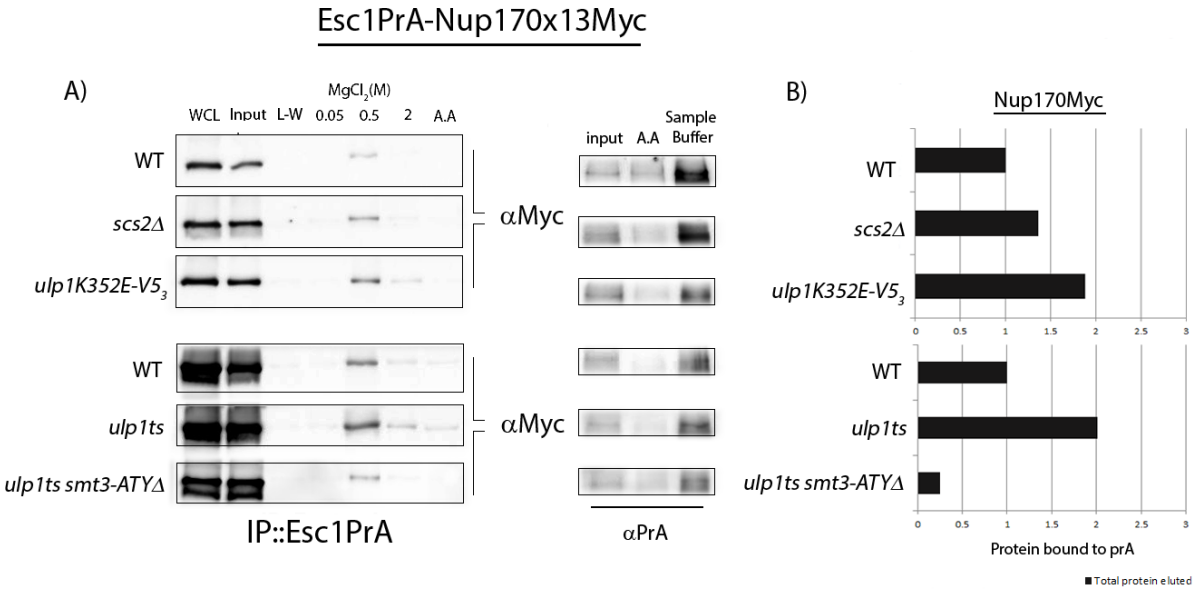

Figure 4-2. The interaction between Nup170 with Esc1 is altered in the ulp1 mutants.

A) Affinity purification of Nup170x13Myc with Esc1-PrA. Whole cell lysates produced from cryo-milled cultures of the indicated strains. Lysates from equal amounts (total number of cells) of each strain were incubated with IgG conjugated Dynabeads to bind PrA tagged Esc1. Nup170x13Myc was subsequently eluted from Esc1-PrA in a stepwise fashion with an increasing $MgCl_2$ concentration gradient, ending with a final wash of acetic acid (left panels). Esc1-PrA was eluted from IgG conjugated beads using washes of acetic acid followed by sample buffer (right panels). Nup170x13Myc and Esc1-PrA was visualized by western blot analysis. B) Quantification of Nup170Myc eluted from Esc1-PrA. The total pixel intensity (TPI) for the eluted Nup170x13Myc (TPI-IP) was summed and set as a ratio to Input (TPI-Input) (TPI-IP/TPI-Input). TPI-IP/TPI-Input was then set as a ratio of the TPI-IP/TPI-Input for the eluted Esc1-PrA ([(TPI-IP/TPI-Input) Nup170x13Myc/(TPI-IP/TPI-Input) Esc1-PrA]). The Nup170x13Myc and Esc1-PrA TPI ratio for the indicated mutants was normalized to WT. Fold-change in TPI is shown as variation from 1. Plotted total protein eluted is an average of two biological replicates.

4.2.2 The interaction between Nup170 with Esc1 is altered in the ulp1 mutants

The interaction between Esc1-PrA and Nup170x13Myc was characterized in the context of mutants that express either the *ulp1ts* or *ulp1K352E-V5*$_3$ alleles. Esc1 and Nup170 have been shown to interact with each other and both promote telomere anchoring during the G1-phase of the cell cycle, so the interaction between these proteins could be affected by mutants with compromised perinuclear telomere tethering. Deleting *SCS2* has been shown to reduce telomere tethering at the NE (Natasha Saik, unpublished observations) and mutants lacking Scs2 showed an increase in the amount of Nup170x13Myc bound to Esc1-PrA (Figure 4-2 A-B). Mutants that express either the *ulp1ts* or *ulpK352E-V5*$_3$ alleles also showed more Nup170x13Myc bound to Esc1-PrA (Figure 4-2 A-B). Supplementing the *ulp1ts* mutant with mature SUMO (*ulp1ts smt3-ATYΔ*) dramatically decreased the amount of Nup170 bound to Esc1-PrA. Together these data suggest that mutants with reduced perinuclear telomere tethering alter the interaction between proteins that promote telomere tethering at the NE during G1-phase of the cell cycle.

4.2.3 The interaction between Sir3 and Sir4 is altered by the different ulp1 mutants

Mutants that express either the *ulpK352E* or *ulp1ts* alleles mislocalized Sir4 and Sir3 away from the NE (Figures 3-6 and 3-7). Because the cellular localization of both Sir3 and Sir4 was altered in the ulp1 mutants, we investigated the interaction between Sir3 and Sir4 using our pulldown assay. Interestingly, analysis of the *ulp1ts* mutant revealed an apparent increase in the amount of Sir3V5$_3$ bound to Sir4-PrA, and this phenotype was also observed in the *ulp1ts smt3-ATYΔ* mutant. Additionally, scs2Δ null

mutants also showed an increased in the amount of Sir3V5$_3$ bound to Sir4-PrA. A similar phenotype was also seen when *NUP170* was deleted (*nup170Δ*, see Figure 4-3). Interestingly, the *ulp1K352E-V5$_3$* mutant did not affect the interaction between Sir3V5$_3$ with Sir4-PrA (Figure 4-3 A-B). This suggests distinct consequences from expressing either the *ulpK352E* or *ulp1ts* alleles in regards to organization of the SIR complex. By assaying for other copurifying proteins with Sir4-PrA and by using antibodies directed against Scs2, the interaction between Sir4-PrA and Scs2 could also be investigated. Scs2 was found not to copurify with Sir4-PrA, suggesting that the interaction between Scs2 and Sir4 is too transient to be detected by this *in vitro* analysis (Figure 4-3 C).

It has been shown that introducing the *ulp1ts* allele causes an increase in the accumulation of SUMO conjugates (Figure 3-2 A; Li & Hochstrasser, 1999). By introducing the *ulp1ts* allele into cells producing both the Sir4-PrA and the Sir3V5$_3$ mutant constructs, a ~150 kDa protein species that corresponds to the predicted mass of SUMOylated Sir3V5$_3$ was apparent by probing for Sir3V5$_3$ with antibodies directed against the V5 tag (Figure 4-3 A, compare the *ulp1ts* and *ulp1ts smt3-ATYΔ* WCL and Input lanes to WT). In cells that express both the *ulp1K352E-V5$_3$* (~100 kDa) and Sir3V5$_s$ (~130 kDa) mutant constructs, separate protein species could be detected for either V5 tagged protein by probing with antibodies directed against the V5 tag (Figure 4-3 D). Additionally, a protein species of ~55 kDa that corresponded to the predicted mass of SUMO conjugated Scs2 was apparent in cells that expressed either the *ulp1ts* or *ulp1K352E-V5$_3$* alleles once probed for with antibodies directed against Scs2 (Figure 4-3 C). By supplementing the ulp1ts mutant with mature SUMO (*ulp1ts smt3-ATYΔ*), there

Figure 4-3. There is an increase in copurifying Sir3 with Sir4 in either the ulp1ts or scs2Δ mutants.

A) Affinity purification of Sir3V5$_3$ with Sir4-PrA. Whole cell lysates produced from cryo-milled cultures of the indicated strains. Lysates from equal amounts (total number of cells) of each strain were incubated with IgG conjugated Dynabeads to bind PrA tagged Sir4. Sir3V5$_3$ was subsequently eluted from Sir4-PrA in a stepwise fashion with an increasing $MgCl_2$ concentration gradient, ending with a final wash of acetic acid (left panels). Sir4-PrA was eluted from IgG conjugated beads using washes of acetic acid followed by sample buffer (right panels). Sir3-V5$_3$ and Sir4-PrA were visualized by western blot analysis. B) Quantification of Sir3-V5$_3$ eluted from Sir4-PrA. The total pixel intensity (TPI) for the eluted Sir3-V5$_3$ (TPI-IP) was summed and set as a ratio to Input (TPI-Input) (TPI-IP/TPI-Input). TPI-IP/TPI-Input was then set as a ratio of the TPI-IP/TPI-Input for the eluted Sir4-PrA ([(TPI-IP/TPI-Input) Sir3-V5$_3$ /(TPI-IP/TPI-Input) Sir4-PrA]). The Sir3-V5$_3$ and Sir4-PrA TPI ratio for the indicated mutants was normalized to WT. Fold-change in TPI is shown as variation from 1. Plotted total protein eluted is an average from three biological replicates (Top graph). Plotted total protein eluted is an average of two biological replicates (Bottom graph). Error bars represent 1 standard deviation. C) Western blot analysis of copurifying Scs2 with Sir4-PrA. Lanes show the same fractions as Figure 4-3 A probed with αScs2. D) Western blot showing whole cell lysates of copurifying Sir3V5$_3$ and *ulp1K352E-V5$_3$* with Sir4-PrA. Asterisks represent potential SUMOylated species. The position of mass markers is shown in kDa.

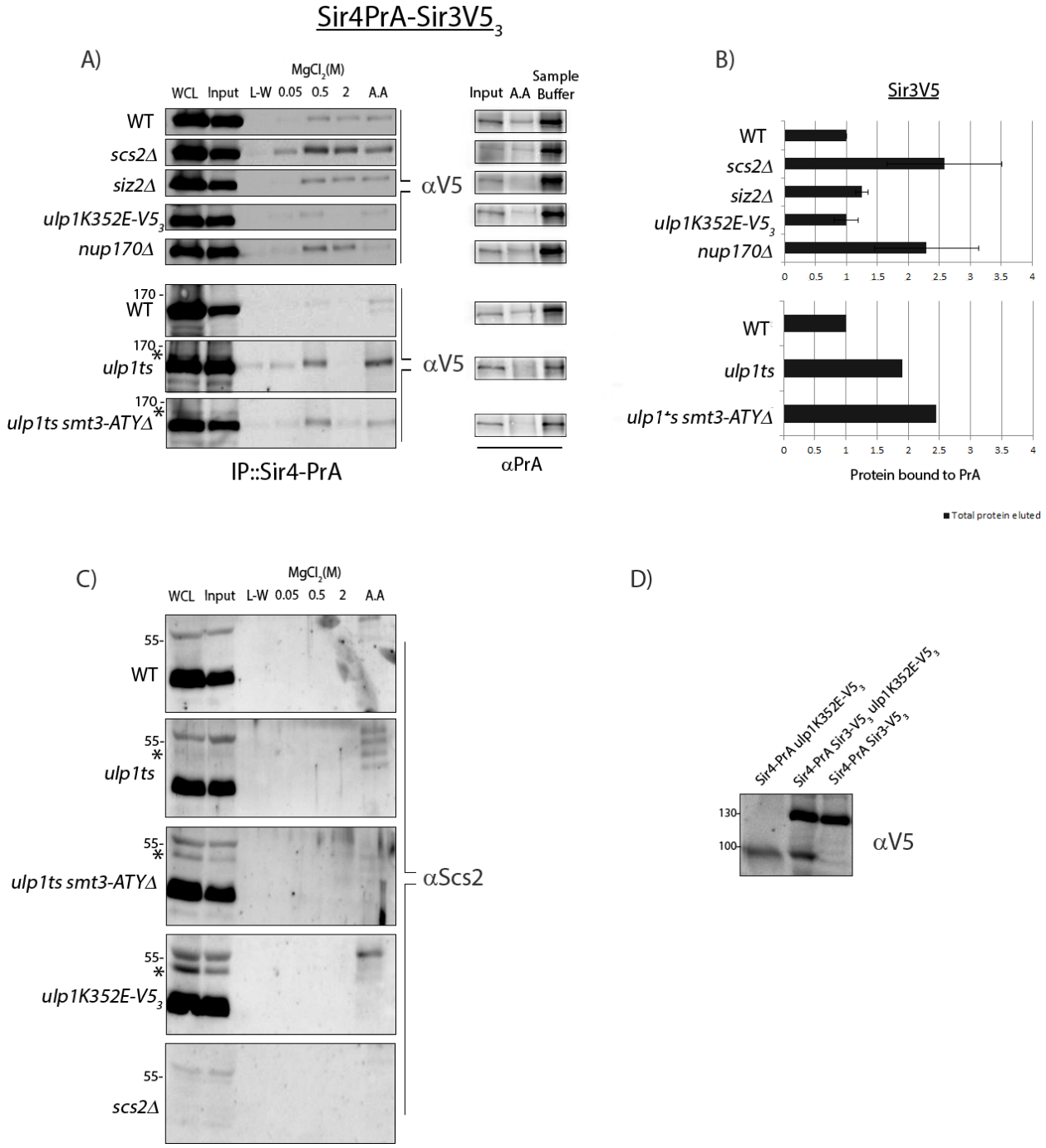

Figure 4-3. There is an increase in copurifying Sir3 with Sir4 in either the ulp1ts or scs2Δ mutants.

was an increase in either the ~150 kDa and ~55 kDa protein species that corresponded to the predicted mass of SUMO-Sir3V5$_3$ and SUMO-Scs2, respectfully (Figure 4-3 A and Figure 4-3 C, compare the *ulp1ts* and *ulp1ts smt3-ATYΔ* WCL and Input lanes).

By removing Siz2, the role that Siz2 plays in organizing the SIR complex could be investigated. Deleting *SIZ2* has been shown to mislocalize telomeres away from the nuclear periphery, but not to alter Sir4 localization away from the NE (Lapetina et. al., 2017; Figure 3-6 B). In order to investigate a consequence in which a loss of Siz2 could facilitate a reduction in telomere positioning at the nuclear periphery, the interaction between Sir4 and Sir3 was characterized. Deleting *SIZ2* had no effect on the interaction between Sir3V5$_3$ with Sir4-PrA, suggesting that the interaction between Sir3 with Sir4 does not reflect the ability of telomeres to localize at the nuclear periphery (Figure 4-3 A-B).

Colocalization between Sir3 and Sir4 was done in order to characterize any observable change in the localization between these SIR complex components related to the increase in copurifying Sir3 from Sir4 in the absence of Scs2. Quantification between fluorescently tagged Sir3-Ruby and Sir4-GFP was performed through the Aro Spot Finding Suite. This software was developed by Scott A. Rifkin's lab and utilizes a 'spot centric' approach over traditional thresholding methods in order to classify local intensity maximum (spots) over background fluorescence (Wu & Rifkin, 2015). Spots localized ~300 nm from one another are identified as overlapping or colocalized. The percent of colocalization between fluorescently tagged proteins is determined as a ratio between the foci identified as overlapping with the total identified foci in a given fluorescence

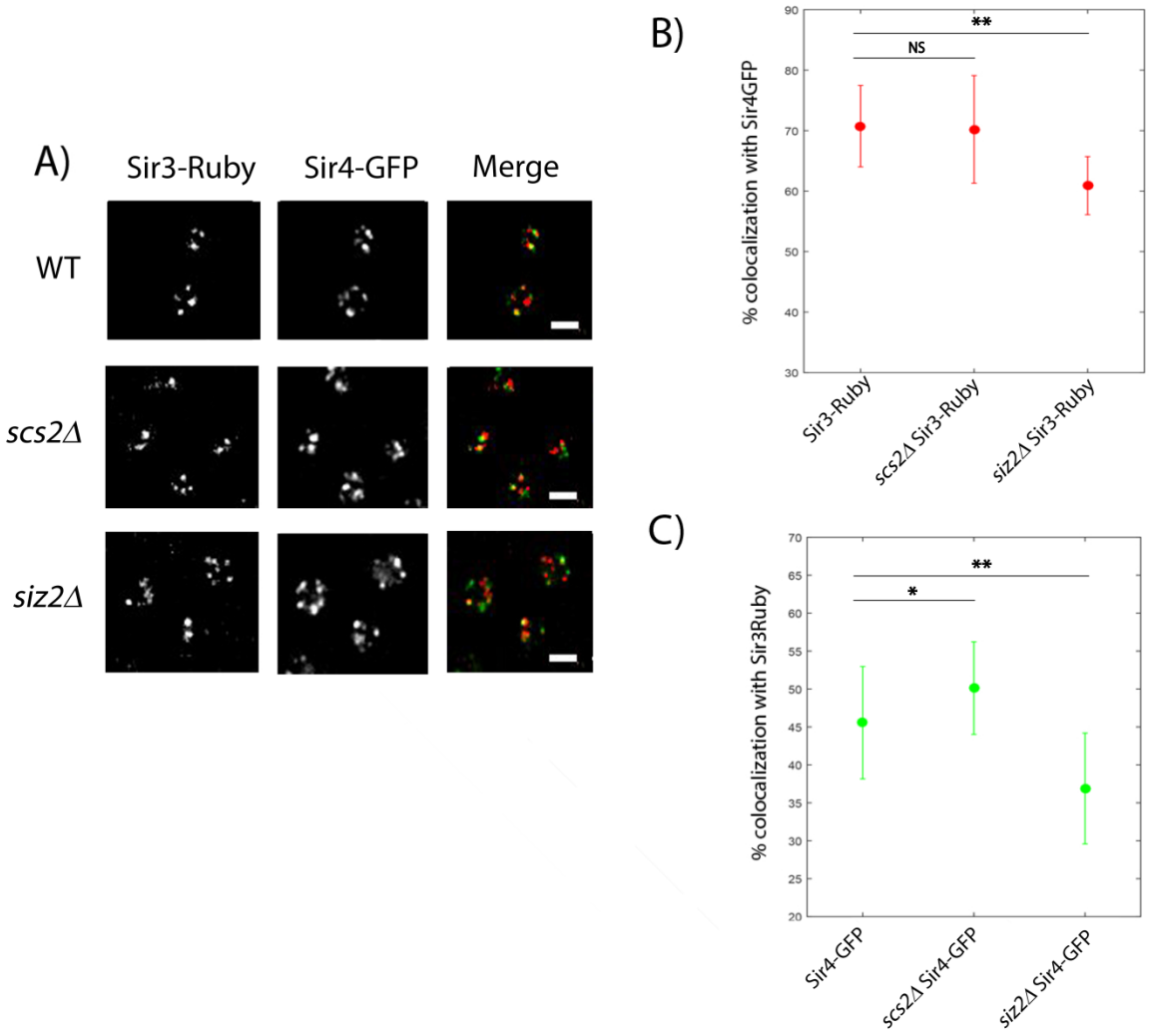

Figure 4-4. Siz2 promotes overlap between Sir3 and Sir4.

A) Representative images of fluorescently tagged Sir4 and Sir3 expressing a deletion in either *SCS2* or *SIZ2*. Samples were collected during log phase growth, washed, and suspended on 2% agarose pads prior to imaging. B) Quantified is the colocalization for the number of overlapping Sir3-Ruby foci with Sir4-GFP set as a ratio to the total number of identified Sir4-GFP foci. C) Quantified is the colocalization for the number of overlapping Sir4-GFP foci with Sir3-Ruby foci set as a ratio to the total number of identified Sir3-Ruby foci. Spots were identified and called by using the Aro Spot Finding Suite software package through the MATLAB programming language (Wu & Rifkin, 2015). The solid circle represents the average of overlapping foci of >300 cells with bars representing 1 Std. Dev. The white scale bar represents 2 μm. Asterisks represents a p-value $\leq$0.01(*) and a p-value $\leq$0.001 (**). NS = Not significant. Statistical significance was calculated by measuring the variance within and between samples using a one way ANOVA.

channel. The percent of colocalization between Sir3-Ruby foci with Sir4-GFP foci averaged ~70% while the inverse (the percent of colocalization between Sir4-GFP foci with Sir3-Ruby foci) showed ~45% colocalization (Figure 4-4). Differences between the percent of colocalization seen between either fluorescent protein highlights the difference in detectability between either tagged protein. Because Sir3-Ruby showed higher levels of background fluorescence, this led to a lower signal-to-noise ratio, which affected spot detection and lowered the overall percent colocalization. Nevertheless, deleting *SIZ2* showed significant reduction in the percent colocalization between Sir3-Ruby and Sir4-GFP, while deleting *SCS2* showed a slight increase in the percent colocalization between Sir4-GFP with Sir3-Ruby (Figure 4-4). Together, these data indicate that the colocalization of Sir3 and Sir4 is dependent on Siz2 and supports observations that show the interaction between Sir3 and Sir4 is favored when Scs2 is absent (Figure 4-3). The reduction in colocalization between Sir3 and Sir4 from deleting *SIZ2* does appear to contradict the evidence that shows no change in the interaction between Sir3 and Sir4. This could be due to the degree in which the colocalization between Sir4 and Sir3 is altered. It is possible that the reduction in the nuclear localization between Sir3 and Sir4 is not detectable by *in vitro* methods that lysis the cell and promote conditions that recapitulate the interaction between these two Sir proteins.

4.2.4 Ulp1 does not colocalize with the Snup complex

Ulp1 mutants showed a loss in the association of Nup170x13Myc with Sir4-PrA. Both Nup170 and Sir4 have been identified as components of the Snup complex, which is composed of a distinct subset of nucleoporins, Siz2, and Sir4 (Lapetina et al., 2017).

Together, these observations could suggest that Ulp1 function could necessitate the organization of the Snup complex. Initially, the localization of Ulp1 was determined in regards to Nup170. Ulp1 associates with Nups at the NPC basket and can localize to different cellular compartments, thus Ulp1 could interact with Nups (such as Nup170) that comprise the Snup complex (Zhao et al., 2004; Makhnevych et al., 2007).

Measuring the degree of colocalization between the protein of interest with Nup170 supports observations that Nups organize into two distinct complexes. Nup170 organizes at both the Snup complex and at intact NPCs, so proteins that share a greater degree of colocalization with Nup170 could be found localizing with Nup170 at both complexes. Proteins that share a lower degree of colocalization with Nup170 are colocalizing only at intact NPCs and not at the pool of Nup170 that is part of the Snup complex (Lapetina et al., 2017). To test this, the colocalization between Ulp1 and Nup170 was assessed. In order to measure the degree of colocalization, the overlap between fluorescently tagged proteins was determined through application of the Aro Spot Finding Suite software. As controls, the colocalization between Nup49-eGFP and Nic96-eGFP with Nup170-RFPT were used. Nic96 has been found to interact with Sir4 and shares a high degree of colocalization with Nup170, suggesting that it organizes at the Snup complex. Nup49 was found not to interact with Sir4 and colocalized with Nup170 to a lesser extent than Nic96, suggesting that it is at NPCs but not part of the Snup complex (Lapetina et al., 2017). Ulp1-eGFP was found to colocalize with Nup170-RFPT in a similar fashion as Nup49-eGFP, indicating that it also is not localizing with the Snup complex. Together, these data suggest that Ulp1 is at NPCs but is not a part of the Snup complex (Figure 4-5).

Figure 4-5. Ulp1 does not colocalize with the Snup complex.

A) Quantification of strains expressing Nup170-RFPT and either an eGFP tagged nucleoporin or the NPC associated protein, Ulp1. Colocalization for the number of overlapping Nup170-RFPT foci with an eGFP tagged protein was set as a ratio to the total number of identified Nup170-RFPT foci. Spots were identified and called by using the Aro Spot Finding Suite software through the MATLAB programming language (Wu & Rifkin, 2015). Distance between overlapping foci was established as ~300 nm. Over 20000 spots from >300 cells were counted for each indicated strain. The solid circle represents the average of overlapping foci and the error bars represent 1 Std. Dev B) Representative, epifluorescence microscopy images showing the overlap in cells expressing eGFP and RFPT tagged proteins. Cells were grown overnight at 30°C and diluted to an $O.D._{600}$ of ~ 1 and were suspended on 2% agarose pads prior to imaging. The white scale bar represents 2 μm.

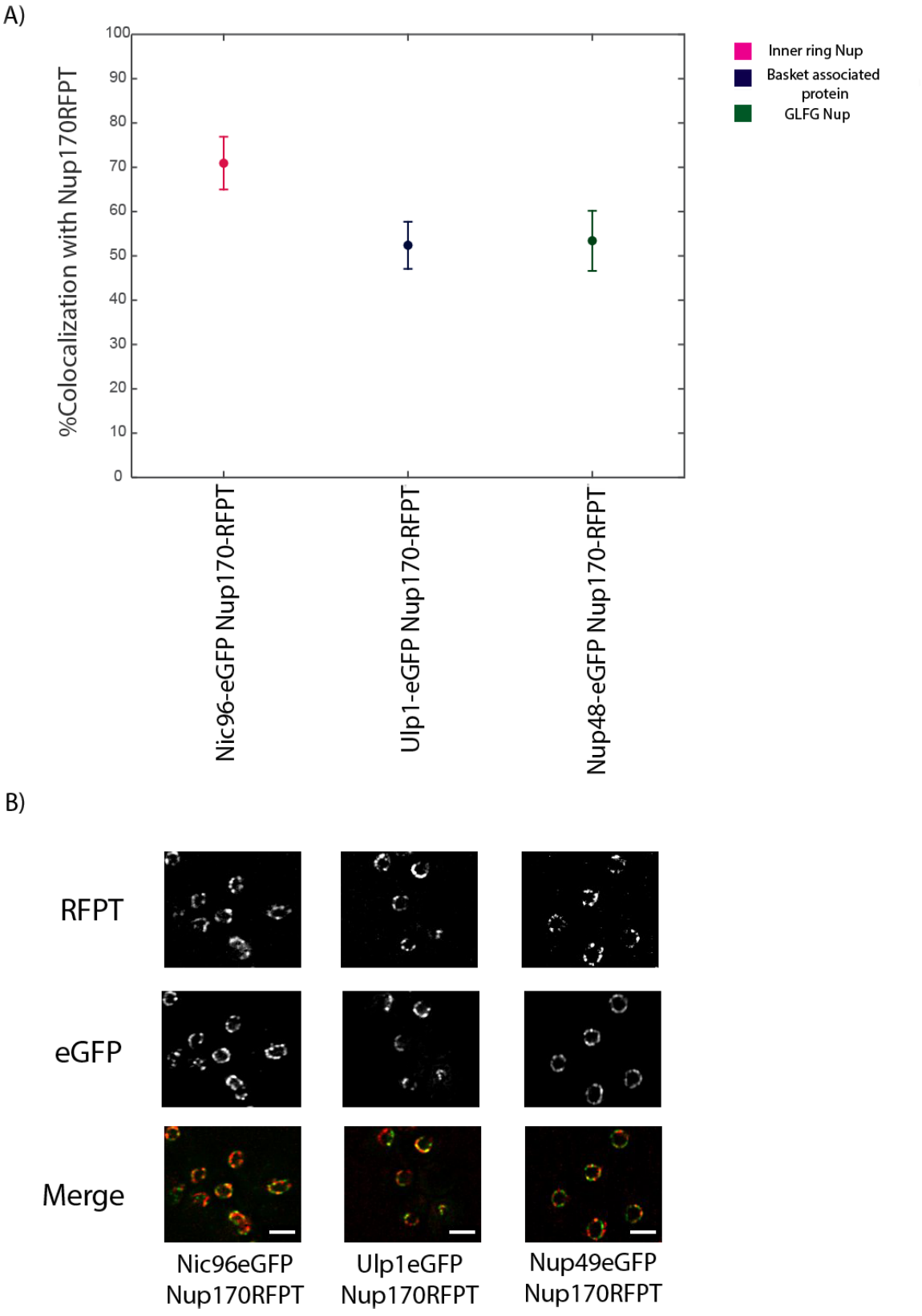

Figure 4-5. Ulp1 does not colocalize with the Snup complex.

4.3 Discussion

Sir4 and Nup170 contribute to the peripheral positioning of telomeres. Nup170 has been shown to be essential for the perinuclear positioning of Sir4 and these proteins establish a subtelomeric tethering complex at the nuclear periphery (Van de Vosse et. al, 2013; Lapetina et al., 2017). The *ulp1K352E-V5$_3$* mutant not only shows a loss in G1-phase telomere tethering but also shows an increase in the SUMOylation of a distinct set of proteins (Figure 3-2 and Figure 3-3 B-C). Additionally, this mutant shows reduced binding of Nup170 to Sir4 (Figure 4-1). Taken together, the reduction in isopeptidase activity of Ulp1 correlated with a loss in the ability of Sir4 and Nup170 to interact, suggesting that the SUMOylation of these proteins could reduce their ability to interact with each other. Telomere tethering at the NE is also reduced in the *ulp1K352E-V5$_3$* mutant, indicating another potential consequence resulting from a loss in the purification of Nup170 from Sir4 (Figure 3-3 B-C). SUMOylated species that correlate to Scs2 noticeably accumulate in both the *ulp1K352E-V5$_3$* and *ulp1ts* mutants, which could be contributing to the loss in interaction between Sir4 and Nup170 (Figure 4-1). The loss in interaction between Sir4 and Nup170 in either the *ulp1K352E-V5$_3$* and *ulp1ts* mutants could also mislocalize Sir4 away from the NE, which in turn could impact telomere tethering at the nuclear periphery (Figure 3-6 and Figure 3-3 B-C). Surprisingly, supplementing the *ulp1ts* strain with mature SUMO restored the copurification of Nup170 from Sir4 to WT levels. Restoring the copurification of Nup170 with Sir4 by supplementing the u*lp1ts* mutant with mature SUMO suggests that the increased availability of mature SUMO can reestablish the interaction between these two proteins.

Mutants expressing either the *ulp1ts* or the *ulp1K352E-V5$_3$* alleles not only increase the accumulation of SUMO conjugates (Felberbaum et al., 2012) but also altered the interaction between Nup170x13Myc with Esc1-PrA (Figure 3-2 and Figure 4-2). SUMO has been shown to alter the ability of proteins to interact with each other and their substrates, suggesting that the increase in SUMOylation by producing ulp1 mutant constructs could affect the ability of proteins localized at the NE to interact with each other (Hannan et al., 2015; Hardeland et al., 2002; Rouvière et al., 2018). Due to the localization of Esc1 at the nuclear periphery and because Nup170 has been shown to localize at different complexes at the INM (Lapetina et al., 2017), SUMOylation could be altering the ability of Nup170 to interact with proteins proximal to the NE. In addition to interacting with Esc1, Nup170 has been shown to interact with Scs2 (Diego Lapetina, unpublished observations). Scs2 is positioned at the NE by its C-terminus and could face towards the nucleoplasm by localizing at the INM (Manford et al., 2012; Smoyer et al., 2016; Chris Ptak, unpublished observations). The SUMOylation of Scs2 seen in either the *ulp1ts* or *ulp1K352E* mutants (Felberbaum et al., 2012) or the deletion of *SCS2* could alter the ability of Nup170 to interact with Scs2 and instead favor an interaction with Esc1 (Figure 4-2).

The increase in the interaction between Esc1 and Nup170 along with the subsequent decrease in interaction between Sir4 and Nup170 seen in either the *ulp1K352E-V5$_3$* or *ulp1ts* mutants supports a potential role for SUMOylation in mediating Snup complex assembly. Nup170, Esc1, and Sir4 are components of the recently identified Snup complex (Lapetina et al., 2017) and mutants that show SUMO species that correspond to SUMOylated Scs2 correlated with alterations in the ability of

Nup170 to organize with other Snup proteins (Figure 4-1 and Figure 4-2). Together, these data suggest that SUMOylation could alter the organization of subtelomeric complexes at the NE.

Esc1 has also been identified as being SUMOylated (Wohlschlegel et al., 2004). In mutants that express the *ulp1K352E-V5*$_3$, the *ulp1ts*, or the *ulp1ts smt3-ATYΔ* alleles, SUMOylated conjugates are seen to accumulate (Figure 3-2), suggesting that Esc1 could be SUMOylated in cells expressing *ulp1* mutant alleles. SUMOylated Sir2 has been shown to not interact with its binding partner, Sir4 (Hannan et al., 2015), suggesting that SUMOylation of Esc1 could also affect the ability of Esc1 to interact with other binding partners. Because the amount of Nup170 bound to Esc1 in mutants expressing the *ulp1ts_smt3-ATYΔ* allele is reduced, it is reasonable to speculate that a SUMO modification on Esc1 could lead to a reduction in the interaction between Esc1 and Nup170. Together, this suggests that deSUMOylation could be required for modulating interactions between perinuclear proteins. Further experiments will need to be done to identify which proteins are being SUMOylated within these mutants to alter the interaction between proteins localized at the nuclear periphery.

The SIR complex (composed of Sir3, Sir4, and Sir2) enriches at subtelomeric chromatin. Sir4 and Sir2 form a heterodimer and associate with Sir3, which homodimerizes through its wing-helix domain (Moazed et al., 1997;Oppikofer et al., 2013). Sir3 can directly bind chromatin through its BAH domain and binds Sir4 within its AAA+ ATPase-like domain (at residues K657, K658, and R659) (Rusché et al., 2002;Ehrentraut et al., 2011). Conversely, the C-terminal residues I1311, M1307, and E1310 of Sir4 are critical for its interaction with Sir3 (Chang et al., 2003). There is

evidence to suggest that the Sir3-Sir4 association is antagonized by the N-terminus of Sir4 and its association with chromatin could promote a conformational change, enabling Sir3 interaction (Moazed et al., 1997). Sir4 has been shown to be SUMOylated (Ferreira et al., 2011).By potentially accumulating SUMO conjugates of Sir4 through the expression of either the *ulp1ts* or *ulp1ts smt3-ATYΔ* alleles, the interaction between Sir3 and Sir4 could be favored. Normally, the Sir3-Sir4 interaction is not very avid (Hoppe et al., 2002) but by increasing the amount of Sir3 bound to Sir4 by SUMOylating Sir4, the interaction between Sir4 and Sir3 could be favored (Figure 4-3). For example, Sir4 could undergo some sort of conformational change resulting from SUMOylation. By changing the conformational state of Sir4, an interaction between Sir4 and Sir3 could be favored over an interaction between other Sir4 binding partners.

An increase in the amount of Sir3 bound to Sir4 could also indicate telomere clustering. Evidenced from early FISH Y′ probing in *S. cerevisiae* cells; Y′sequences that are found in half of the 32-telomeres in budding yeast were contained within 3-8 discrete foci, suggesting telomere clustering. Rap1, Sir4, and Sir3 foci were found to colocalize at these foci, implicating them as components of these clusters (Gotta et al., 1996). Deleting *SCS2* caused an increase in the total copurifying Sir3 with Sir4-PrA (Figure 4-3). Additionally, the colocalization between Sir4 and Sir3 was increased when *SCS2* was deleted, which suggests that these Sir proteins could be clustering at telomeres (Figure 4-4). Alternatively, deleting *SIZ2* caused a reduction in the colocalization between Sir3 and Sir4. This could indicate either that the nucleoplasmic distribution between Sir3 and Sir4 is altered when *SIZ2* is deleted or that there is a loss of telomere clustering mediated by

Siz2 (Figure 4-4). Together, these data suggest that both Scs2 and Siz2 play a role in spatially organizing Sir proteins, which could affect the ability of telomeres to cluster.

Recently, different nucleoporin subcomplexes that are distinct from NPCs have been identified. In *S. cerevisiae*, Lapetina et al. (2017) have identified the assembly of a chromatin associated, Sir4-Nup subcomplex that promotes proper telomere tethering. In *Drosophilia*, the MINT complex, that is composed of Ulp1, Mtor (the NPC basket proteins), Raf2, Mad1, and Mad2, has been identified (Raich et al., 2018). The Mad proteins are components of the mitotic checkpoint complex (MCC), which prevents the continuation of mitosis following irregular chromosomal alignment prior to the onset of anaphase. Both the Snup complex and the MINT complex are composed of Nups that function on chromatin, away from NPCs. Ulp1 was found not to colocalize with the Snup complex (Figure 4-5) but being a component of the nucleoplasmic MINT complex, Ulp1 could function away from NPCs to regulate the spindle assembly checkpoint (SAC). Given that nucleoporins can organize away from NPCs and that Nups that are not part of the Snup complex can interact with chromatin bound proteins (such as Nup53 with Rap1 or Mtor with MINT components at kinetochores) (Van de Vosse et al., 2013; Raich et al., 2018), Ulp1 could be localizing with different Nups at chromatin. Coupled with the evidence that Ulp1 deSUMOylates septins during M-phase of the cell cycle, its localization is dynamic and can transition away from the NPC. The dynamic localization of Ulp1 within the cell could allow Ulp1 to localize to different cellular compartments, depending on cell cycle progression (Takahashi et al., 2000, Makhnevych et al., 2007).

Chapter V: Perspectives

5.1 Synopsis

Transcriptionally silent, heterochromatin organizes at the nuclear periphery. In *S. cerevisiae*, heterochromatin can be defined as either the rDNA, subtelomeric chromatin, or the HM loci. All of these repressed regions localize at the periphery and require components of the SIR complex in order to maintain a silenced state at the nuclear envelope periphery (Rusché et al., 2002; Chien et al., 1993; Smith & Boeke, 1997; Fritze et al.,1997). The mechanism that establishes the peripheral positioning of telomeres occurs in a cell cycle dependent manner and is dependent on SUMOylation (Taddei et al., 2004; Bupp et al., 2007; Schober et al., 2009; Ferreira et al., 2011). Because the deSUMOylase, Ulp1, is tethered to the NPC basket, it can access substrates localized at the nuclear periphery (Panse et al., 2003). As a result of this perinuclear localization, Ulp1 can potentially deSUMOylate proteins involved in telomere tethering in order to facilitate the localization of telomeres at the NE.

We have shown that mutants that express the *ulp1ts* allele promote a loss of subtelomeric silencing. The different ulp1 mutants showed mislocalization of telomeres away from the nuclear periphery. This loss in telomere tethering at the NE correlates with the mislocalization of both Sir4 and Sir3 from the NE. Both Nup170 and Sir4 have been shown to promote subtelomeric anchoring at the NE (Van de Vosse et al., 2013; Taddei et al., 2004), suggesting that the ulp1 mutants could be affecting telomere tethering by the reduction in Nup170 bound to Sir4. Additionally, there was an increase in amount of Sir3 bound to Sir4, which could indicate telomere clustering. In this chapter, I discuss the impact that SUMOylation has on telomere biology with other research that has expanded on the consequences of SUMOylation. Specifically, I speculate on the consequences of

inhibiting the cycling of SUMO and how persistent SUMO could be implicated in altering the interaction between proteins that affect the ability of chromatin to maintain a repressive state at the nuclear periphery.

5.2 The cycling of SUMO regulates telomere positioning

SUMOylation, as a reversible post-translational modification, has been implicated in a wide variety of different cellular processes. It can function to modulate protein interactions, affect protein stability, change the localization of proteins, and regulate processes such as gene expression and DSB repair (Desterro et al., 1998; Lin et al., 2003; Psakhye & Jentsch, 2012). Changes in SUMOylation are evident in several different cancers and the precise consequence of SUMOylation varies depending on context (Bertolotto et al., 2011; Kessler et al., 2012). The SUMOylation of proteins has been shown to necessitate the interaction between proteins, such as RanGAP1 with RanBP2 at the NPC cytoplasmic filaments (Matunis et al., 1996; Matunis et al., 1998). This indicates that the direct consequence of SUMOylation can be persistent and can function to mediate the binding of one protein with another. RanGAP1 serves as a unique example due to the fact that ~50% of it is SUMOylated at any given time. Normally, less than one percent of any given SUMOylated conjugate is apparent at any time. This suggests a more transient role for SUMOylation in modifying substrates. An example of this can be seen with the SUMOylation of human thymine-DNA glycosylase (TDG). The function of TDG is to initiate base excision repair (BER) at mismatched thymine or uracil bases. SUMOylation is required to disassociate TDG from the abasic sites that are the products of its function. In order for TDG to regain activity, it must be deSUMOylated (Hardeland

et al., 2002). This method of activation supports the notion that the cycling of SUMO necessitates its functionality as a post translational modification. Because of this, the mechanisms regulating telomere tethering that are dependent on SUMOylation could be functioning in a similar fashion. The fact that mutants that exhibit both increases in SUMOylation and a loss of SUMOylation similarly affect the ability of telomeres to tether to the periphery, suggests that the cycling of SUMO could play a role in telomere anchoring (Figure 3-3 B-C; Ferreira et al., 2011).

5.3 The organization of scaffolding proteins requires Ulp1 mediated desumoylation

SUMO could also be implicated in the organization of proteins at the NE periphery in order to properly establish the perinuclear tethering of telomeres. Ulp1 is tethered to the NPC basket by its N-terminus, through interactions with the importins Kap60, Kap95, and Kap121. Because Ulp1 localizes at the nuclear periphery, substrates that are SUMOylated at the NE can potentially be deSUMOylated by Ulp1, which is the case with Scs2 (Panse et al., 2003; Felberbaum et al., 2012). In addition to providing a platform for the association of Ulp1 with the NPC, the Mlps function as a scaffold for a variety of different proteins, such as a components of the spindle pole body (SPB), RNPs proceeding export, and components that mediate the spindle assemble checkpoint (SAC) (Niepel et al., 2005; Fasken et al., 2008; Green et al., 2003; Iouk et al., 2002). Niepel et al., (2013) further suggests that the Mlps extend from the nuclear basket to form an interacting network that provides stability to the NE as well as uniformity to NPC spacing. Esc1 was found to necessitate the localization of the NPC basket proteins at the NE and to interact with them, thus supporting a platform in which the Mlps could extend

from and connect to other NPCs (Lewis et al., 2007; Niepel et al., 2013). This scaffold of proteins that is composed of the Mlps and Esc1 is thought to provide structure to the NE in a manner similar to the lamina of higher eukaryotes (reviewed in Broers et al., 2006 and Burke & Stewart, 2014). Similarly to Esc1, which functions to organize proteins at the nuclear periphery, Scs2 has been shown to interact with proteins localized at nucleoplasmic side of the INM, such as Nup170, Rap1, and Opi1, indicating that it too could organize proteins at the INM (Loewen & Levine, 2005; Manford et al., 4-6; Diego Lapetina, unpublished observations). Potentially, the increase level of SUMOylated Scs2 seen in either the *ulp1K352E* or *ulp1ts* mutants could be altering the ability of Scs2 to organize proteins at the NE, to instead favor an interaction with Esc1. This has been seen by altering the organization of proteins localized at the nuclear periphery by producing mutant ulp1 proteins that change the interaction between Nup170 and Esc1. Additionally, deleting *SCS2* would serve to alter the organization of perinuclear proteins in a similar fashion, if modifying Scs2 with SUMO impairs its ability to interact with proteins at the nuclear periphery. The *siz2Δ*, the *ulp1K352E-V5*$_3$, and the *ulp1ts* mutants increased copurifying Nup170 from Esc1, suggesting that either the SUMOylation of Scs2 or deletion of *SCS2* could favor the interaction between Nup170 and Esc1 (Figure 4-2). By further accumulating SUMO conjugates by expressing the *ulp1ts smt3-ATYΔ* allele (Figure 3-2), additional INM proteins could be targeted by SUMO. If SUMO is inhibiting the ability of tethering proteins to interact at the NE, than the reduced amount Nup170 bound to Esc1 in the *ulp1ts smt3-ATYΔ* mutant could be from SUMOylation of Esc1, which has been previously shown to be conjugated by SUMO (Wohlschlegel et al., 2004). Together, these observations suggest that Scs2 could be a component of the

Esc1/Mlp scaffolding network and that SUMOylation could alter the interaction of proteins within this network. Additional support for this conclusion can be seen from cells that express the *ulp1K352E-V5$_3$* allele, which shows alterations in the localization of Esc1. The *ulp1K352E-V5$_3$* mutant showed mislocalization of Esc1 into regions of the NE adjacent to the nucleolus, where normally it is excluded (Figure 3-9), in a similar fashion to deleting both *MLP* genes (Niepel et al., 2013). Together, these observations suggest that the SUMOylation of proteins localized at the INM could alter the organization of proteins that comprise the Esc1/Mlp scaffolding network.

5.4 SUMO promotes an increase in protein-protein interaction which could favor telomere clustering

Similar to the system described in yeast, where subtelomeric chromatin is organized at the nuclear periphery through interactions between the chromatin bound protein, Sir4, with the INM protein, Esc1; metazoans organize chromatin at the NE through the interaction of chromatin bound proteins with the nuclear envelope transmembrane (NET) proteins (Zullo et al., 2012; Polioudaki et al., 2001). Additionally, the nuclear lamina (which is lacking in yeast but parallels could be drawn from the Mlp scaffolding network) has been shown to bind to DNA and regulate gene expression (Zhao, Harel, Stuurman, Guedalia, & Gruenbaum, 1996; Zheng et al., 2000). The nuclear lamina is composed of lamins. The two types of lamins are A-type and B-type. In mammals, A-type lamins are derived from one gene through alternative splicing resulting in lamin A and lamin C, while B-type lamins are encoded by two different genes, LMNB1 and LMNB2 (reviewed in Broers et al., 2006 and Burke & Stewart, 2014). SUMO has been implicated in promoting the clustering of proteins and an example of

this can be seen with the aggregation of the nuclear lamina in patients suffering from dilated cardiomyopathy. Primary mouse myoblasts expressing mutant pAsp192Gly lamin C derived from patients suffering from dilated cardiomyopathy accumulated aggregates with WT lamin A/C and SUMO-1 (Boudreau et al., 2012). Parallels could be drawn from SUMO lamins forming aggregates, to SUMO being involved in increasing in the interaction between proteins that are components of the yeast Mlp scaffolding network (Figure 4-2). Additionally, the copurification of Sir3 from Sir4 was shown to increase, further suggesting that SUMOylation can favor the interaction between proteins (Figure 4-3). This increase in the interaction between Sir3 and Sir4 could be from an increase in the clustering of telomeres, which would promote additional interactions between Sir3 and Sir4.

Telomere clusters are visualized by labeling telomeres with FISH Y′ probes. All 32 labeled telomeres stain in a limited number of 3 to 8 foci, which suggests that they cluster (Gotta et al., 1996). Rap1, Sir3, and Sir4 colocalize at these foci, indicating that they cluster with telomeres. The over expression of Sir3 has been shown to promote hypertelomere clustering. In strains that over expressed Sir3 at the endogenous locus with a strong GAL1p promoter, Ruault et al., (2011) showed that telomere clustering is dependent on the degree of Sir3 expression. By monitoring the localization of telomeres by overlapping fluorescently labeled Sir4, Sir2, and Sir3 with telomeres probed for Y′ elements through FISH, SIR3 overexpression was seen to cluster telomeres into a single bright focus that localized away from the nuclear periphery (Ruault et al., 2011). Similarly, a loss in telomere tethering at the NE was seen when either *SCS2* was deleted (Natasha Saik, unpublished observations) or when SUMO conjugates accumulated in the

ulp1 mutants. Both the *scs2Δ* and the *ulp1ts* or *ulp1ts smt3-ATYΔ* mutants mislocalized telomeres from the periphery and increased the amount of Sir3 bound to Sir4, showing similar phenotypes as *SIR3* over expression that clustered telomeres away from the periphery into one bright focus. Together, this suggests that telomeres are clustering in either the *ulp1ts* or *ulp1ts smt3-ATYΔ* mutants potentially by increasing levels of SUMOylation or by deleting *SCS2* (Figure 3-3, and Figure 4-2). SUMO could be facilitating the interaction between Sir proteins in much the same way as the over expression of Sir3 increased telomere-telomere interactions through an increase in interaction between Sir3 proteins. SUMOylated Sir3 or SUMOylated Sir4 could promote an increase in the interaction between Sir4 and Sir3 seen within either the *ulp1ts* or *ulp1ts smt3-ATYΔ* mutants, which could further indicate an increase in telomere-telomere interaction (Figure 4-3).

5.5 Silencing as it relates to the organization of the SIR complex

SUMOylation has been implicated in regulating gene expression. For example, SUMOylation of the tumor suppressor, p53, has been shown to increase its ability to act as a transactivator , indicating that SUMOylation can promote gene expression (Gostissa et al., 1999; Rodriguez et al., 1999). The increase in subtelomeric gene expression shown in the *ulp1ts* and *ulp1ts smt3-ATYΔ* mutants could result from inhibiting proteins that bind on chromatin to facilitate silencing. How SUMO could be functioning at telomeres to promote the loss of silencing seen in either the *ulp1ts* or *ulp1ts smt3ATYΔ* would be through alterations in the ability of silencing proteins to establish repressed chromatin. Overexpressing Siz2 has been shown to alter silencing at both subtelomeric chromatin

and at HMR; potentially through an increase in Siz2 mediated SUMOylation. This loss in silencing is further exacerbated by deleting *ESC1* (Pasupala et al.,2012). The organization of the SIR complex at silenced chromatin can also be disrupted by increasing Siz2 expression. Over expressing Siz2, coupled with deleting *ESC1*, caused both Sir4 and Sir2 to bind less at HMR and prevented Sir2 from binding at subtelomeric chromatin (Pasupala et al., 2012). Additionally, the organization of the SIR complex is altered when Sir2 is modified with SUMO. SUMOylated Sir2 is unable to bind Sir4 and SUMOylated Sir2 preferentially localizes to the nucleolus (Hannan et al., 2015). Together, this suggests that increasing SUMOylation can affect SIR complex organization and affect the recruitment of Sir proteins onto silenced chromatin, thus promote a loss of silencing (Figure 3-4 and Figure 3-5).

5.6 SUMO mediates complex organization

The binding of Nups with chromatin has been shown to alter the ability of chromatin to localize at the nuclear periphery. In *Drosophilia malanogaster* cells, the orthologue of Nup170 (Nup155) mediates chromatin binding to the NE and this binding can be inhibited with the recruitment of Nup62 (Breuer & Ohkura, 2015). In this way, Lapetina et al., (2017) speculate that the binding of a non-Snup protein, Nup53, with Nup170 could alter the ability of Nup170 to associate with the Snup complex. This would suggest that the Snup complex could function as a NPC intermediate, where the binding of Nups would transistion the pool of Nups that associate with the Snup complex to favor integrating into NPCs. An alternative to this notion would involve the cycling of SUMO as a switch to mediate the organization of Nups at the Snup complex into

integrating into nascent NPCs. In this way, the isopeptidase activity of Ulp1 could function to orgainize the Snup complex. The reduction in Nup170 bound to Sir4 seen in both the *ulp1ts* and *ulp1K352E-V5*$_3$ mutant would support this notion (Figure 4-1). Siz2, being a component of the Snup complex, could SUMOylate Snup proteins and the removal of SUMO would occur following the transition of this complex to the nuclear periphery. At the nuclear periphery, Ulp1 could gain acess to these substrates, where upon the removal of SUMO could alter Snup complex oragnaization into a state more favorible for Nup integration into NPCs. In this way, the cycling of SUMO would mediate the interactions between Snup components as a method to promote the integration of Nups into nascent NPCs.

Our studies reveal how different ulp1 mutants impact the ability of proteins to interact with each other. Expressing different mutant *ulp1* alleles mislocalized telomeres from the nuclear periphery, altered the ability of subtelomeric proteins to organize with each other, and mislocalized Sir proteins away from the nuclear periphery. There were additional defects in the establishment of subtelomeric silencing by expressing either the *ulp1ts* or the *ulp1ts smt3ATYΔ* mutant alleles. The mislocalization of Sir4 away from the NE, along with a loss in the copurification of Nup170 from Sir4 suggest potential consequences that can be seen by impairing the isopeptidase activity of Ulp1. Additionally, the copurification between proteins of the SIR complex is increased when either *SCS2* is deleted or when ulp1 is mutated, suggesting that telomeres are potentially clustering. Future studies will need to be done to identify which targets are being SUMOylated in these different Ulp1 mutants and whether the SUMOylation of these targets are promoting the altered organization of proteins localized at the NE.

References

Abraham, J., Nasmyth, K. A., Strathern, J. N., Klar, A. J., & Hicks (1984). Regulation of mating-type information in yeast: negative control requiring sequences both 5′ and 3′ to the regulated region. *The Journal of Molecular Biology, 176*(3), 307-331.

Aitchison, J. D., Rout, M. P., Marelli, M., Blobel, G., & Wozniak, R. W. (1995). Two novel related yeast nucleoporins Nup170p and Nup157p: complementation with the vertebrate homologue Nup155p and functional interactions with the yeast nuclear pore-membrane protein Pom152p. *The Journal of cell biology*, *131*(5), 1133-1148.

Aksenova, A. Y., Greenwell, P. W., Dominska, M., Shishkin, A. A., Kim, J. C., Petes, T. D., & Mirkin, S. M. (2013). Genome rearrangements caused by interstitial telomeric sequences in yeast. *PNAS, 110*(49), 19866-19871.

Alber, F., Dokudovskaya, S., Veenhoff, L. M., Zhang, W., Kipper, J., Devos, D., . . . Chait, B. T. (2007a). Determining the architectures of macromolecular assemblies. *Nature, 450*(7170), 683-694.

Andrulis, E. D., Zappulla, D. C., Ansari, A., Perrod, S., Laiosa, C. V., Gartenberg, M. R., & Sternglanz, R. J. (2002). Esc1, a nuclear periphery protein required for Sir4-based plasmid anchoring and partitioning. *Molecular and Cellular Biology, 22*(23), 8292-8301.

Bernier-Villamor, V., Sampson, D. A., Matunis, M. J., & Lima, C. D. (2002). Structural basis for E2-mediated SUMO conjugation revealed by a complex between ubiquitin-conjugating enzyme Ubc9 and RanGAP1. *Cell, 108*(3), 345-356.

Berterame, N. M., Porro, D., Ami, D., & Branduardi, P. (2016). Protein aggregation and membrane lipid modifications under lactic acid stress in wild type and OPI1 deleted Saccharomyces cerevisiae strains. *Microbial Cell Factories, 15*(1), 39.

Berthiau, A. S., Yankulov, K., Bah, A., Revardel, E., Luciano, P., Wellinger, R. J., . . . Gilson, E. J. (2006). Subtelomeric proteins negatively regulate telomere elongation in budding yeast. *25*(4), 846-856.

Bi, X., & Broach, J. R. (1999). UASrpg can function as a heterochromatin boundary element in yeast. *Genes & Development, 13*(9), 1089-1101.

Blobel, G. J. (1985). Gene gating: a hypothesis. *PNAS, 82*(24), 8527-8529.

Boudreau, É., Labib, S., Bertrand, A. T., Decostre, V., Bolongo, P. M., Sylvius, N., . . . Tesson, F. (2012). Lamin A/C mutants disturb sumo1 localization and sumoylation in vitro and in vivo. *PLoS One, 7*(9), e45918.

Boulton, S. J., & Jackson, S. P. (1996a). Identification of a Saccharomyces cerevisiae Ku80 homologue: roles in DNA double strand break rejoining and in telomeric maintenance. *Nucleic Acids Research, 24*(23), 4639-4648.

Boulton, S. J., & Jackson, S. P. (1996b). Saccharomyces cerevisiae Ku70 potentiates illegitimate DNA double-strand break repair and serves as a barrier to error-prone DNA repair pathways. *The EMBO Journal, 15*(18), 5093-5103.

Bourgeois, C., Laquerriere, F., Hemon, D., Hubert, J., & Bouteille, M. J. (1985). New data on the in situ position of the inactive X chromosome in the interphase nucleus of human fibroblasts. *Human Genetics, 69*(2), 122-129.

Brachmann, C. B., Sherman, J. M., Devine, S. E., Cameron, E. E., Pillus, L., & Boeke, J. D. (1995). The SIR2 gene family, conserved from bacteria to humans, functions

in silencing, cell cycle progression, and chromosome stability. *Genes & Development, 9*(23), 2888-2902.
Braunstein, M., Rose, A. B., Holmes, S. G., Allis, C. D., Broach, J. R. (1993). Transcriptional silencing in yeast is associated with reduced nucleosome acetylation. *Genes and Development, 7*(4), 592-604.
Breuer, M., & Ohkura, H. (2015). A negative loop within the nuclear pore complex controls global chromatin organization. *Genes & Development, 29*(17), 1789-1794.
Broers, J., Ramaekers, F., Bonne, G., Yaou, R. B., & Hutchison, C. (2006). Nuclear lamins: laminopathies and their role in premature ageing. *Physiological Reviews, 86*(3), 967-1008.
Bupp, J. M., Martin, A. E., Stensrud, E. S., & Jaspersen, S. L. (2007). Telomere anchoring at the nuclear periphery requires the budding yeast Sad1-UNC-84 domain protein Mps3. *The Journal of Cell Biology, 179*(5), 845-854.
Burke, B., & Stewart, C. L. (2014). Functional architecture of the cell's nucleus in development, aging, and disease. *Current Topics in Developmental Biology* (Vol. 109, pp. 1-52): Elsevier.
Callan, H. G., & Tomlin, S. J. (1950). Experimental studies on amphibian oocyte nuclei I. Investigation of the structure of the nuclear membrane by means of the electron microscope. *Proceeings of the Royal Society of Biological Sciences, 137*(888), 367-378.
Campbell, J. L., Lorenz, A., Witkin, K. L., Hays, T., Loidl, J., & Cohen-Fix, O. (2006). Yeast nuclear envelope subdomains with distinct abilities to resist membrane expansion. *Molecular Biology of the Cell, 17*(4), 1768-1778.
Capelson, M., Liang, Y., Schulte, R., Mair, W., Wagner, U., & Hetzer, M. W. (2010). Chromatin-bound nuclear pore components regulate gene expression in higher eukaryotes. *Cell, 140*(3), 372-383.
Capitanio, J. S. (2016). Github-ImageJ Script.
Cavalli, G., & Misteli, T. (2013). Functional implications of genome topology. *Nature Structural & Molecular Biology, 20*(3), 290-299.
Chan, C. S., Tye, B.-K., & Herskowitz, I. J.(1983). A family of Saccharomyces cerevisiae repetitive autonomously replicating sequences that have very similar genomic environments. *Journal of Molecular Biology, 168*(3), 505-523.
Chan, C. S., & Tye, B.-K. (1983). Organization of DNA sequences and replication origins at yeast telomeres. *Cell, 33*(2), 563-573.
Chang, J.-F., Hall, B. E., Tanny, J. C., Moazed, D., Filman, D., & Ellenberger, T. (2003). Structure of the coiled-coil dimerization motif of Sir4 and its interaction with Sir3. *Structure, 11*(6), 637-649.
Chien, C.-t., Buck, S., Sternglanz, R., & Shore, D. (1993). Targeting of SIR1 protein establishes transcriptional silencing at HM loci and telomeres in yeast. *Cell, 75*(3), 531-541.
Chung, I., Zhao, X. J. (2015). DNA break-induced sumoylation is enabled by collaboration between a SUMO ligase and the ssDNA-binding complex RPA. *Genes and Development, 29*(15), 1593-1598.

Churikov, D., Charifi, F., Eckert-Boulet, N., Silva, S., Simon, M.-N., Lisby, M., & Géli, V. (2016). SUMO-dependent relocalization of eroded telomeres to nuclear pore complexes controls telomere recombination. *Cell Reports, 15*(6), 1242-1253.

Cowan, C. R., Carlton, P. M., & Cande, W. Z. (2001). The polar arrangement of telomeres in interphase and meiosis. Rabl organization and the bouquet. *Plant Physiology, 125*(2), 532-538.

Cremer, T., & Cremer, M. (2010). Chromosome territories. *Cold Spring Harbor Perspectives in Biology, 2*(3), a003889.

Cremona, C. A., Sarangi, P., & Zhao, X. (2012). Sumoylation and the DNA damage response. *Biomolecules, 2*(3), 376-388.

Croft, J. A., Bridger, J. M., Boyle, S., Perry, P., Teague, P., & Bickmore, W. A. (1999). Differences in the localization and morphology of chromosomes in the human nucleus. *The Journal of Cell Biology, 145*(6), 1119-1131.

D'Amours, D., Jackson, S. P. (2001). The yeast Xrs2 complex functions in S phase checkpoint regulation. *Genes and Development, 15*(17), 2238-2249.

del Dedo, J. E., Idrissi, F.-Z., Fernandez-Golbano, I. M., Garcia, P., Rebollo, E., Krzyzanowski, M. K., . . . Geli, M. I.(2017). ORP-Mediated ER Contact with Endocytic Sites Facilitates Actin Polymerization. *Developmental Cell, 43*(5), 588-602.

Desterro, J. M., Rodriguez, M. S., & Hay, R. T. (1998). SUMO-1 modification of IκBα inhibits NF-κB activation. *Molecular Cell, 2*(2), 233-239.

Dhillon, N., Raab, J., Guzzo, J., Szyjka, S. J., Gangadharan, S., Aparicio, O. M., . . . Kamakaka, R. T. (2009). DNA polymerase ε, acetylases and remodellers cooperate to form a specialized chromatin structure at a tRNA insulator. *The EMBO Journal, 28*(17), 2583-2600.

Diffley, J. F., & Stillman, B. (1989). Transcriptional silencing and lamins. *Nature, 342*(6245), 24-24.

Donze, D., & Kamakaka, R. T. (2001). RNA polymerase III and RNA polymerase II promoter complexes are heterochromatin barriers in Saccharomyces cerevisiae. *The EMBO Journal, 20*(3), 520-531.

Dreger, M., Bengtsson, L., Schöneberg, T., Otto, H., & Hucho, F. J. (2001). Nuclear envelope proteomics: novel integral membrane proteins of the inner nuclear membrane. *PNAS, 98*(21), 11943-11948.

Ebrahimi, H., & Donaldson, A. D. (2008). Release of yeast telomeres from the nuclear periphery is triggered by replication and maintained by suppression of Ku-mediated anchoring. *Genes & Development, 22*(23), 3363-3374.

Ehrentraut, S., Hassler, M., Oppikofer, M., Kueng, S., Weber, J. M., Mueller, J. W., . . . Ehrenhofer-Murray, A. E. (2011). Structural basis for the role of the Sir3 AAA+ domain in silencing: interaction with Sir4 and unmethylated histone H3K79. *Genes & development, 25*(17), 1835-1846.

Ellahi, A., Thurtle, D. M., & Rine, J. J. G. (2015). The chromatin and transcriptional landscape of native Saccharomyces cerevisiae telomeres and subtelomeric domains. *Genetics*, *200*(2), 505-521.

Evans, S. K., & Lundblad, V. J. (1999). Est1 and Cdc13 as comediators of telomerase access. *Science, 286*(5437), 117-120.

Fajardo, V. A., McMeekin, L., & LeBlanc, P. J. (2011). Influence of phospholipid species on membrane fluidity: a meta-analysis for a novel phospholipid fluidity index. *The Journal of Membrane Biology, 244*(2), 97-103.

Felberbaum, R., Wilson, N. R., Cheng, D., Peng, J., & Hochstrasser, M. (2012). Desumoylation of the endoplasmic reticulum membrane VAP family protein Scs2 by Ulp1 and SUMO regulation of the inositol synthesis pathway. *Molecular and Cellular Biology, 32*(1), 64-75.

Feldman, J. B., Hicks, J. B., & Broach, J. R. (1984). Identification of sites required for repression of a silent mating type locus in yeast. *Journal of Molecular Biology, 178*(4), 815-834.

Ferreira, H. C., Luke, B., Schober, H., Kalck, V., Lingner, J., & Gasser, S. M. (2011). The PIAS homologue Siz2 regulates perinuclear telomere position and telomerase activity in budding yeast. *Nature Cell Biology, 13*(7), 867-874.

Feuerbach, F., Galy, V., Trelles-Sticken, E., Fromont-Racine, M., Jacquier, A., Gilson, E., . . . Nehrbass, U. J. (2002). Nuclear architecture and spatial positioning help establish transcriptional states of telomeres in yeast. *Nature Cell Biology*, *4*(3), 214.

Fisher, T. S., Taggart, A. K., & Zakian, V. A.(2004). Cell cycle-dependent regulation of yeast telomerase by Ku. *Nature Structural and Molecular Biology11*(12), 1198.

Flotho, A., & Melchior, F. (2013). Sumoylation: a regulatory protein modification in health and disease. *Annual Review of Biochemistry, 82*, 357-385.

Fourel, G., Revardel, E., Koering, C. E., & Gilson, É. J. (1999). Cohabitation of insulators and silencing elements in yeast subtelomeric regions. *The EMBO Journal, 18*(9), 2522-2537.

Fritze, C. E., Verschueren, K., Strich, R., & Esposito, R. E. (1997). Direct evidence for SIR2 modulation of chromatin structure in yeast rDNA. *The EMBO Journal, 16*(21), 6495-6509.

Frolova, E., Majors, J., & Johnston, M. (1999). Binding of the glucose-dependent Mig1p repressor to the GAL1 and GAL4 promoters in vivo: regulation by glucose and chromatin structure. *Nucleic Acids Research, 27*(5), 1350-1358.

Galy, V., Olivo-Marin, J.-C., Scherthan, H., Doye, V., Rascalou, N., & Nehrbass, U. J. (2000). Nuclear pore complexes in the organization of silent telomeric chromatin. *Nature, 403*(6765), 108.

Gao, H., Cervantes, R. B., Mandell, E. K., Otero, J. H., & Lundblad, V. J. (2007). RPA-like proteins mediate yeast telomere function. *Nature Structural and Molecular Biology, 14*(3), 208.

Geiss-Friedlander, R., & Melchior, F. (2007). Concepts in sumoylation: a decade on. *Nature reviews Molecular Cell Biology, 8*(12), 947.

Golebiowski, F., Matic, I., Tatham, M. H., Cole, C., Yin, Y., Nakamura, A., . . . Hay, R. T. (2009). System-wide changes to SUMO modifications in response to heat shock. *Sci. Signal., 2*(72).

Gostissa, M., Hengstermann, A., Fogal, V., Sandy, P., Schwarz, S. E., Scheffner, M., & Del Sal, G. (1999). Activation of p53 by conjugation to the ubiquitin-like protein SUMO-1. *The EMBO Journal, 18*(22), 6462-6471.

Gotta, M., Laroche, T., Formenton, A., Maillet, L., Scherthan, H., & Gasser, S. M. (1996). The clustering of telomeres and colocalization with Rap1, Sir3, and Sir4

proteins in wild-type Saccharomyces cerevisiae. *The Journal of Cell Biology, 134*(6), 1349-1363.
Gottlieb, S., & Esposito, R. E. (1989). A new role for a yeast transcriptional silencer gene, SIR2, in regulation of recombination in ribosomal DNA. *Cell, 56*(5), 771-776.
Gottschling, D. E., Aparicio, O. M., Billington, B. L., & Zakian, V. A. (1990). Position effect at S. cerevisiae telomeres: reversible repression of Pol II transcription. *Cell, 63*(4), 751-762.
Grossman, E., Medalia, O., & Zwerger, M. (2012). Functional architecture of the nuclear pore complex. *Annual Review of Biophysics*, *41*, 557-584.
Hannan, A., Abraham, N. M., Goyal, S., Jamir, I., Priyakumar, U. D., & Mishra, K. (2015). Sumoylation of Sir2 differentially regulates transcriptional silencing in yeast. *Nucleic Acids Research, 43*(21), 10213-10226.
Hardeland, U., Steinacher, R., Jiricny, J., & Schär, P. (2002). Modification of the human thymine-DNA glycosylase by ubiquitin-like proteins facilitates enzymatic turnover. *The EMBO Journal, 21*(6), 1456-1464.
Hardy, C., Sussel, L., & Shore, D. J. (1992a). A RAP1-interacting protein involved in transcriptional silencing and telomere length regulation. *Genes and Development, 6*(5), 801-814. Hardy, C., Balderes, D., & Shore, D. (1992b). Dissection of a carboxy-terminal region of the yeast regulatory protein RAP1 with effects on both transcriptional activation and silencing. *Molecular and cellular biology, 12*(3), 1209-1217.
Hardy, C., Balderes, D., & Shore, D. (1992b). Dissection of a carboxy-terminal region of the yeast regulatory protein RAP1 with effects on both transcriptional activation and silencing. *Molecular and cellular biology, 12*(3), 1209-1217.
Hattier, T., Andrulis, E. D., & Tartakoff, A. M. (2007). Immobility, inheritance and plasticity of shape of the yeast nucleus. *BMC Cell Biology, 8*(1), 47.
Hediger, F., Berthiau, A. S., van Houwe, G., Gilson, E., & Gasser, S. M. (2006). Subtelomeric factors antagonize telomere anchoring and Tel1-independent telomere length regulation. *The EMBO Journal, 25*(4), 857-867.
Hediger, F., Dubrana, K., & Gasser, S. M. (2002). Myosin-like proteins 1 and 2 are not required for silencing or telomere anchoring, but act in the Tel1 pathway of telomere length control. *The Journal of Structural Biology, 140*(1-3), 79-91.
Hediger, F., Neumann, F. R., Van Houwe, G., Dubrana, K., & Gasser, S. M. (2002). Live imaging of telomeres: yKu and Sir proteins define redundant telomere-anchoring pathways in yeast. *Current Biology, 12*(24), 2076-2089.
Hickey, C. M., Wilson, N. R., & Hochstrasser, M. J.(2012). Function and regulation of SUMO proteases. *Nature Reviews Molecular and Cell Biology, 13*(12), 755.
Hoppe, G. J., Tanny, J. C., Rudner, A. D., Gerber, S. A., Danaie, S., Gygi, S. P., & Moazed, D. (2002). Steps in assembly of silent chromatin in yeast: Sir3-independent binding of a Sir2/Sir4 complex to silencers and role for Sir2-dependent deacetylation. *Molecular and Cellular Biology, 22*(12), 4167-4180.
Horigome, C., Bustard, D. E., Marcomini, I., Delgoshaie, N., Tsai-Pflugfelder, M., Cobb, J. A., & Gasser, S. M. (2016). PolySUMOylation by Siz2 and Mms21 triggers relocation of DNA breaks to nuclear pores through the Slx5/Slx8 STUbL. *Genes & Development, 30*(8), 931-945.

Hughes, T. R., Evans, S. K., Weilbaecher, R. G., & Lundblad, V. (2000). The Est3 protein is a subunit of yeast telomerase. *Current Biology, 10*(13), 809-812.

Jain, D., & Cooper, J. P.(2010). Telomeric strategies: means to an end. *Annual Review of Genetics, 44*, 243-269.

Jin, Q.-W., Fuchs, J., & Loidl, J. (2000). Centromere clustering is a major determinant of yeast interphase nuclear organization. The *Journal of Cell Science, 113*(11), 1903-1912.

Johnson, E. S., & Gupta, A. A. (2001). An E3-like factor that promotes SUMO conjugation to the yeast septins. *Cell, 106*(6), 735-744.

Kaiser, S. E., Brickner, J. H., Reilein, A. R., Fenn, T. D., Walter, P., & Brunger, A. T. (2005). Structural basis of FFAT motif-mediated ER targeting. *Structure*, *13*(7), 1035-1045.

Koehler, D., Zakhartchenko, V., Froenicke, L., Stone, G., Stanyon, R., Wolf, E., . . . Brero, A. J.(2009). Changes of higher order chromatin arrangements during major genome activation in bovine preimplantation embryos. *Experimental Cell Research, 315*(12), 2053-2063.

Krull, S., Dörries, J., Boysen, B., Reidenbach, S., Magnius, L., Norder, H., . . . Cordes, V. C. (2010). Protein Tpr is required for establishing nuclear pore-associated zones of heterochromatin exclusion. *The EMBO Journal, 29*(10), 1659-1673.

Kupiec, M. (2014). Biology of telomeres: lessons from budding yeast. *FEMS Microbiology Reviews, 38*(2), 144-171.

Kyrion, G., Liu, K., Liu, C., & Lustig, A. (1993). RAP1 and telomere structure regulate telomere position effects in Saccharomyces cerevisiae. *Genes & Development, 7*(7a), 1146-1159.

Lapetina, D. L., Ptak, C., Roesner, U. K., & Wozniak, R. W. (2017). Yeast silencing factor Sir4 and a subset of nucleoporins form a complex distinct from nuclear pore complexes. *The Journal of Cell Biology, 216*(10), 3145-3159.

Laroche, T., Martin, S. G., Gotta, M., Gorham, H. C., Pryde, F. E., Louis, E. J., & Gasser, S. M.(1998). Mutation of yeast Ku genes disrupts the subnuclear organization of telomeres. *Current Biology, 8*(11), 653-657.

Lee, S., Lim, W. A., & Thorn, K. S. (2013). Improved blue, green, and red fluorescent protein tagging vectors for S. cerevisiae. *PloS One*, *8*(7), e67902.

Levy, D. L., & Blackburn, E. H. (2004). Counting of Rif1p and Rif2p on Saccharomyces cerevisiae telomeres regulates telomere length. *Molecular and Cellular Biology, 24*(24), 10857-10867.

Lewis, A., Felberbaum, R., & Hochstrasser, M. (2007). A nuclear envelope protein linking nuclear pore basket assembly, SUMO protease regulation, and mRNA surveillance. *The Journal of Cell Biology, 178*(5), 813-827.

Li, S.-J., & Hochstrasser, M. (1999). A new protease required for cell-cycle progression in yeast. *Nature, 398*(6724), 246-251.

Li, S.-J., & Hochstrasser, M. (2003). The Ulp1 SUMO isopeptidase: distinct domains required for viability, nuclear envelope localization, and substrate specificity. *The Journal of Cell Biology, 160*(7), 1069-1082.

Li, S.-J., & Hochstrasser, M. J. (2000). The yeast ULP2 (SMT4) gene encodes a novel protease specific for the ubiquitin-like Smt3 protein. *Molecular and Cellular Biology, 20*(7), 2367-2377.

Light, W. H., Brickner, D. G., Brand, V. R., & Brickner, J. H. (2010). Interaction of a DNA zip code with the nuclear pore complex promotes H2A. Z incorporation and INO1 transcriptional memory. *Molecular Cell, 40*(1), 112-125.

Lin, X., Sun, B., Liang, M., Liang, Y.-Y., Gast, A., Hildebrand, J., . . . Feng, X.-H. (2003). Opposed regulation of corepressor CtBP by SUMOylation and PDZ binding. *Molecular Cell, 11*(5), 1389-1396.

Loewen, C. J., & Levine, T. P. (2005). A highly conserved binding site in vesicle-associated membrane protein-associated protein (VAP) for the FFAT motif of lipid-binding proteins. *The Journal of Biological Chemistry, 280*(14), 14097-14104.

Longtine, M. S., Mckenzie III, A., Demarini, D. J., Shah, N. G., Wach, A., Brachat, A., ... & Pringle, J. R. (1998). Additional modules for versatile and economical PCR-based gene deletion and modification in Saccharomyces cerevisiae. *Yeast*, *14*(10), 953-961.

Louis, E. J., & Haber, J. E. (1992). The structure and evolution of subtelomeric Y'repeats in Saccharomyces cerevisiae. *Genetics, 131*(3), 559-574

Louis, E., Naumova, E., Lee, A., Naumov, G., & Haber, J. (1994). The chromosome end in yeast: its mosaic nature and influence on recombinational dynamics. *Genetics, 136*(3), 789-802.

Luo, K., Vega-Palas, M. A., & Grunstein, M. (2002). Rap1–Sir4 binding independent of other Sir, yKu, or histone interactions initiates the assembly of telomeric heterochromatin in yeast. *Genes & Development, 16*(12), 1528-1539.

Mahajan, R., Delphin, C., Guan, T., Gerace, L., & Melchior, F. J. (1997). A small ubiquitin-related polypeptide involved in targeting RanGAP1 to nuclear pore complex protein RanBP2. *Cell, 88*(1), 97-107.

Makhnevych, T., Ptak, C., Lusk, C. P., Aitchison, J. D., & Wozniak, R. (2007). The role of karyopherins in the regulated sumoylation of septins. *The Journal of Cell Biology, 177*(1), 39-49.

Manford, A. G., Stefan, C. J., Yuan, H. L., MacGurn, J. A., & Emr, S. D. J. (2012). ER-to-plasma membrane tethering proteins regulate cell signaling and ER morphology. *Developmental Cell, 23*(6), 1129-1140.

Marcand, S., Gilson, E., & Shore, D. (1997). A protein-counting mechanism for telomere length regulation in yeast. *Science, 275*(5302), 986-990.

Martin, S. G., Laroche, T., Suka, N., Grunstein, M., & Gasser, S. M. (1999). Relocalization of telomeric Ku and SIR proteins in response to DNA strand breaks in yeast. *Cell, 97*(5), 621-633.

Matunis, M. J., Coutavas, E., & Blobel, G. J. (1996). A novel ubiquitin-like modification modulates the partitioning of the Ran-GTPase-activating protein RanGAP1 between the cytosol and the nuclear pore complex. *The Journal of Cell Biology, 135*(6), 1457-1470.

Matunis, M. J., Wu, J., & Blobel, G. J. (1998). SUMO-1 modification and its role in targeting the Ran GTPase-activating protein, RanGAP1, to the nuclear pore complex. *The Journal of Cell Biology, 140*(3), 499-509.

Mekhail, K., Seebacher, J., Gygi, S. P., & Moazed, D. (2008). Role for perinuclear chromosome tethering in maintenance of genome stability. *Nature, 456*(7222), 667

Mishra, K., & Shore, D. (1999). Yeast Ku protein plays a direct role in telomeric silencing and counteracts inhibition by rif proteins. *Current Biology, 9*(19), 1123-S1122.

Mondoux, M. A., Scaife, J. G., & Zakian, V. A. (2007). Differential nuclear localization does not determine the silencing status of Saccharomyces cerevisiae telomeres. *Genetics, 177*(4), 2019-2029.

Moazed, D., Kistler, A., Axelrod, A., Rine, J., & Johnson, A. D. (1997). Silent information regulator protein complexes in Saccharomyces cerevisiae: a SIR2/SIR4 complex and evidence for a regulatory domain in SIR4 that inhibits its interaction with SIR3. *PNAS, 94*(6), 2186-2191.

Negrini, S., Ribaud, V., Bianchi, A., & Shore, D. (2007). DNA breaks are masked by multiple Rap1 binding in yeast: implications for telomere capping and telomerase regulation. *Genes & Development, 21*(3), 292-302.

Niepel, M., Molloy, K. R., Williams, R., Farr, J. C., Meinema, A. C., Vecchietti, N., . . . Strambio-De-Castillia, C. (2013). The nuclear basket proteins Mlp1p and Mlp2p are part of a dynamic interactome including Esc1p and the proteasome. *Molecular Biology of the Cell, 24*(24), 3920-3938.

Niepel, M., Strambio-de-Castillia, C., Fasolo, J., Chait, B. T., & Rout, M. P. (2005). The nuclear pore complex–associated protein, Mlp2p, binds to the yeast spindle pole body and promotes its efficient assembly. *The Journal of Cell Biology, 170*(2), 225-235.

Nikawa, J.-i., Murakami, A., Esumi, E., & Hosaka, K. J. (1995). Cloning and sequence of the SCS2 gene, which can suppress the defect of IN01 expression in an inositol auxotrophic mutant of Saccharomyces cerevisiae. *The Journal of Biochemistry, 118*(1), 39-45.

Oki, M., & Kamakaka, R. T. (2005). Barrier function at HMR. *Molecular Cell, 19*(5), 707-716.

Olsen, S. K., Capili, A. D., Lu, X., Tan, D. S., & Lima, C. D. (2010). Active site remodelling accompanies thioester bond formation in the SUMO E1. *Nature, 463*(7283), 906.

Onishi, M., Liou, G.-G., Buchberger, J. R., Walz, T., & Moazed, D. J. (2007). Role of the conserved Sir3-BAH domain in nucleosome binding and silent chromatin assembly. *Molecular Cell, 28*(6), 1015-1028.

Oppikofer, M., Kueng, S., Keusch, J. J., Hassler, M., Ladurner, A. G., Gut, H., & Gasser, S. M. (2013). Dimerization of Sir3 via its C-terminal winged helix domain is essential for yeast heterochromatin formation. *The EMBO Journal, 32*(3), 437-449.

Palancade, B., Liu, X., Garcia-Rubio, M., Aguilera, A., Zhao, X., & Doye, V. (2007). Nucleoporins prevent DNA damage accumulation by modulating Ulp1-dependent sumoylation processes. *Molecular Biology of the Cell, 18*(8), 2912-2923.

Panse, V. G., Küster, B., Gerstberger, T., & Hurt, E. J. (2003). Unconventional tethering of Ulp1 to the transport channel of the nuclear pore complex by karyopherins. *Nature Cell Biology, 5*(1), 21.

Pasupala, N., Easwaran, S., Hannan, A., Shore, D., & Mishra, K. (2012). The SUMO E3 ligase Siz2 exerts a locus-dependent effect on gene silencing in Saccharomyces cerevisiae. *Eukaryotic cell, 11*(4), 452-462.

Pennock, E., Buckley, K., & Lundblad, V. (2001). Cdc13 delivers separate complexes to the telomere for end protection and replication. *Cell, 104*(3), 387-396.

Peric-Hupkes, D., Meuleman, W., Pagie, L., Bruggeman, S. W., Solovei, I., Brugman, W., . . . van Lohuizen, M. (2010). Molecular maps of the reorganization of genome-nuclear lamina interactions during differentiation. *Molecular cell, 38*(4), 603-613.

Plechanovová, A., Jaffray, E. G., Tatham, M. H., Naismith, J. H., & Hay, R. T. (2012). Structure of a RING E3 ligase and ubiquitin-loaded E2 primed for catalysis. *Nature, 489*(7414), 115.

Polioudaki, H., Kourmouli, N., Drosou, V., Bakou, A., Theodoropoulos, P. A., Singh, P. B., . . . Georgatos, S. D. (2001). Histones H3/H4 form a tight complex with the inner nuclear membrane protein LBR and heterochromatin protein 1. *EMBO reports, 2*(10), 920-925.

Pryde, F. E., Huckle, T. C., & Louis, E. J. (1995). Sequence analysis of the right end of chromosome XV in Saccharomyces cerevisiae: an insight into the structural and functional significance of sub-telomeric repeat sequences. *Yeast, 11*(4), 371-382.

Psakhye, I., & Jentsch, S. (2012). Protein group modification and synergy in the SUMO pathway as exemplified in DNA repair. *Cell, 151*(4), 807-820.

Rabl, C. (1885). Uber zelltheilung. *Morphol. Jahrb., 10*, 214-330. .

Raich, N., Mahmoudi, S., Emre, D., & Karess, R. E. (2018). Mad1 influences interphase nucleoplasm organization and chromatin regulation in Drosophila. *Open Biology, 8*(10), 180166.

Richards, O. W. (1928). The growth of the yeast Saccharomyces cerevisiae. I. The growth curve, its mathematical analysis, and the effect of temperature on the yeast growth. *Annals of Botany*, *42*(165), 271-283.

Rine, J., & Herskowitz, I. (1987). Four genes responsible for a position effect on expression from HML and HMR in Saccharomyces cerevisiae. *Genetics, 116*(1), 9-22.

Robbins, J., Dilwortht, S. M., Laskey, R. A., & Dingwall, C. (1991). Two interdependent basic domains in nucleoplasmin nuclear targeting sequence: identification of a class of bipartite nuclear targeting sequence. *Cell, 64*(3), 615-623.

Rodriguez, M. S., Desterro, J. M., Lain, S., Midgley, C. A., Lane, D. P., & Hay, R. T. (1999). SUMO-1 modification activates the transcriptional response of p53. *The EMBO Journal, 18*(22), 6455-6461.

Rohner, S., Gasser, S. M., & Meister, P. (2008). Modules for cloning-free chromatin tagging in Saccharomyces cerevisae. *Yeast*, *25*(3), 235-239.

Rout, M. P., & Aitchison, J. D. (2001). The nuclear pore complex as a transport machine. *Journal of Biological Chemistry, 276*(20), 16593-16596.

Rouvière, J. O., Bulfoni, M., Tuck, A., Cosson, B., Devaux, F., & Palancade, B. (2018). A SUMO-dependent feedback loop senses and controls the biogenesis of nuclear pore subunits. *Nature Communications, 9*.

Ruault, M., De Meyer, A., Loïodice, I., & Taddei, A. (2011). Clustering heterochromatin: Sir3 promotes telomere clustering independently of silencing in yeast. *The Journal of Cell Biology, 192*(3), 417-431.

Rusché, L. N., Kirchmaier, A. L., & Rine, J. (2002). Ordered nucleation and spreading of silenced chromatin in Saccharomyces cerevisiae. *Molecular Biology of the Cell, 13*(7), 2207-2222.

Ryan, K. J., & Wente, S. R. (2002). Isolation and characterization of new Saccharomyces cerevisiae mutants perturbed in nuclear pore complex assembly. *BMC genetics, 3*(1), 17.

Sabourin, M., Tuzon, C. T., & Zakian, V. A. (2007). Telomerase and Tel1p preferentially associate with short telomeres in S. cerevisiae. *Molecular Cell, 27*(4), 550-561.

Schober, H., Ferreira, H., Kalck, V., Gehlen, L. R., & Gasser, S. M. (2009). Yeast telomerase and the SUN domain protein Mps3 anchor telomeres and repress subtelomeric recombination. *Genes & Development, 23*(8), 928-938.

Shampay, J., Szostak, J. W., & Blackburn, E. H. (1984). DNA sequences of telomeres maintained in yeast. *Nature, 310*(5973), 154.

Singer, M. S., & Gottschling, D. E. (1994). TLC1: template RNA component of Saccharomyces cerevisiae telomerase. *Science, 266*(5184), 404-409

Smith, J. S., & Boeke, J. D. (1997). An unusual form of transcriptional silencing in yeast ribosomal DNA. *Genes & Development, 11*(2), 241-254.

Smoyer, C. J., Katta, S. S., Gardner, J. M., Stoltz, L., McCroskey, S., Bradford, W. D., . . . Unruh, J. R. (2016). Analysis of membrane proteins localizing to the inner nuclear envelope in living cells. The *Journal of Cell Biology*. 215(4), 575-590.

Song, J., Durrin, L. K., Wilkinson, T. A., Krontiris, T. G., & Chen, Y. (2004). Identification of a SUMO-binding motif that recognizes SUMO-modified proteins. *PNAS, 101*(40), 14373-14378.

Soustelle, C., Vernis, L., Fréon, K., Reynaud-Angelin, A., Chanet, R., Fabre, F., & Heude, M. (2004). A new Saccharomyces cerevisiae strain with a mutant Smt3-deconjugating Ulp1 protein is affected in DNA replication and requires Srs2 and homologous recombination for its viability. *Molecular and Cellular Biology, 24*(12), 5130-5143.

Stancheva, I., & Schirmer, E. C. (2014). Nuclear envelope: connecting structural genome organization to regulation of gene expression. In *Cancer Biology and the Nuclear Envelope* , 209-244

Stellwagen, A. E., Haimberger, Z. W., Veatch, J. R., & Gottschling, D. E. (2003). Ku interacts with telomerase RNA to promote telomere addition at native and broken chromosome ends. *Genes & Development, 17*(19), 2384-2395.

Strahl-Bolsinger, S., Hecht, A., Luo, K., Grunstein, M. J. (1997). SIR2 and SIR4 interactions differ in core and extended telomeric heterochromatin in yeast. *Genes and Development, 11*(1), 83-93.

Strambio-de-Castillia, C., Blobel, G., & Rout, M. P. (1999). Proteins connecting the nuclear pore complex with the nuclear interior. *The Journal of Cell Biology, 144*(5), 839-855.

Sun, J.-Q., Hatanaka, A., & Oki, M. (2011). Boundaries of transcriptionally silent chromatin in Saccharomyces cerevisiae. *Genes & Genetic Systems, 86*(2), 73-81.

Suzuki, R., Shindo, H., Tase, A., Kikuchi, Y., Shimizu, M., & Yamazaki, T. (2009). Solution structures and DNA binding properties of the N-terminal SAP domains of SUMO E3 ligases from Saccharomyces cerevisiae and Oryza sativa. *Proteins, Structures, Function and Bioinfomatics, 75*(2), 336-347.

Taddei, A., Hediger, F., Neumann, F. R., Bauer, C., & Gasser, S. M. (2004). Separation of silencing from perinuclear anchoring functions in yeast Ku80, Sir4 and Esc1 proteins. *The EMBO Journal, 23*(6), 1301-1312.

Taddei, A., Schober, H., & Gasser, S. M. (2010). The budding yeast nucleus. *Cold Spring Harbor perspectives in biology*, *2*(8).

Taggart, A. K., Teng, S.-C., & Zakian, V. A. (2002). Est1p as a cell cycle-regulated activator of telomere-bound telomerase. *Science, 297*(5583), 1023-1026.

Takahashi, Y., Mizoi, J., Toh-e, A., & Kikuchi, Y. (2000). Yeast Ulpl, an Smt3-specific protease, associates with nucleoporins. *The Journal of Biochemistry, 128*(5), 723-725.

Takahashi, Y., Toh-e, A., & Kikuchi, Y. (2003). Comparative analysis of yeast PIAS-type SUMO ligases in vivo and in vitro. *Journal of Biochemistry, 133*(4), 415-422.

Tanabe, H., Müller, S., Neusser, M., von Hase, J., Calcagno, E., Cremer, M., . . . Cremer, T. (2002). Evolutionary conservation of chromosome territory arrangements in cell nuclei from higher primates. *PNAS, 99*(7), 4424-4429.

Teixeira, M. T., Arneric, M., Sperisen, P., & Lingner, J. (2004). Telomere length homeostasis is achieved via a switch between telomerase-extendible and-nonextendible states. *Cell, 117*(3), 323-335.

Texari, L., Dieppois, G., Vinciguerra, P., Contreras, M. P., Groner, A., Letourneau, A., & Stutz, F. (2013). The nuclear pore regulates GAL1 gene transcription by controlling the localization of the SUMO protease Ulp1. *Molecular Cell, 51*(6), 807-818.

Tham, W.-H., Wyithe, J. S. B., Ferrigno, P. K., Silver, P. A., & Zakian, V. A. (2001). Localization of yeast telomeres to the nuclear periphery is separable from transcriptional repression and telomere stability functions. *Molecular Cell, 8*(1), 189-199.

Therizols, P., Fairhead, C., Cabal, G. G., Genovesio, A., Olivo-Marin, J.-C., Dujon, B., & Fabre, E. (2006). Telomere tethering at the nuclear periphery is essential for efficient DNA double strand break repair in subtelomeric region. The *Journal of Cell Biology, 172*(2), 189-199.

Therizols, P., Duong, T., Dujon, B., Zimmer, C., & Fabre, E. (2010). Chromosome arm length and nuclear constraints determine the dynamic relationship of yeast subtelomeres. *PNAS*, 200914187.

Treitel, M. A., & Carlson, M. (1995). Repression by SSN6-TUP1 is directed by MIG1, a repressor/activator protein. *PNAS, 92*(8), 3132-3136.

Valenzuela, L., Dhillon, N., & Kamakaka, R. T. (2009). Transcription independent insulation at TFIIIC dependent insulators. *Genetics*.

Van de Vosse, D. W., Wan, Y., Lapetina, D. L., Chen, W.-M., Chiang, J.H., Aitchison, J. D., & Wozniak, R. W. (2013). A role for the nucleoporin Nup170p in chromatin structure and gene silencing. *Cell, 152*(5), 969-983.

Van Leeuwen, F., & Gottschling, D. E. (2002). Assays for gene silencing in yeast. *Methods in Enzymology, 350*, 165-186.

Vodenicharov, M. D., Laterreur, N., & Wellinger, R. J. (2010). Telomere capping in non-dividing yeast cells requires Yku and Rap1. *The EMBO Journal, 29*(17), 3007-3019.

Wang, S., & Zakian, V. A. (1990). Sequencing of Saccharomyces telomeres cloned using T4 DNA polymerase reveals two domains. *Moleucalr and Cellular Biology, 10*(8), 4415-4419.

Wang, X., Connelly, J. J., Wang, C.-L., & Sternglanz, R. (2004). Importance of the Sir3 N terminus and its acetylation for yeast transcriptional silencing. *Genetics, 168*(1), 547-551.

Watson, M. L. (1955). The nuclear envelope: Its structure and relation to cytoplasmic membranes. *The Journal of Biophysical and Biochemical Cytology, 1*(3), 257.

Walters, A. D., Amoateng, K., Wang, R., Chen, J.-H., McDermott, G., Larabell, C. A., . . . Cohen-Fix, O. (2018). Nuclear envelope expansion in budding yeast is independent of cell growth and does not determine nuclear volume. *Molecular Biology of the Cell*, mbc. E18-04-0204.

Wohlschlegel, J. A., Johnson, E. S., Reed, S. I., & Yates, J. R. (2004). Global analysis of protein sumoylation in Saccharomyces cerevisiae. *Journal of Biological Chemistry, 279*(44), 45662-45668.

Wotton, D. & Shore, D. J. (1997). A novel Rap1p-interacting factor, Rif2p, cooperates with Rif1p to regulate telomere length in Saccharomyces cerevisiae. *Genes and Development, 11*(6), 748-760.

Wright, J. H., Gottschling, D. E., Zakian, V. A. (1992). Saccharomyces telomeres assume a non-nucleosomal chromatin structure. *Genes and Development, 6*(2), 197-210.

Wu, A. C.-Y., & Rifkin, S. A. (2015). Aro: a machine learning approach to identifying single molecules and estimating classification error in fluorescence microscopy images. *BMC Bioinformatics, 16*(1), 102.

Yunus, A. A., & Lima, C. D. (2009). Structure of the Siz/PIAS SUMO E3 ligase Siz1 and determinants required for SUMO modification of PCNA. *Molecular Cell, 35*(5), 669-682.

Zhao, K., Harel, A., Stuurman, N., Guedalia, D., & Gruenbaum, Y. (1996). Binding of matrix attachment regions to nuclear lamin is mediated by the rod domain and depends on the lamin polymerization state. *FEBS, 380*(1-2), 161-164.

Zhao, X., Wu, C.-Y., & Blobel, G. (2004). Mlp-dependent anchorage and stabilization of a desumoylating enzyme is required to prevent clonal lethality. *The Journal of Cell Biology, 167*(4), 605-611.

Zheng, R., Ghirlando, R., Lee, M. S., Mizuuchi, K., Krause, M., & Craigie, R. J. (2000). Barrier-to-autointegration factor (BAF) bridges DNA in a discrete, higher-order nucleoprotein complex. *PNAS 97*(16), 8997-9002.

Zullo, J. M., Demarco, I. A., Piqué-Regi, R., Gaffney, D. J., Epstein, C. B., Spooner, C. J., . . . Reddy, K. L. (2012). DNA sequence-dependent compartmentalization and silencing of chromatin at the nuclear lamina. *Cell, 149*(7), 1474-1487.